This is to certify that the

dissertation entitled

Diagenesis of aluminosilicate minerals in the
New Haven Arkose and East Berlin Formation
(Triassic-Jurassic), southern Hartford Basin,
Connecticut.

presented by

Mounir K. Saad

has been accepted towards fulfillment
of the requirements for

_____Ph.D._____ degree in ___Geology___

_____
Major professor

Date _FEB. 22, 1991_

PLACE IN RETURN BOX to remove this checkout from your record.
TO AVOID FINES return on or before date due.

DATE DUE	DATE DUE	DATE DUE
_____	_____	_____
_____	_____	_____
_____	_____	_____
_____	_____	_____
_____	_____	_____
_____	_____	_____
_____	_____	_____

c:\circ\datedue.pm3-p.1

DIAGENESIS OF ALUMINOSILICATE MINERALS IN THE NEW HAVEN ARKOSE AND EAST BERLIN FORMATION (TRIASSIC-JURASSIC), SOUTHERN HARTFORD BASIN, CONNECTICUT.

by

Mounir K. Saad

A THESIS

Submitted to
Michigan State University
in partial fulfillment of the requirements
for the degree of

DOCTOR OF PHILOSOPHY

Department of Geological Sciences

1991

ABSTRACT

**DIAGENESIS OF ALUMINOSILICATE MINERALS IN THE NEW HAVEN
ARKOSE AND EAST BERLIN FORMATION (TRIASSIC-JURASSIC),
SOUTHERN HARTFORD BASIN, CONNECTICUT.**

BY

MOUNIR KAMEL SAAD

Late Triassic and Early Jurassic fluvial sandstones of
the Hartford Basin contain of a complex assemblage of
diagenetic minerals. Sample examination using thin-section
petrography, SEM, BSEM, EDS, and EMPA techniques was performed
in order to constrain compositional and textural relationships
among authigenic aluminosilicate minerals in the New Haven
and East Berlin Formation.

The diagenetic history of the New Haven Arkose (fluvial)
and the East Berlin Formation (fluvial/lacustrine) is similar
and shows that compaction was the earliest process in these
rocks. However, albitization, illitization, and zeolite
cementation are more extensive in the more deeply buried New
Haven Arkose.

XRD analysis reveals that illite is the predominant clay
mineral present in these sandstones. The presence of
interstratified illite-smectite layers suggest possible

formation of illite from a smectite precursor.

The abundance and distribution of albitized feldspars, chlorites, and zeolites varies between the stratigraphically shallower East Berlin Formation and the deeply buried New Haven Arkose. Albitization of K-feldspars, and authigenic chlorites, increase down section. Type 1 albite is common in the East Berlin Formation, whereas type 2 albite is common in the New Haven Arkose. Detrital chlorite is present in both formations, whereas authigenic pore-filling and pore-lining chlorite cement is confined to the New Haven Arkose. Chlorite increases in abundance with depth among the deeper samples. Petrographic and XRD results suggest the authigenic chlorites are polytype Ib and detrital chlorite is polytype IIb. Throughout the stratigraphic thickness of the New Haven Arkose, diagenetic facies varies from a zeolite (laumontite) facies, to zeolite/chlorite facies, and finally to chlorite facies with increasing burial depth.

The variation in abundance and distribution of different diagenetic cements and replacements found in the New Haven Arkose and the East Berlin Formation suggests that the main diagenetic processes are temperature and depth related.

Dedicated to my lovely wife and my daughter

"Without your support and sacrifice, my wife,

this work will never be done".

--Feb. 22, 1990

graduate work.

I would like also to acknowledge the assistance and help given to me by Amideast and the Egyptian Cultural and Educational Bureau during this "american" experience.

Finally, I thank my beloved wife and daughter for their understanding and unconditional love, support and sacrifice.

TABLE OF CONTENTS

LIST OF TABLES

CHAPTER 1

INTRODUCTION

This study is concerned with the clay mineralogy and sandstone diagenesis of the clastic sedimentary red-bed sequence of Lower Mesozoic age located in the Hartford Basin, Connecticut Valley and generally referred to as the Newark Supergroup (Van Houten, 1977; Olsen, 1978). These sedimentary rocks consist of alluvial-fan, fluvial and lacustrine deposits interlayered with extrusive basalt flows and intrusive basalt dikes and sills (Hubert et al., 1978).

The Hartford Basin is one of the most studied Mesozoic closed basins of eastern North America (Krynine, 1950; Hubert et al., 1978; Hubert et al., 1982). The Hartford Basin is a part of a linear system of fault-bounded basins extending for a distance of 2000 km along the eastern continental margin of North America (Figure 1). These basins developed during rifting which formed the Atlantic Ocean (Van Houten, 1977; Austin et al., 1980). The Newark Supergroup of sedimentary rocks within the Connecticut Valley forms a homocline that generally dips east and strikes north-south (Krynine, 1950; Van Houten, 1977). The Hartford Basin is a half-graben about 150 km long and up to 30 km across. The strata dip uniformly toward the eastern edge of the basin, where there is a complex west-dipping normal fault system bounding the basin on the east. The basin is bounded to the west by pre-Triassic metamorphic basement rocks. These faults separate the

1
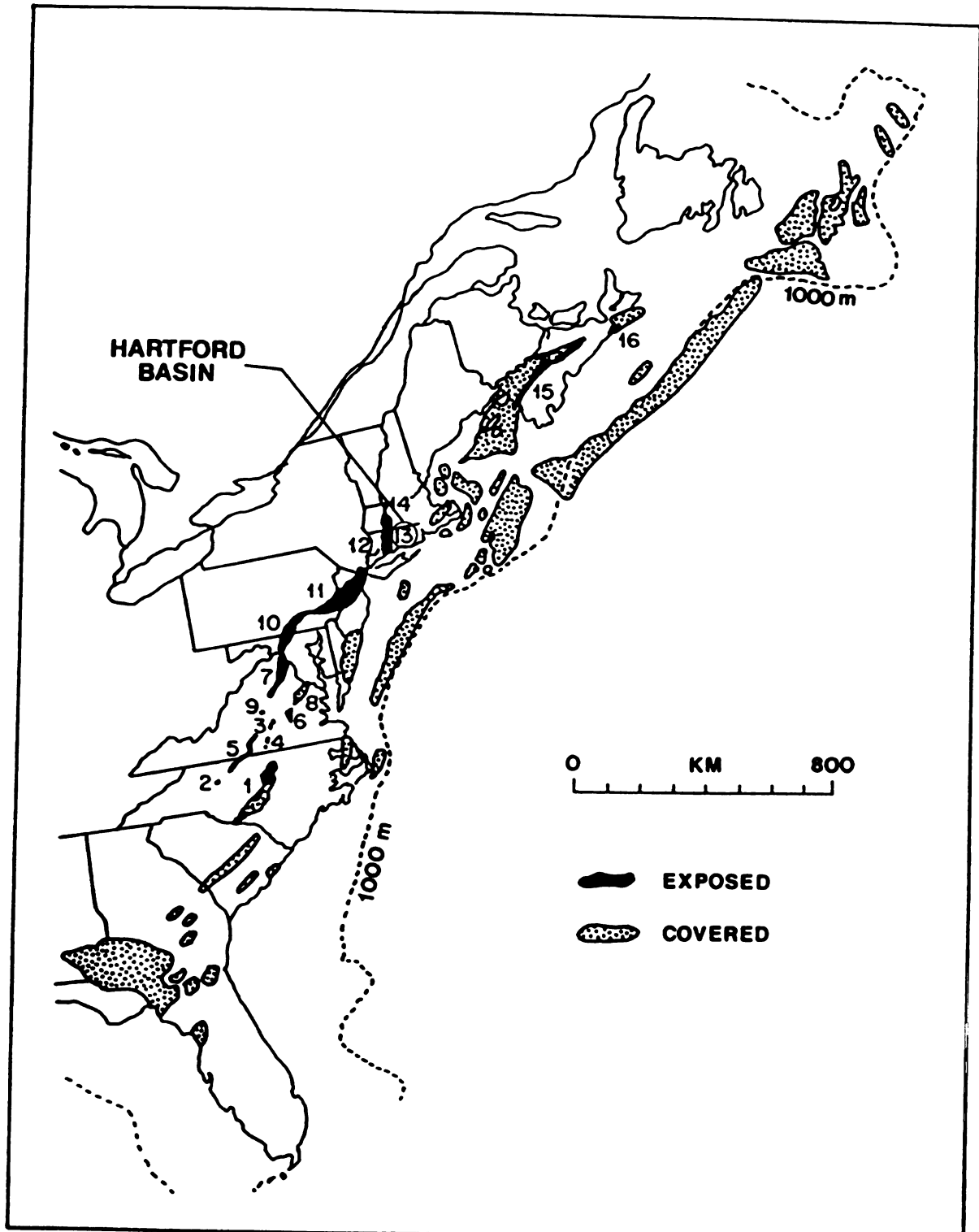
Figure 1. Basins of the Newark Supergroup along eastern North America (after Van Houten, 1977).

uplifted Lower Paleozoic metamorphic rocks to the east from the down-dropped valley (Hubert et al., 1978).

The Hartford Basin contains sedimentary and volcanic igneous rocks of Late Triassic and Early Jurassic age (Krynine, 1950). These rocks have a maximum thickness of about 4 km (Hubert et al., 1978). The Triassic strata of the Hartford Basin were subdivided into seven main formations of the Meriden Group; from bottom to top: New Haven Arkose, Talcott Formation, Shuttle Meadow Formation, Holyoke Formation, East Berlin Formation, Hampden Formation, and Portland Formation (Rodgers, 1968; Sanders, 1970). This classification is based upon lithology. The Hampden, Holyoke, and Talcott Formations are basalt flows; the other four units consist of terrigenous clastic sedimentary rocks. The stratigraphic framework of the Connecticut Valley is depicted in Figure 2.

PALEOGEOGRAPHIC HISTORY

In its pre-continental drift position, the rift valley was located in the tropics at about 15 degrees north paleolatitude (Hubert et al., 1978). The valley was floored by multiply-deformed, high grade metamorphic rocks of Early Paleozoic age. The initial sedimentary fill was the 2000 m New Haven Arkose of Late Triassic-Early Jurassic age (Krynine, 1950). Rivers flowed from the eastern highlands, depositing conglomerate and sandstone in alluvial fans along the base of a fault-bounded escarpment. The rivers coursed south-west,

KM

4

3

2

1

0
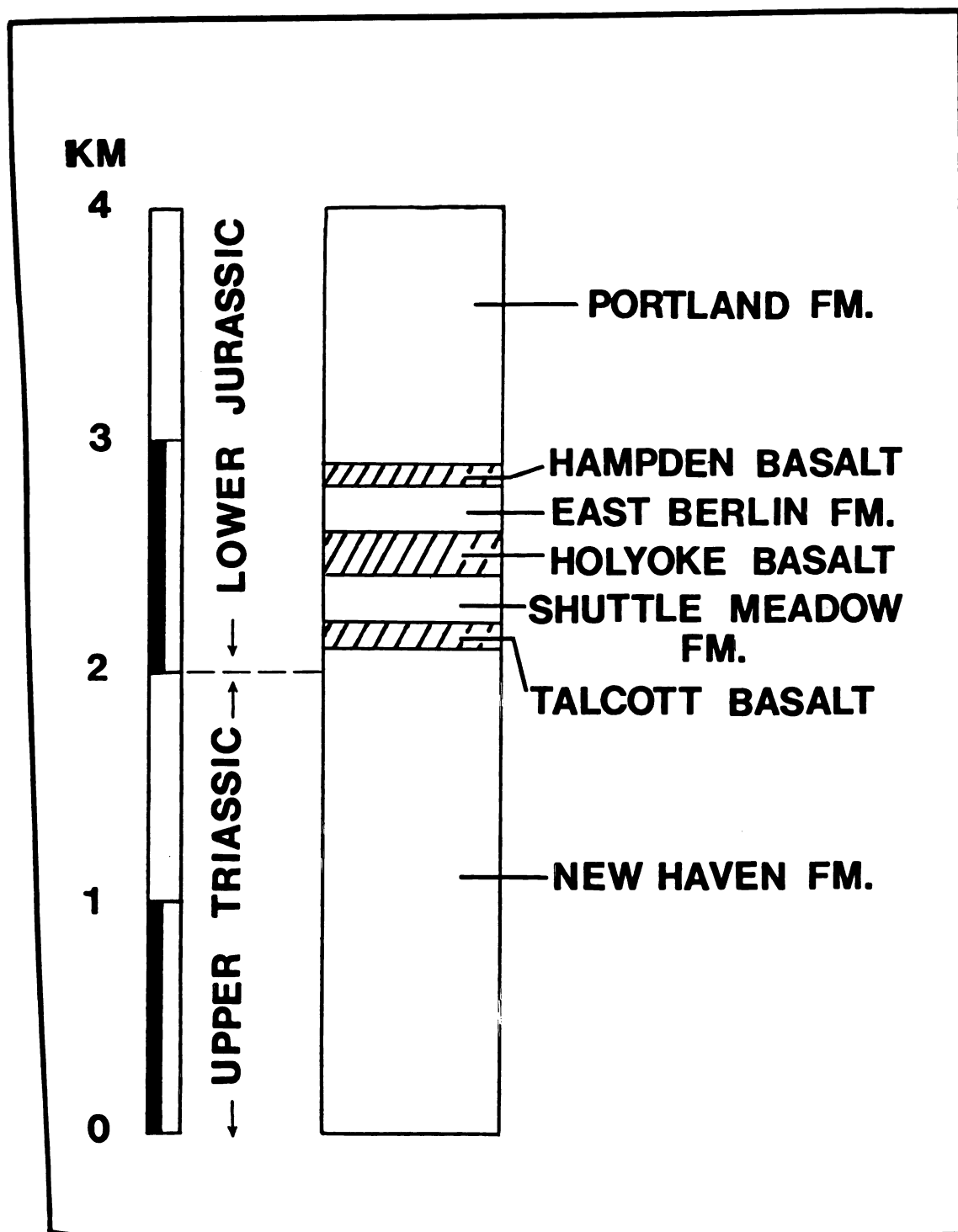
Figure 2. The stratigraphic framework of the Upper
Triassic and Lower Jurassic in the
Hartford Basin, Central Connecticut
(Hubert et al., 1976).

mistru

mistc

Sach,

scndar

sai-az

n 'Ib

In

kng c

merbe

he flo

foor

below

mt e

precipi

builde

Restor

Kqueno

Racks

Ymati

Ymati

Vo

kng f

Revoke

Admistr

Ymati

Rules

Kstory

constructing an alluvial-plain sequence of braided-river
sandstone and pebbly sandstone and floodplain red mudstone
(Smith, 1971 and 1972). Caliche paleosol profiles are
abundant, reflecting a paleoclimate dominated by tropical
semi-aridity with seasonal precipitation of about 100 to 500
mm (Hubert et al., 1978).

In Early Jurassic time, tholeiitic basaltic magma rose
along deep crustal fractures to form the fissure flows and
interbedded volcanic agglomerate of the 65 m Talcott Basalt.
The flows substantially lowered the gradient of the valley
floor (Hubert et al., 1978). The overlying 100m Shuttle
Meadow Formation is dominated by playa and perennial lakes
that existed during intervals of relatively increased
precipitation (Hubert et al., 1982). The lacustrine rocks
include laminated dolomite-gray mudstone, gray sandstone,
limestone, and thin, evenly bedded redbeds. Thin fluvial
sequences of redbeds separate the lacustrine rocks. Dinosaur
tracks are found in the mudstones of the Shuttle Meadow
Formation, as well as in the East Berlin and Portland
Formations (Hubert et al., 1978).

Volcanic activity then resumed with huge outpourings
along fissures of highly fluid basalt that form the 100 m
Holyoke Basalt. The lava flows were succeeded by the
lacustrine and fluvial strata of the 170 m East Berlin
Formation. One third of the formation consists of lacustrine
cycles of gray mudstone and sandstone-black shale-gray
mudstone and sandstone. The lakes were perennial with

alkaline hard water (Hubert et al., 1978).

Later, thin lava flows spread from fissures and vents located southwest of central Connecticut to form the 60 m Hampden Basalt. The overlying Portland Arkose is a 1200 m sequence consisting mostly of braided-river sandstone and floodplain red mudstone. Alluvial fans continued to coalesce along the front of the eastern highlands. Thin lacustrine beds of gray mudstone and sandstone are present in the lower half of the Portland Arkose (Hubert et al., 1978).

The strata in the rift valley have been intruded by basalt dikes and sills, tilted to the southeast, locally folded and faulted, and subjected to erosion (Krynine, 1950; Hubert et al., 1978).

Geographic Position

Recently, with the advent of plate tectonic theory and paleomagnetic research, the geographic position of the Connecticut Valley during Late Triassic and Early Jurassic time has been tentatively placed between 10 to 25 degree north of the paleoequator (Hallam, 1971; Philipps and Forsyth, 1972). With this information and numerous lacustrine paleocurrent and slump fold measurements Hubert et al. (1976), in their sedimentologic study of the East Berlin Formation, proposed that the valley was under the influence of a predominant northwest paleowind. In a later paper, Hubert (1977) suggested that the northwesterly winds blowing over outcroppings of Paleozoic carbonate rocks to the west of the

rift valley provided calcareous dust for the formation of caliche deposits in the New Haven Arkose (Late Triassic-Early Jurassic).

The research conducted by Hubert et al., (1976) provides detailed interpretations of the fluvial and lacustrine sedimentary depositional environments of the East Berlin Formation. They conclude that the sediments were deposited in fluvial and lacustrine-paludal environments (Figure 3). Stream-channel sandstone, floodplain red mudstone and lacustrine red sandstone and siltstone were deposited under oxidizing and alkaline conditions. The black shale and gray mudstone and sandstone were laid down in large, perennial, oligomictic lakes, which at times extended over wide areas of the rift valley.

DESCRIPTION OF THE STUDIED FORMATIONS

Previous sedimentologic work by Krynine (1950), Sanders (1970) and Hubert et al. (1978) has yielded a stratigraphic framework, petrographic history and a broad understanding about depositional environment. Krynine's work emphasized the mineralogy and petrology of the sedimentary rocks and the climatic significance of the red color of the sediments. Sanders (1970) revised the stratigraphy and developed a lacustrine model of deposition for the fine-grained sediments of the East Berlin Formation. Hubert et al. (1978) have summarized many of the currently accepted interpretations of depositional environments for the different formations found
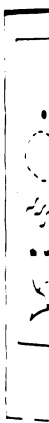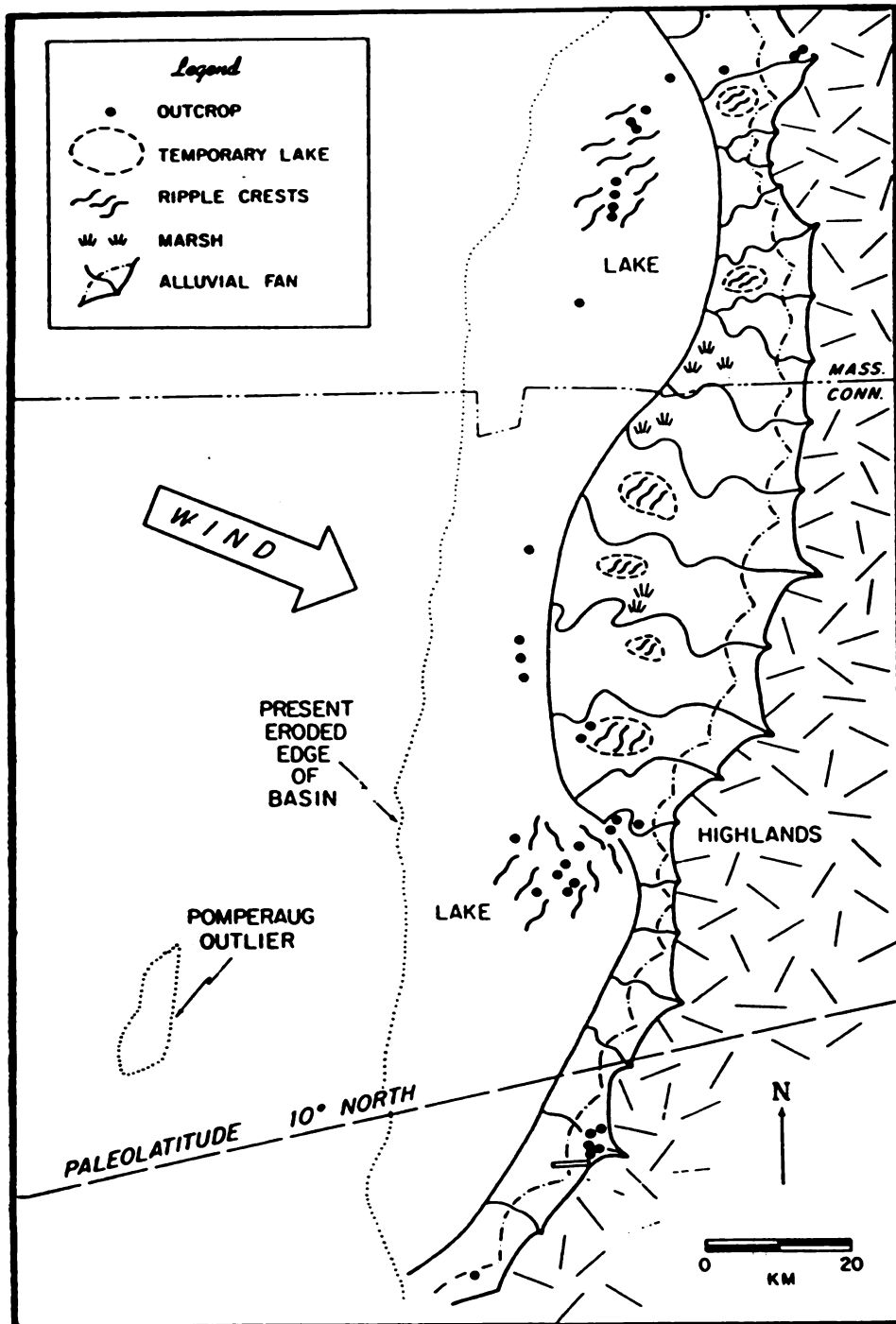
Figure 3. Paleogeographic map showing various depositional environments of the East Berlin Fm. Paleowind direction was determined from paleocurrent readings in shallow water and shoreline sandstone of temporary and perennial lakes (Hubert et al., 1976).

in the Hartford Basin.

Four accessible exposures representing East Berlin and New Haven Arkose Formations were selected for this study (stops 1-4, Figure 4a). An idealized cross-section of the Hartford Basin (A-A', perpendicular to structural strike) illustrates the approximate geographic and stratigraphic location of stops 2-4, showing that stop 3 of the New Haven Arkose is stratigraphically higher than stop 2 and 4 (Figure 4b). The following is a description of the stratigraphy and sedimentation of both formations.

New Haven Arkose

A large outcrop of about 72 m of the New Haven Arkose is exposed along the North Haven section, Connecticut (stop 2, Figure 4).

The rocks of the New Haven Arkose contain an alluvial plain sequence of channel pale red sandstones and conglomerate interbedded with floodplain red sandy mudstone (Figure 5a). Cross-bed sets of pebbly sandstone commonly exceed 0.5 m in thickness, suggesting avalanche deposition on prograding slipfaces of braid bars (Hubert et al., 1978).

At this stop, numerous caliche profiles were observed, produced by paleosol calcification of channel sand and floodplain mud. A combination of a slow sedimentation rate with a paleoclimate dominated by semi-aridity generated about 35 caliche horizons in the 72 m section. Hubert (1977) discovered widely distributed caliche paleosol profiles in
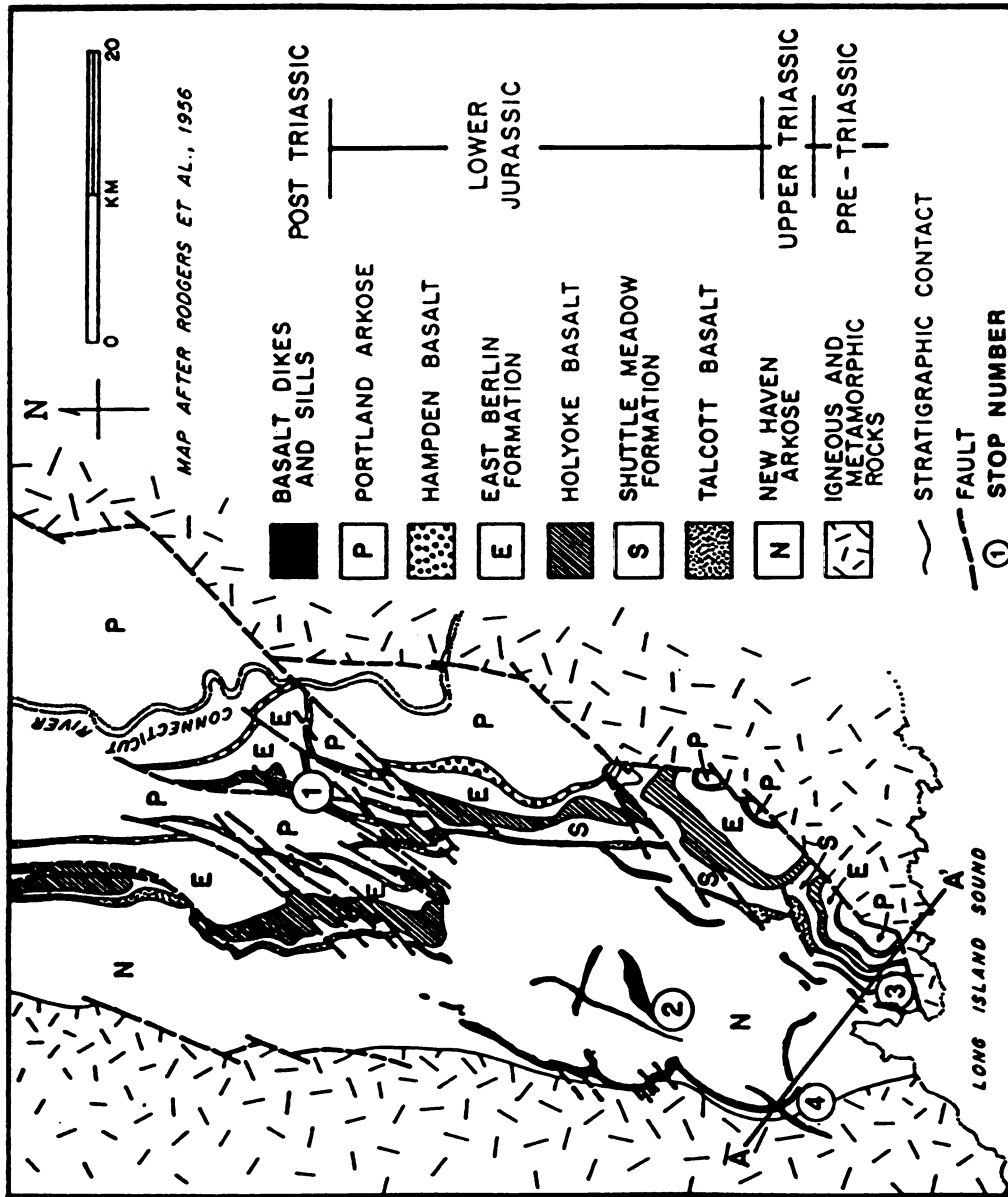
Figure 4a Geological map of central Connecticut showing the location of the four sampling stops.
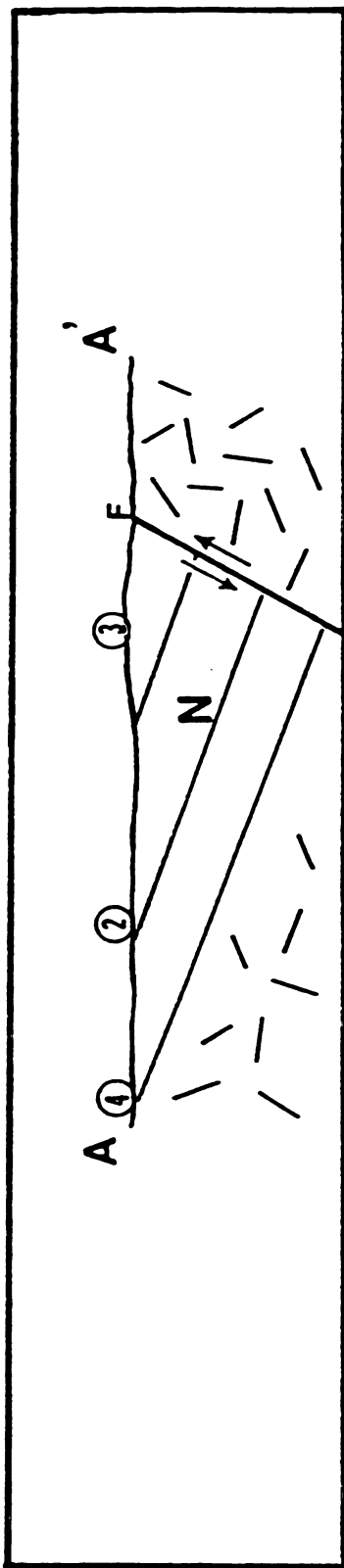
Figure 4b Schematic cross-section (A-A') of the Hartford Basin
showing the relative stratigraphic position of the
three stops of the New Haven Arkose. Cross-section
direction is illustrated in Figure 4a.
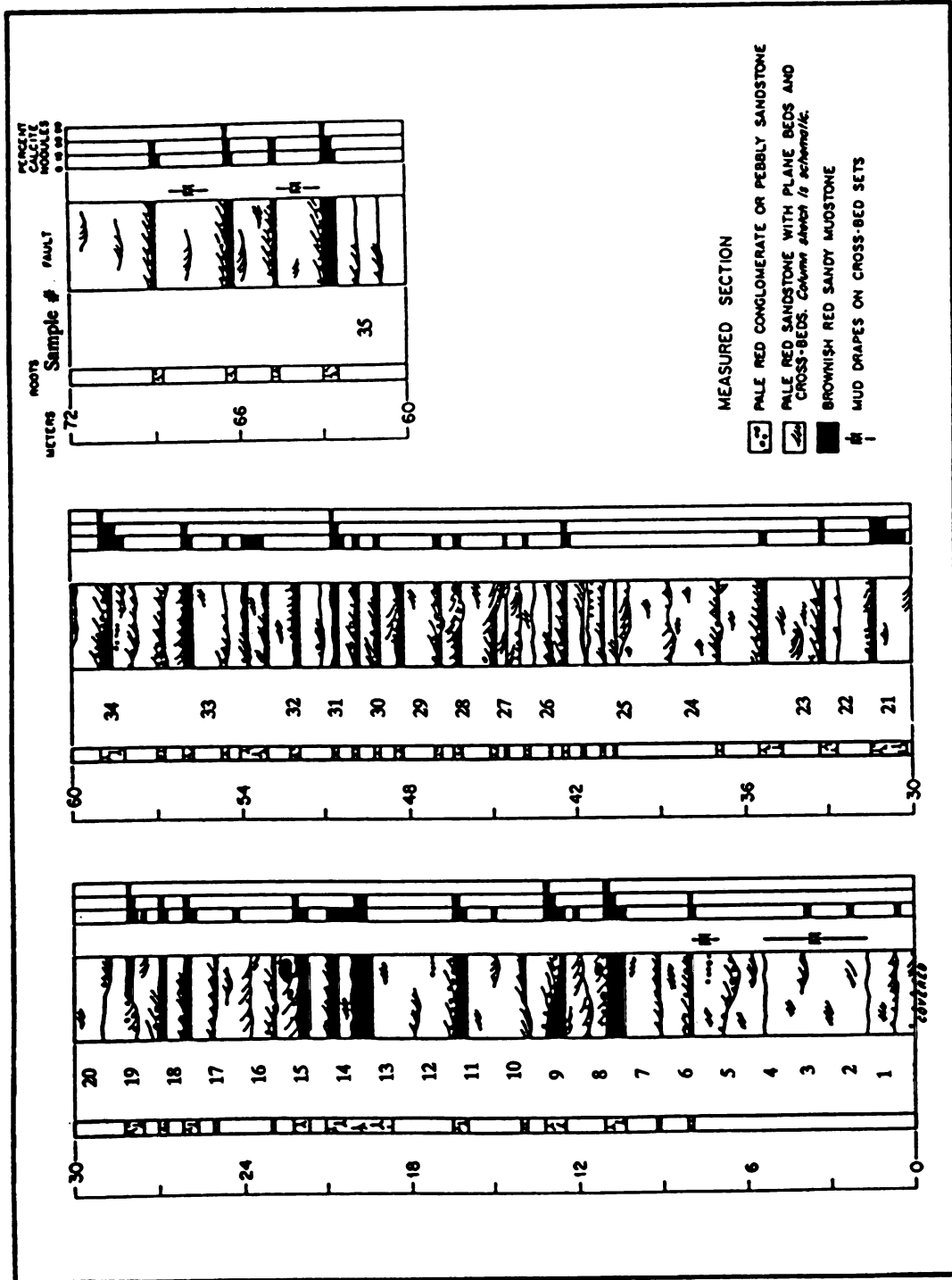
Figure 5a Measured section of the New Haven Arkose at stop 2 along route 40, North Haven (modified after Hubert et al., 1978).

braided-stream sandstone and overbank mudstone in this section of the New Haven Arkose. Caliche profiles were not observed in the other studied outcrops of the New Haven Arkose (Stops 3 and 4, Figure 4).

The alluvial plain sequence was deposited by braided rivers as evident by the presence of a complex pattern of plane beds, and planar tangential cross-beds overlain by pebbly sandstone and conglomerate (Hubert et al., 1978). The rivers were ephemeral, with a large fluctuations in water discharge, shallow, floored by bars and channels, of high gradient and low sinuosity, and with a coarse bedload of pebbly sand (Smith, 1971 and 1972).

The New Haven Arkose exposed in an old abandoned quarry (currently the Hamden Dump) consists mainly of floodplain facies that are cut by a dolerite dike, about 3 meters thick (stop 3, Figures 4 and 5b). These rocks consist of coarse-grained, thick-bedded sandstone and interbedded, thin-bedded siltstone. The sandstones are coarse-grained, arkosic, poorly sorted and pebbly.

An outcrop of proximal alluvial fan facies of the basal New Haven Arkose at Woodbridge, Connecticut (stop 4, Figures 4 and 5b) shows that these rocks unconformably overly the pre-Triassic Milford Chlorite Schist. The New Haven Arkose consists of interlayered and intertonguing cobble- and pebble-conglomerate and green, epidotic (detrital), arkosic sandstone. Both the conglomerate and sandstone are poorly sorted. Bedding is extremely crude, roughly parallel to the

14
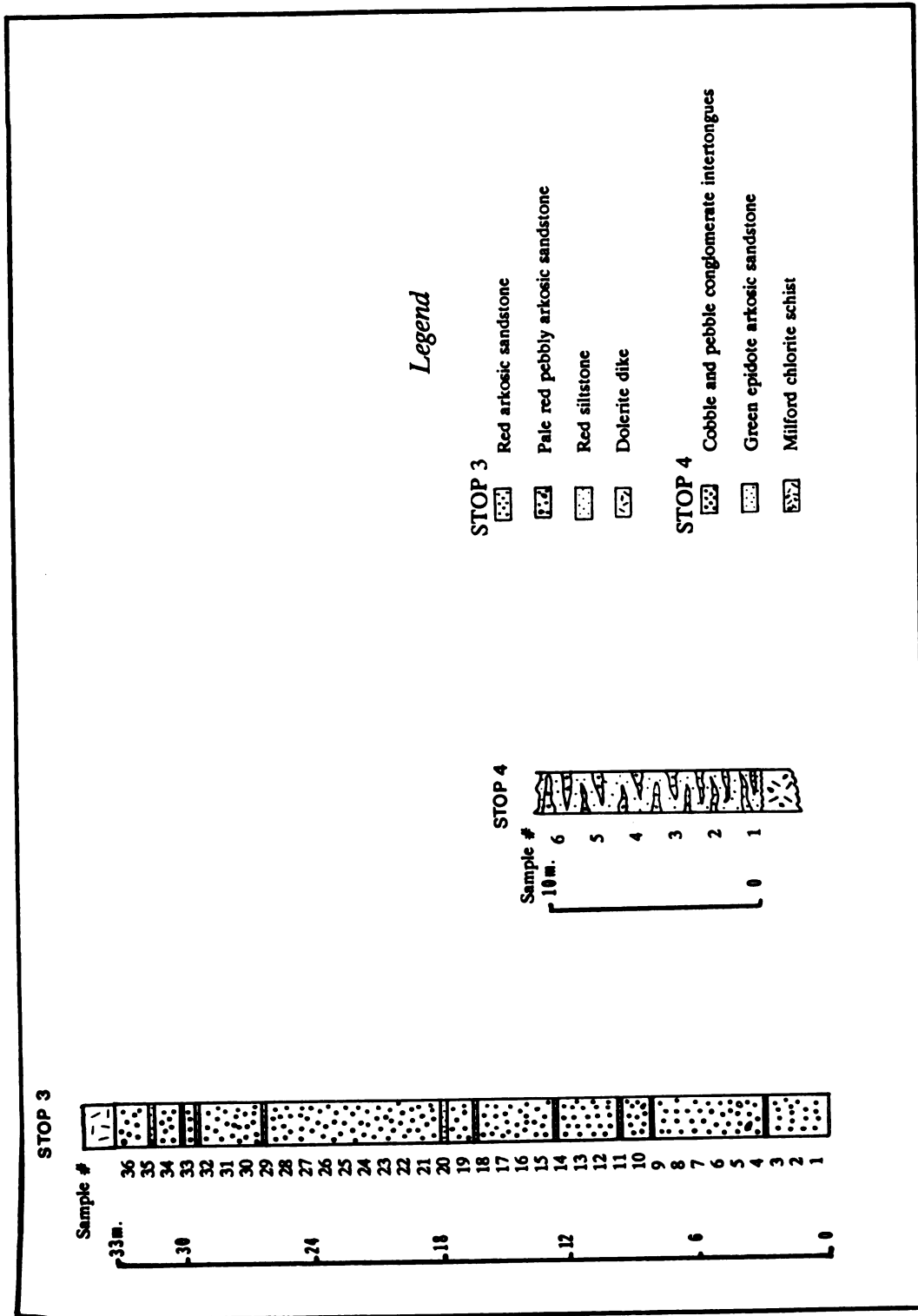
Figure 5b Measured sections of the New Haven Arkose at stop 3 and 4.

basa

asso

pebli

Lkos

Lle

and

Len

iqli

if th

Iten

iit

ii

lasa

il.

may

Fen

lexke

tive

lat

iecp

ice

basal unconformity.

The conglomerate shows two distinct size composition associations, phyllitic cobbles and quartzo-feldspathic pebbles, suggesting two sources for the basal New Haven Arkose. The cobble fraction was derived locally from the Milford Chlorite Schist, whereas the pebble fraction and the sand fraction were probably derived from a more distant source (Klein, 1968).

The mixed sorting of the rocks, the sand-grain angularity, the poor stratification, and the mixed population of the conglomerates support the proximal alluvial fan facies interpretation.

East Berlin Formation

About 62 m of the upper part of the East Berlin Formation, plus the contact with the overlying 60 m Hampden Basalt, are exposed near Cromwell, Connecticut (stop 1, Figure 4).

The rock types are mainly gray mudstone, black shale, and gray sandstone (perennial lakes); red mudstone (floodplains); evenly bedded red sandstone and siltstone with abundant ripple marks (shallow oxidized lakes); and pale-red channel sandstone (river channels).

The black shale and gray mudstone record perennial lakes that existed from time to time in the rift valley (Krynine, 1950; Klein, 1969; Hubert et al., 1976). At some localities in central Connecticut these beds contain different groups of

fossi

the se

large

of ver

contr

c

a dep

kelli

poli

appra

of pe

is si

spher

Inter

sllas

Tple

of ea

deepe

distr

whol

Almos

Sone

Rain

Thor

Trans

fossil fish (Hubert et al., 1978). Olsen (1986) believes that the sediments of the early Mesozoic Newark Supergroup consist largely of sedimentary cycles produced by the rise and fall of very large lakes that responded to periodic climate changes controlled by variations in the earth's orbit.

The recent study by Demicco and Kordesch (1986) provides a detailed sedimentary facies classification of the East Berlin Formation. They conclude that the mudstone facies are cyclic and record long periods of dry playa mudflat aggradation punctuated by the rapid expansion and contraction of perennial lakes. On the other hand, the sandy facies occur as single sedimentation units that record sheet floods across ephemeral floodplains. I agree with Hubert et al. (1978) interpretation of the mudstone facies cycles as representing climatic changes from wet-dry periods.

The black shale and gray mudstone form symmetrical cycles, mostly 2 to 7 m in thickness (Figure 6). The center of each cycle is pyritic black shale that accumulated in the deeper, more central parts of a lake. Above and below is gray mudstone with structures indicative of shallower water, including dolomite concretions, ripple marks, mud cracks, and dinosaur footprints. Ferroan dolomite laminae are present in some of the black shale and gray mudstone. The terrigenous grains in these drab-colored rocks were originally coated with limonite stains which were removed in solution, evidently as organic-ferrous iron complexes (Hubert et al., 1978).
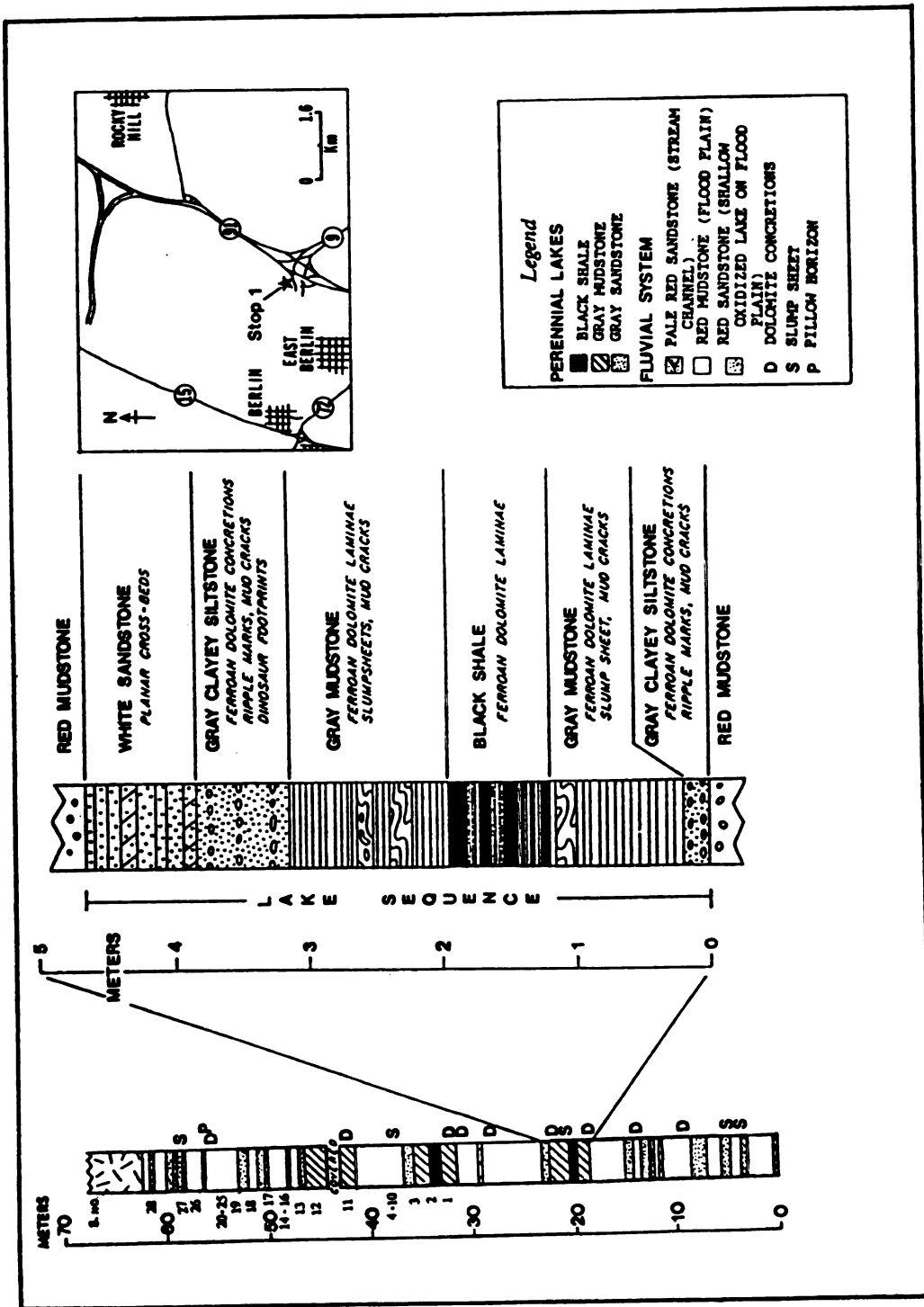
Figure 6. Stratigraphic section of the perennial lake cycle in the East Berlin Formation, stop 1, Cromwell (modified after Hubert et al., 1976).

Thin beds of gray, fine- to very fine-grained sandstone occur in some of the gray mudstones, forming intervals of thin-bedded sandstone and gray mudstone. Most of the sandstone is horizontally laminated, but there are some planar cross-beds. The sandstones are near the top and bottom of the cycles, implying accumulation in shallow water near the lake shores. The gray mudstone-black shale-gray mudstone symmetrical cycles require expansion and contraction of perennial lakes (Hubert et al., 1978).

The Early Jurassic palynoflorule in the East Berlin Formation comprises more than 90% Corollina pollen from conifers that lived most abundantly on sandy areas of the alluvial fans and highlands (Cornet and Traverse, 1975). The rarity of xeromorphic cuticular adaptations in the flora, plus the many kinds of cryptograms based on spore diversity, suggest to these authors a humid climate with a short dry season. The palynoflorule is found in lacustrine gray mudstone and black shale, recording periods of increased rainfall that coincided with the existence of large perennial lakes.

The paleoclimate of the Hartford Basin during Early Mesozoic time has been variously described as: glacial (Dana 1883), arid to semi-arid (Hubert, 1977), and warm and humid or seasonally wet (Krynine, 1950; Cornet and Traverse, 1975; Hubert et al., 1976). The two latter hypotheses are considered viable on the bases of fossil as well as petrographic, mineralogical, and sedimentological evidence.

Ebert

nle t

xurre

or th

lterna

prevail

i. (1

ydroge

asins

alcitr

mpos

ndit

b re

irass

REVIO

V

of the

been p

that

similar

Kypni

early

strat

Trias

rift

Hubert et al., (1978) suggest that no one climate fits the whole time span during which deposition in the rift valley occurred. A semiarid (wet/dry) climate appears characteristic for the Upper Triassic (New Haven Arkose), whereas an alternating subhumid (wet/dry)-semiarid (wet/dry) climate prevailed in Lower Jurassic (East Berlin) time. Suchecki et al. (1988) studied the isotopic imprint of climate and hydrogeochemistry on the strata of the Hartford and Fundy basins. They concluded that in the Hartford Basin, caliche calcites in fluvial mudstones and sandstones have isotopic compositions that reflect paleosol processes during climatic conditions that varied from warm and dry in Late Triassic time to relatively cooler and probably wetter in the Early Jurassic.

PREVIOUS WORK AND OBJECTIVES

Various theories addressing the depositional environment of the sedimentary rocks in the Connecticut rift valley have been proposed, since Sir Charles Lyell (1845) first suggested that the sediments were deposited in a large tidal estuary similar to the Bay of Fundy. The facies interpretations of Krynine (1950), Hubert et al. (1976 and 1978) were discussed early in this chapter.

In spite of considerable tectonic, structural, stratigraphic, and sedimentologic research carried out on the Triassic-Jurassic rocks of the Hartford Basin (Connecticut rift valley), very little is known about the mineralogy,

petrology and diagenesis of these rocks. Particularly interesting problems are: the variations in the paleoclimate and its effect on diagenesis of the various detrital mineral assemblages; the extent of sediment diagenesis; the influence of the hot basalt flows on the underlying sediments; and the origin and paragenesis of certain authigenic minerals.

Few sedimentological studies of the Triassic rift basins have made extensive use of thin-section petrography. Krynine (1950) studied the petrography, stratigraphy and origin of the Triassic sedimentary rocks of Connecticut. He included detailed, somewhat exhaustive, petrographic descriptions and characterizations of the sediments. In his stratigraphic classification, the East Berlin Formation was incorporated as a part of the Meriden Formation, a term no longer used. He specified three petrographic and textural components: 1) a coarse-grained (sandy or pebbly) arkose; 2) a fine-grained detrital clayey matrix; and 3) a chemical carbonate cement (generally calcite). Texturally, Krynine mentioned that the Triassic rocks of Connecticut are made up of conglomerates, sandstones, and shales of different degrees of rounding. These rocks are extremely coarse-grained and very poorly sorted. The mineralogy of the rocks allowed him to conclude that there was no significant contribution of sediments from sources west of the main basin's eastern border fault. Krynine was able to decipher the sequence of erosion in the source area by demonstrating an inverted metamorphic-to-granitic compositional sequence within the sediments. Such

vertical distributions allowed him to subdivide some of the formations, but to date, these divisions have had little application to sedimentological problems (Lorenz, 1988).

Krynine also used his suite of over twenty trace or heavy minerals for purposes of east-west stratigraphic correlation, documenting that the bulk of the sediments in the Pomperaug outlier (west of the Hartford Basin; basin 12 on Figure 1) correlate with the New Haven Arkose. Another important use of the heavy-mineral study was in documenting primarily east-to-west paleodrainage. The heavy mineral grains are subangular to subrounded, reflecting the few tens of kilometers of stream transport from the source highlands east of the rift valley (Hubert and Reed, 1978).

Weddle and Hubert (1983), according to Lorenz (1988), combined the distribution of petrographic characteristics of rocks with paleoflow patterns and facies distributions. They showed that, although Triassic sediments probably extended beyond their present limits in the Newark and Hartford/Deerfield basins, the two general areas were not connected as a continuous, broad area of subsidence and sedimentation.

Vetter and Brakenridge (1986) tested the paleogeographic reconstructions derived from cross-bedding by means of petrographic techniques. Their study is an attempt to produce a framework for the subsurface stratigraphic correlation of petrographic horizons in drill holes.

Hubert et al. (1976) discussed the mineralogy of the East Berlin Formation and suggested that the evaporation of the perennial lake led to the formation of dolomite concretions and cement. The climate was wet-tropical with a pronounced dry season. Illite was found to occur abundantly in the red and gray mudstone and black shale. Corrensite in the gray mudstones of the perennial lake cycle sequences may have formed in shallow pools where waters were enriched in dissolved salts. April (1980) reported the presence of a regularly interstratified chlorite/vermiculite (corrensite) in red beds of the East Berlin Formation. The mineral is restricted to a zone of contact metamorphosed strata adjacent to and underlying the Hampden Basalt. Trioctahedral smectite and regularly interstratified chlorite/smectite are restricted to black shale and gray mudstone deposited in alkaline, perennial lakes of the East Berlin Formation (April, 1981). Vergo and April (1982) also reported the presence of an interstratified chlorite/smectite in contact aureoles produced by tholeiitic, basaltic intrusives at West Rock in New Haven Connecticut.

Most of the aforementioned petrographic studies emphasized provenance or stratigraphic correlation. Few petrographic studies have addressed diagenetic processes in the Hartford Basin. Heald (1956) studied the cementation of the Triassic arkoses in Connecticut and Massachusetts away from and near the eastern border fault and intrusives. He concluded that large amounts of cryptocrystalline quartz,

potash feldspar, and sericite were deposited in the sediments along the border fault, while microcrystalline secondary albite is the abundant cement type in the arkoses near intrusives.

Hubert and Reed (1978) used thin-section data, by observing the textural and diagenetic relationships between detrital grains and the authigenic cements, to document the source of red coloration and diagenetic sequence in the Early Jurassic rocks of the East Berlin Formation. They concluded that the red coloration of the sandstones and mudstones is mainly due to hematite and this red color is authigenic. Hematite was produced by different post-depositional diagenetic processes including: aging of limonite; intrastratal solution of Fe-silicate grains; oxidation of magnetite; and replacement of Fe-silicate grains by dolomite cement. Hubert and Reed (1978) also noted that the proportion of quartz and feldspar among the grains are statistically similar in both of the fluvial and lacustrine environments, as are the authigenic mineral cements and their proportions. Plagioclase grains dominate over K-spar in a 7:1 ratio in the arkoses of the lacustrine deposits (Hubert and Reed, 1978). Microcline is more abundant than sodic plagioclase feldspar in the fluvial deposits (Heald, 1956).

Recently, Hubert and Meriney (1988) studied the cementation and paragenetic sequence of the Hartford Basin sediments in Connecticut and Massachusetts. They conclude that albite overgrowths occur in all formations, environments

and parts of the basin.

This dissertation began as an attempt to test the hypothesis that the clay mineral diagenesis in the sandstones and mudstones of the East Berlin Formation and the New Haven Arkose has influenced the evolution of sandstone reservoir properties. After work had begun, the lack of petrographic evidence on porosity evolution and, on the other hand, the enormity of a detailed mineralogical and diagenetic investigation soon became apparent. Research then focused on the diagenesis and mineralogy of the East Berlin Formation and the New Haven Arkose, which proved to display a great diversity in terms of diagenetic alterations and clay-mineral assemblages. The investigation of both paleoclimatically different formations eventually led to a detailed study of the paragenesis and origin of authigenic, detrital, and clay mineral assemblages. The reader should be aware, however, that the regional results and implications are by no means conclusive. They should be regarded as stepping stones for future detailed investigations in this and other basins.

CHAPTER 2

SAMPLING AND ANALYTICAL METHODS

SAMPLE COLLECTION AND LOCALITIES

A total of 105 samples were collected from 4 localities in Connecticut. Samples were obtained from the New Haven Arkose and the East Berlin Formation. Locations of the sampling sites are shown in Figure 4. Twenty-eight samples were collected from the East Berlin Formation (stop 1, Figure 6) near Cromwell. These rocks are exposed along the excavated but unpaved access roads of the interchange between I-91 and route 9 in Cromwell, Connecticut (Figure 6). Sixty-nine samples were collected from three outcrops of the New Haven Arkose. Thirty-five samples were collected from the large exposure of the New Haven Arkose along route 40 (stop 2, Figure 5a) in North Haven, Connecticut. Thirty-six samples of New Haven Arkose were collected from an exposure near a Hampden basalt intrusion (stop 3, Figure 5b) in the Hamden dump. Finally, six samples of the basal New Haven Arkose were collected from a small outcrop behind buildings of the Amity Shopping Center (stop 4, Figure 5b), Woodbridge, Connecticut.

PETROGRAPHIC THIN SECTIONS

Ninety-five thin sections were prepared from all rock types selected from the East Berlin and New Haven Arkose Formations. Hand samples were cut into chips, and blue dyed epoxy was vacuum impregnated into the pore space. Each chip

was then ground on a coarse and then fine grinding wheel and then attached to a petrographic slide. Each thin section was ground to 30 microns thickness and coated with immersion oil and a coverslip. Selected feldspar rich-samples were later cleaned with acetone and stained with sodium cobaltinitrite and rhodizonate reagent for the identification of untwinned potash- and plagioclase feldspar respectively, following the method described by Bailey and Stevens (1960).

Selected sandstone thin sections were point counted (500 point counts) for the different detrital and authigenic minerals using the "traditional" method discussed by Ingersoll et al. (1984). Counts were made by using the microscope's medium magnification power (field of view = 1.8 mm).

Both thin sections and sample chips were carbon coated for the Scanning Electron Microscopy (SEM) and Energy Dispersive Spectroscopy (EDS) analysis. SEM analysis was performed on a JEOL JSM-35C and JEOL T20-CSI; EDS analysis were made by using a Tracor Northern 2000 and 5000. Selected thin sections were polished and carbon coated for the Electron Microprobe (EMP) and Back Scattered Electron Microscopy (BSEM) analyses. A total of 167 analyses were performed using a CAMECA MBX Automated Electron Microprobe Analyzer (EMPA) equipped with three wavelength dispersive spectrometers and secondary and backscattered electron detectors. The operating conditions for the analyses were an accelerating voltage of 15 kV, 10 nA beam current, and a 3 micron beam diameter. BSEM was performed using a KE four-

element solid-state back scattered electron detector. BSEM produces an image in which brightness relates to mean atomic number (Hall and Lloyd, 1981; Pye and Krinsley, 1983; Krinsley, Pye and Kearsley, 1983; Pye and Krinsley, 1984).

X-RAY DIFFRACTION AND CLAY PREPARATION TECHNIQUES

Approximately 5 grams of rock sample was crushed and ground with a ceramic mortar and pestle. The powder was washed in a 500 ml beaker where deionized water was added. Further disaggregation was accomplished by submerging the beaker into an ultrasonic bath for 5 minutes. The less-than-two micron fraction was separated by gravity settling in the beaker at 20 degrees celsius using Stokes law for settling. After 3 hours of settling, the top 5 cm of the beaker was transferred by pipeting to a sealable container. If significant flocculation occurred the sample was treated with sodium hexametaphosphate (Calgon) and the fraction was then agitated in the ultrasonic bath for 5 minutes.

An oriented specimen mount was then made by the method of Drever (1973) as modified by Keller et al. (1986). This involved placing the clay dispersion in a clean cylinder attached by clamp to a porous fritted glass filter overlain by a cellulose ester <0.45 micron filter. A vacuum pump was used to rapidly draw out the liquid, producing an oriented film of clay on the cellulose filter. The untreated clay specimen was then mounted on a glass slide by rolling a glass rod over the filter on to the glass slide. Prior to mounting,

treated samples were saturated with 1N KCl or 1N $MgCl_2$ by passing them through the clay fraction. The samples were glycerol-solvated in the same way. Potassium saturated samples were heated to 300°C and 550°C for 1 hour in a furnace. The x-ray radiation used in the Rigaku-Geigerflex CN-2013 was CuK-alpha, run at 35kV and 25 mA. Scanning speeds were 1 degree-2 theta per minute, run at 1K cps. The divergence slit used was 1/6 degrees (2-theta); the receiving slit, 0.3 mm; and the antiscatter slit was 2 degrees (2-theta). The chart speed was 10 millimeters per minute and the time constant used was 2 seconds.

CHAPTER 3

PETROGRAPHY

The Triassic-Jurassic sediments of the Hartford Basin, Connecticut Valley consist of a mixture of arkosic sandstones and conglomerates, siltstones, red mudstones, black shales, and very subordinate limestones.

NEW HAVEN ARKOSE

Petrographically, the New Haven Arkose consists of a coarse, very poorly to poorly sorted mixture of angular to subangular quartz and feldspar, together with a little mica set in a red, ferruginous clayey matrix.

Generally, these sandstones contain an average of 44% quartz, 37% feldspars, less than 3% rock fragments, and about 2% hematite-stained clay matrix (Table 1). They are classified as arkose according to the classification of Pettijohn et al. (1987) to be arkose (Figure 7a). Figure 7b illustrates the distribution of the mean QFR (quartz, feldspar, and rock fragments) values at the four stops. The distribution of quartz, plagioclase, and K-feldspar (QPK) is illustrated in figure 7c. Point counting for the rock fragments component (R) was made using the "traditional" method as discussed by Ingersoll et al. (1984). The QFR diagram differs from the QFL in that, in the latter, rock fragment counts are made by using the Gazzi-Dickinson method of point counting, which assigns the sand sized crystals and

Table 1. Petrographic point counts of the New Haven Arkose

Stop	Sample	Monoct Qz	Polyt Qz	Detrital Feldspar Micr.	Orth.	Plag.	Rockt Frag.	Opaqt	Micat	Chloritet Det.	P.F.	P.L.	Calcitet Cem.	Rep.	Port	Scolt	Overgrowth Qz	Feldt	Fract	Albt
	MH-4-6	35	5	23	6	2	3	8	-	-	-	10	-	-	-	-	-	-	1	7
	MH-4-5	34	15	15	1	5	2	7	1	-	15	-	-	-	-	-	-	-	2	3
	MH-4-4	37	2	4	-	6	3	10	-	1	25	-	-	-	-	-	-	-	8	4
4	MH-4-3	38	2	25	1	4	2	11	1	-	13	-	-	-	-	-	-	-	1	2
	MH-4-2	41	2	11	1	3	0	8	-	1	22	-	-	-	-	-	-	-	5	3
	MH-4-1	23	8	14	-	4	2	9	2	-	-	30	-	-	-	-	-	-	4	4
	MH-3-36	40	16	32	-	1	3	4	1	-	-	-	-	-	-	-	1	-	-	6
	MH-3-35	39	10	15	-	2	-	4	2	-	-	-	-	-	-	-	-	-	1	28
	MH-3-34	46	4	16	-	4	4	1	-	1	1	-	-	-	-	-	-	-	2	21
	MH-3-33	29	-	42	1	1	2	5	-	-	-	-	-	-	-	-	-	-	1	19
	MH-3-32	25	-	48	-	3	-	7	-	-	-	-	-	-	4	-	-	-	5	8
	MH-3-31	38	2	35	-	4	1	5	4	-	-	-	-	-	-	-	-	-	2	9
	MH-3-30	55	7	10	-	1	-	6	1	-	-	-	-	-	-	-	-	-	1	19
	MH-3-29	49	8	14	-	1	-	9	9	1	-	-	-	-	1	-	-	-	1	10
3	MH-3-28	25	4	30	1	20	-	2	6	1	-	-	-	-	1	-	-	-	1	9
	MH-3-27	32	1	39	-	10	1	6	-	-	1	-	-	-	-	-	-	-	2	8
	MH-3-26	28	1	36	-	8	5	8	1	-	-	-	-	-	-	-	-	-	-	13
	MH-3-25	32	2	36	-	1	-	10	5	-	-	-	-	-	-	-	3	-	9	2
	MH-3-24	35	-	20	-	-	12	8	4	4	-	-	-	-	-	-	6	-	8	3
	MH-3-23	50	-	34	-	-	-	-	-	-	1	-	-	-	-	-	2	-	9	4
	MH-3-22	37	14	30	-	-	-	-	12	-	2	-	-	-	-	-	-	-	-	5
	MH-3-21	30	5	33	-	10	8	1	7	-	-	-	-	-	-	-	-	-	-	6
	MH-3-20	33	6	35	-	6	-	-	3	-	-	-	-	-	-	-	-	-	-	17
	MH-3-19	48	3	25	-	5	5	-	6	-	-	-	-	-	-	-	-	-	-	8

Table 1 (cont'd.)

Stop	Sample	Monot Qs	Polyt Qs	Detrital Feldspar Micr.	Orth.	Plag.	Rock Frag.	Opaqt	Micat	Chloritet Det.	P.F.	P.L.	Calcitet Cem.	Rep.	Port	Seolt	Overgrowth Qs	Feldt	Fract	Albt
	MM-3-18	47	2	21	-	-	-	15	4	-	-	-	-	-	-	-	-	-	2	9
	MM-3-17	40	4	20	-	-	1	20	2	-	1	-	-	-	2	-	-	-	1	10
	MM-3-16	24	17	30	-	1	1	-	4	-	1	-	-	-	1	-	-	-	9	12
	MM-3-15	42	2	31	-	2	4	1	1	-	1	-	-	-	-	4	-	-	1	11
	MM-3-14	38	6	31	-	5	-	9	5	-	1	-	-	-	-	3	-	-	-	2
	MM-3-13	31	5	26	-	2	-	8	8	-	-	-	-	-	-	2	-	-	-	18
	MM-3-12	35	2	26	-	4	-	-	-	-	-	-	-	-	-	5	1	-	18	9
	MM-3-11	30	1	31	-	1	-	-	4	-	-	-	-	-	1	5	15	-	2	11
3	MM-3-10	21	-	28	-	-	8	-	9	-	1	-	-	-	2	4	10	-	4	21
	MM-3-9	42	1	39	-	-	8	4	-	-	-	-	-	-	-	2	-	-	1	3
	MM-3-8	37	-	43	1	-	1	8	-	-	-	-	-	-	-	-	-	-	1	9
	MM-3-7	33	-	30	-	-	4	12	10	-	-	-	-	-	-	-	-	-	2	9
	MM-3-6	28	8	34	-	-	-	11	3	1	1	-	-	-	-	-	4	1	4	11
	MM-3-5	27	2	39	-	-	-	10	-	-	1	-	-	-	1	-	4	-	10	5
	MM-3-4	44	1	38	-	-	-	-	2	-	-	-	-	-	-	-	7	-	2	6
	MM-3-3	35	3	38	-	-	-	-	-	-	-	-	-	-	-	-	11	5	1	7
	MM-3-2	30	5	21	-	-	-	-	-	-	-	-	-	-	-	-	12	13	8	11
	MM-3-1	32	-	30	-	-	-	-	-	-	-	-	-	-	-	-	15	10	3	10
	MM-2-35	40	5	25	-	10	2	1	1	1	-	-	2	-	-	-	-	-	-	13
	MM-2-34	37	-	18	-	11	-	-	9	9	-	-	1	-	-	-	-	-	-	15
	MM-2-33	34	15	11	-	12	5	-	10	8	-	-	-	4	-	-	-	-	-	1
	MM-2-32	39	20	19	-	-	7	1	-	1	-	-	-	5	-	-	-	-	-	8
	MM-2-31	40	11	19	-	10	2	2	8	-	-	-	-	1	-	-	-	-	-	7
2	MM-2-30	39	24	18	-	6	4	1	-	-	-	-	-	1	2	-	-	-	-	5

Table 1 (cont'd.)

stop	Sample	Monot Qz	Polyt Qz	Detrital Feldspar			Rock Frag.	Opaqt	Micat	Chlorit			Calcit		Port	Scolt	Overgrowth		Fract	Albt
				Micr.	Orth.	Plag.				Det.	P.F.	P.L.	Cem.	Rep.			Qz	Feldt		
	MH-2-29	34	22	22	-	-	-	-	9	-	-	-	-	2	-	-	-	-	-	11
	MH-2-28	37	12	33	-	-	3	-	-	1	-	-	-	4	-	-	-	-	-	10
	MH-2-27	36	2	33	-	11	-	-	-	2	-	-	3	1	-	-	-	-	-	12
	MH-2-26	23	1	37	-	12	-	1	10	-	-	-	2	2	-	-	-	-	1	11
	MH-2-25	37	2	20	-	13	-	-	9	-	-	-	1	-	-	-	-	-	8	10
	MH-2-24	34	20	19	-	-	3	-	1	1	-	-	2	2	-	-	-	-	7	11
	MH-2-23	34	-	20	-	-	11	1	-	2	-	-	10	-	-	-	-	-	1	21
	MH-2-22	32	-	-	-	18	-	2	11	-	-	-	19	11	-	-	-	-	2	5
	MH-2-21	21	-	42	-	10	-	5	1	-	1	-	2	4	-	-	-	-	3	11
	MH-2-20	40	3	18	-	11	-	4	2	1	2	-	2	2	-	-	-	-	5	16
	MH-2-19	27	4	19	-	5	6	1	3	1	-	-	11	12	-	-	-	-	10	1
	MH-2-18	40	11	20	-	-	2	-	-	1	1	-	-	9	-	-	-	-	11	5
2	MH-2-17	38	12	40	-	10	3	10	-	8	-	-	-	8	-	-	-	-	1	8
	MH-2-16	34	10	19	-	4	3	-	1	8	-	-	1	7	-	-	-	-	4	9
	MH-2-15	38	12	22	-	5	-	6	4	-	-	-	1	-	-	-	-	-	2	10
	MH-2-14	30	20	18	-	13	-	-	9	-	-	-	6	1	-	-	-	-	1	11
	MH-2-13	38	7	20	-	11	8	8	9	-	-	-	4	1	-	-	-	-	1	1
	MH-2-12	42	11	2	-	7	-	-	8	-	-	-	20	-	-	-	-	-	1	1
	MH-2-11	45	9	-	-	18	2	-	10	-	1	-	11	2	-	-	-	-	-	2
	MH-2-10	47	4	-	-	29	-	-	-	-	2	-	9	2	-	-	-	-	1	6
	MH-2-9	25	28	4	-	20	-	-	11	-	-	-	8	1	-	-	-	-	1	2
	MH-2-8	35	2	29	-	14	1	1	-	-	-	-	5	1	-	-	-	-	2	11
	MH-2-7	30	9	11	-	-	15	1	-	9	-	-	4	-	-	-	-	-	2	19
	MH-2-6	34	-	14	-	10	-	-	-	8	-	-	4	8	-	-	-	-	4	18

Table 1 (cont'd.)

stop	sample	Monot Qz	Polyt Qz	Detrital Feldspar			Rockt Frag.	Opaqt	Micat	Chloritet			Calcitet		Port	Seolt	Overgrowth		Fract	Albt
				Micr.	Orth.	Plag.				Det.	P.F.	P.L.	Cem.	Rep.			Qz	Feldt		
	MH-2-5	38	1	2	-	17	-	-	-	10	-	-	7	9	-	-	-	-	3	13
	MH-2-4	47	3	12	-	10	1	-	11	1	-	-	1	-	-	3	-	-	-	11
2	MH-2-3	40	2	18	-	9	-	-	-	12	-	-	1	-	-	2	-	-	1	15
	MH-2-2	41	11	11	-	8	-	1	-	1	-	-	2	1	-	1	-	-	1	22
	MH-2-1	45	2	10	-	11	2	-	-	2	-	-	1	4	-	4	-	-	2	17
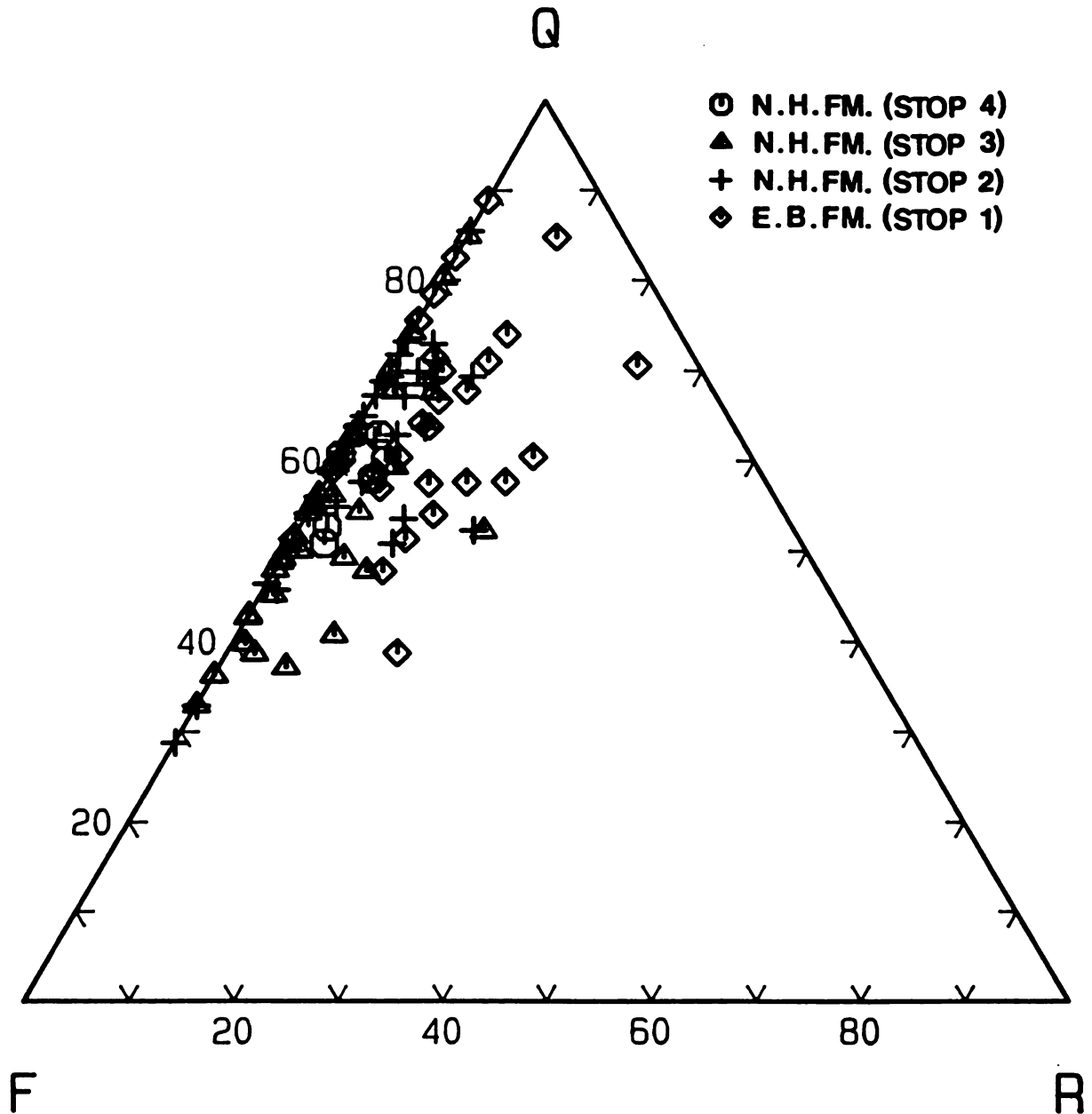
Figure 7a QFR ternary diagram illustrating the
sandstone composition of the New Haven
Arkose and the East Berlin Formation
(after Pettijohn et al., 1987).
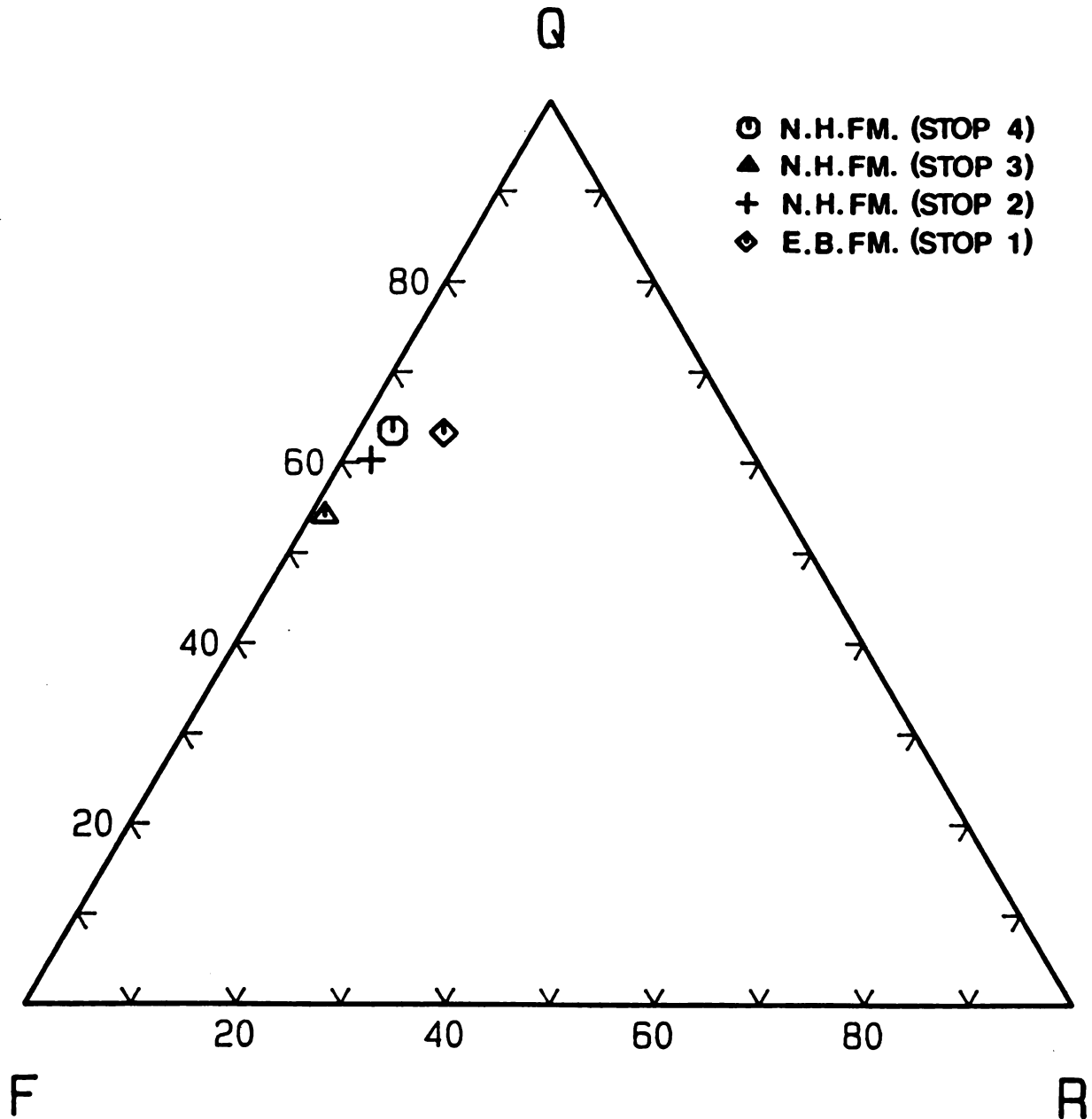
Figure 7b QFR ternary diagram of the mean values of
percent point counts of the different
stops.
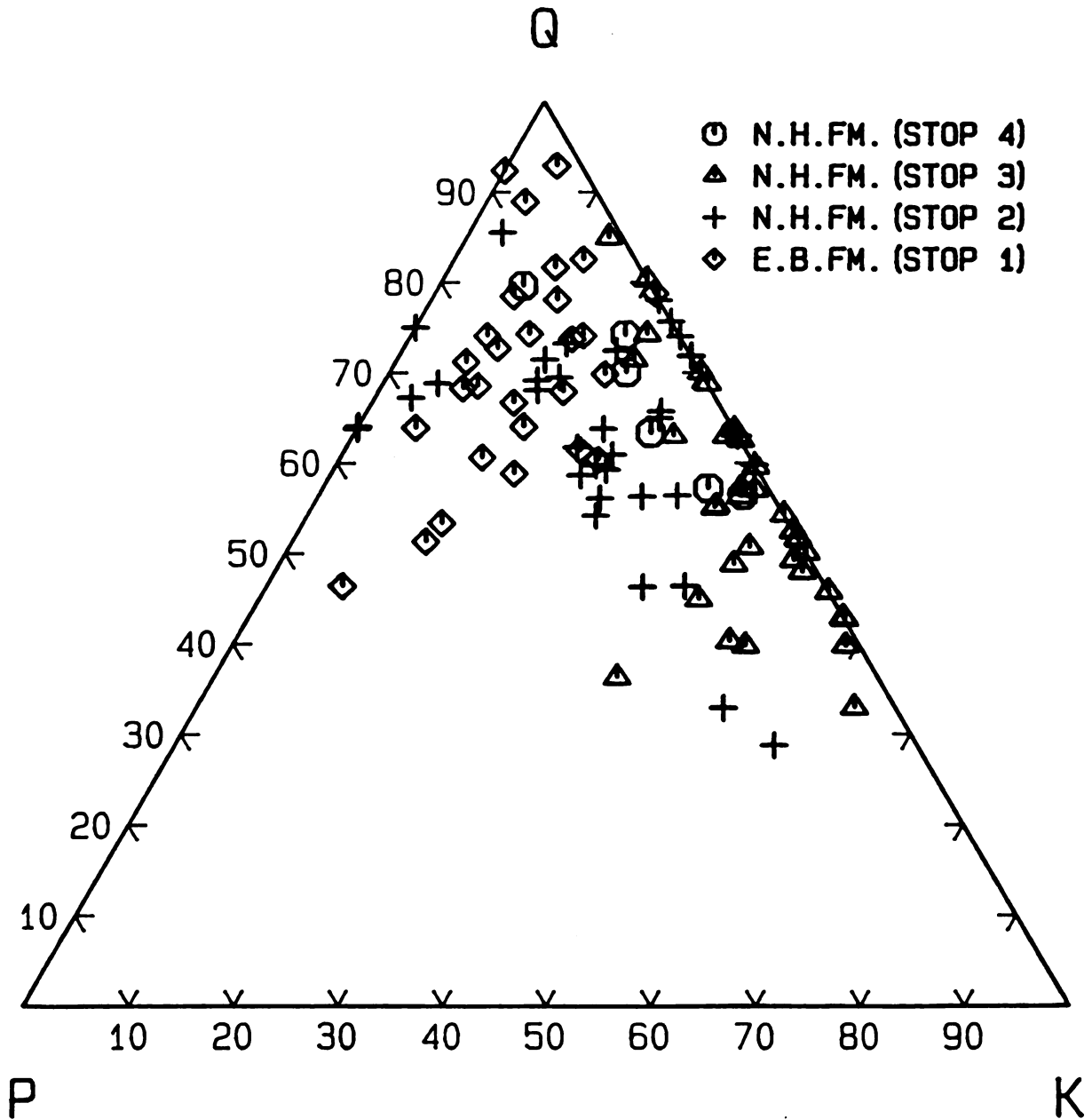
Figure 7c QPK ternary diagram of point count data
of the different stops.

grains within larger fragments to the category of the individual crystal or grain. The "traditional" method (QFR, in this study) assigns such sand sized crystals and grains to the category of the larger fragments. However, results of point counting of rock fragments by both methods (traditionally or by the Gazzi-Dickinson method) are expected to be similar in this study, as the Hartford Basin arkoses are low in their rock fragment content of finely crystalline rock fragments.

Stop 4

At this outcrop, representing the base of the rift-valley fill sequence, the New Haven Arkose unconformably overlies the Milford Chlorite Schist. The New Haven Arkose consists of poorly sorted arkosic sandstone and conglomerate cemented mainly by authigenic pore-filling chlorites. The conglomerates are pebble and cobble in size. The cobble fraction contains angular and blade-shaped fragments of epidotic phyllite derived from the underlying Milford Chlorite Schist (Klein, 1969). Accessory cobbles of rounded, milky quartz also occur. The pebble fraction consists almost exclusively of rounded fragments of orthoclase and microcline, milky quartz, and granite pegmatite. The pebbles show better rounding than the cobbles; they are disc-shaped and spheroidal (Figure 8).

The sandstones are green, coarse- to very coarse-grained, angular, poorly-sorted, arkosic and epidotic. Sizes range

Figure 8. Pebble and cobble conglomerate in epidotic arkosic sandstone matrix of stop 4 of the New Haven Arkose. Notice the unconformity surface between Paleozoic Milford chlorite schist and Upper Triassic New Haven Arkose basal conglomerate.

from 0.6 to 1.4mm. The sandstones contain about 35% monocrystalline quartz, 6% polycrystalline quartz, 15% microcline, 2% orthoclase, 4% plagioclase, 2% rock fragments, 9% opaque minerals and epidote, and 19% chlorite cement (Table 1). The sandstone is cemented by pore-filling and pore-lining chlorites (Figure 9).

Fracturing of feldspars is prominent in all specimens. Fractures in microcline and plagioclase are filled with late diagenetic hematite-stained chlorite, sericite, and minor amounts of calcite cement (Figures 10 and 11). Deformed mica (Figure 12) suggests compaction due to burial of the New Haven Arkose. Quartz-overgrowth is more common than feldspar-overgrowth. The growths are small, euhedral, and clear rims (Figure 13). SEM shows pyramidally terminated quartz overgrowths on detrital quartz grains (Figure 14). A double hematite line is observed in some of the overgrowths (Figure 15). Partially altered metamorphic rock fragments are noted.

Albitization of feldspars, particularly microcline, is prominent in the lower part of the section. Under the optical microscope albitized feldspar grains are characteristically untwinned and mostly riddled with abundant minute brownish inclusions (Figure 16).

Stop 3

The New Haven Arkose exposed in this abandoned quarry (currently the Hamden dump) consists of sandstones with siltstone interbeds. The sandstones are coarse- to medium-
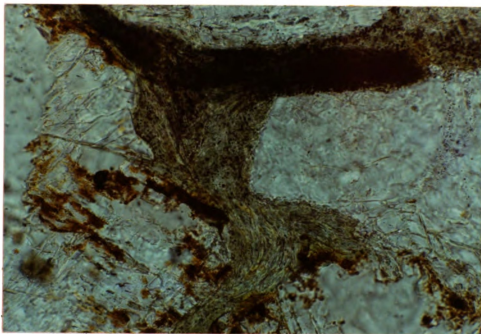
Figure 9. Photomicrograph of pore-lining chlorite.
Notice hematite coating of detrital
quartz and absence of chlorite at grain
contacts. Sample # NH-4-6.
(Frame dimensions: 0.4 mm x 0.6 mm)
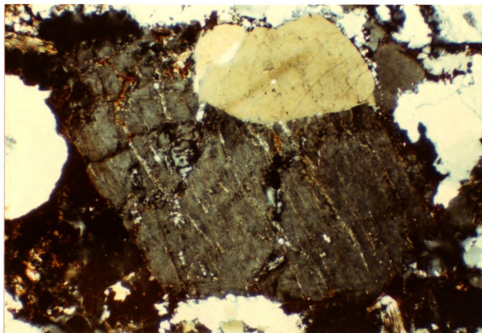
Figure 10 Fractured potash feldspar filled with
hematite-stained clay. Sample # NH-4-5.
(Frame dimensions: 2.5 mm x 3.8 mm)
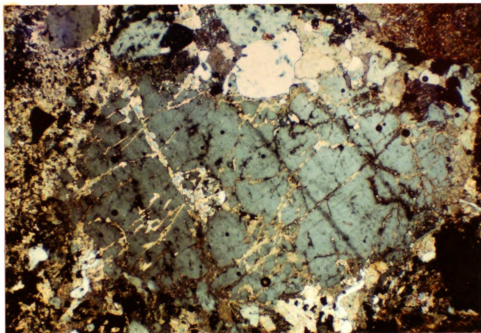
Figure 11 Minor calcite cement filling fractured feldspar. Notice the optical continuity between fracture and pore-filling calcite. Sample # NH-4-3. (Frame dimensions: 2.5 mm x 3.8 mm)
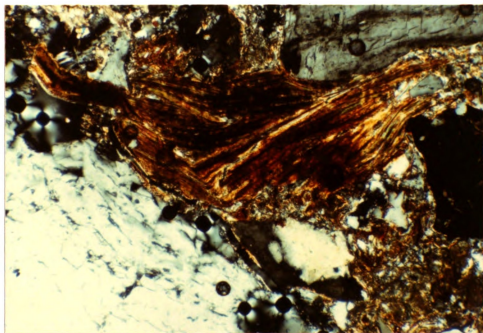
Figure 12 Deformed mica (biotite) during compaction of early cementing material. Sample # NH-4-5. (Frame dim.: 1.0 mm x 1.5 mm)
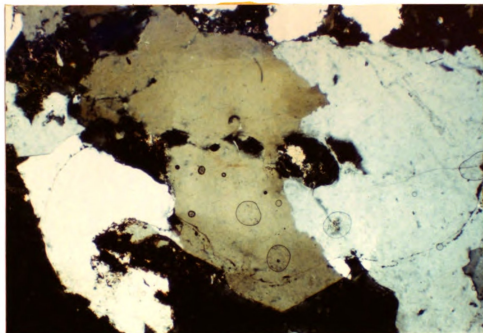
Figure 13 Clear euhedral quartz overgrowths rim
detrital quartz grains. Sample # NH-4-3.
(Frame dim.: 2.5 mm x 3.8 mm)
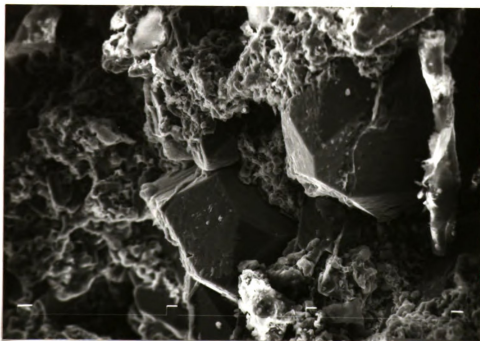
Figure 14 SEM photomicrograph of pyramidally
terminated quartz overgrowths. Sample #
NH-4-5.

Fi

Fi
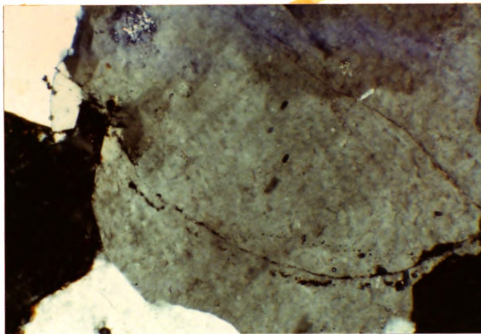
Figure 15 Double hematite line outlines the boundary between the quartz-overgrowth and the detrital quartz grain. Sample # NH-4-3. (Frame Dim.: 1.0 mm x 1.5 mm)
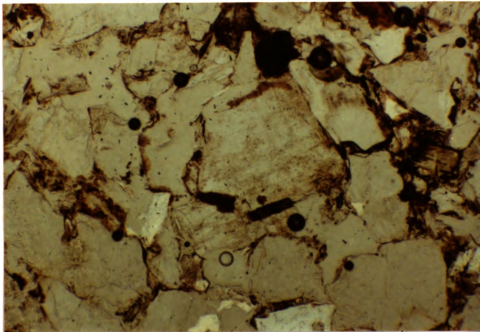
Figure 16 Photomicrograph of partly albitized K-feldspar riddled with abundant minute inclusions. Sample # NH-3-16. (Frame dim.: 2.5 mm x 3.8 mm)

grained, angular to subangular, poorly sorted, pebbly and arkosic. Grain size ranges from 0.3 to 0.7mm. Pebbles of milky quartz, granite, schist and gneiss rock fragments are scattered throughout the sandstones.

The sandstones consist of about 36% monocrystalline quartz, 4% polycrystalline quartz, 30% microcline, 2% plagioclase, 3% mica (biotite and muscovite), 1% zeolite cement, and 4% hematite-stained chlorite matrix (Table 1).

Fracturing and albitization of potash feldspar are common (Chapter 5). Minor feldspar- and quartz-overgrowth are restricted to samples near the base of the section (Figure 17a). SEM examination shows small euhedral overgrowths partly covering a detrital feldspar grain (Figure 17b). A complex assemblage of clay minerals including sericite, chlorite, and illite represents the main type of cement in these sandstones (Figure 18). Local pore-lining and pore-filling chlorites (Chapter 6) and illites or mixed-layer illite-smectites were observed in these samples (Figure 19). A minor amount of calcite is present in these arkoses, but most of it occurs as a replacement of detrital feldspar grains rather than as an interstitial cement.

Thin-sections show that zeolite, mainly laumontite (from XRD analysis; Chapter 7), is optically clear to light yellow in color, low birefringence, with well developed cleavage and undulatory extinction. It occurs as pore-filling cement and partly replaces the feldspar (Figure 20). Laumontite has been found only in samples NH-3-9 through NH-3-15 in the lower
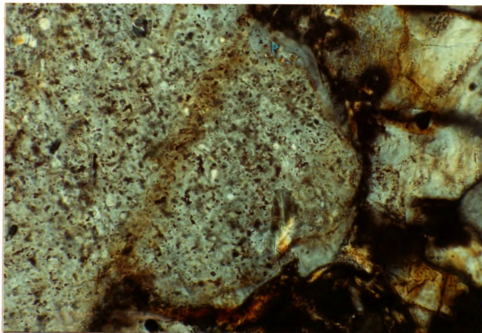
Figure 17a   Clear feldspar overgrowths rim
              detrital core filled with
              inclusions.   Sample # NH-3-3.
              (Frame dim.: 0.16 mm x 0.24 mm)
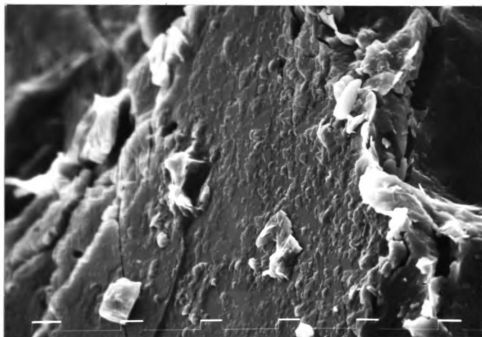
(A)
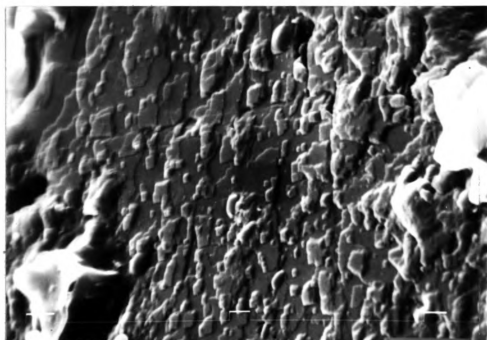
(B)

Figure 17b   SEM photomicrograph of detrital K-feldspar (a) grain rimmed with small, jagged overgrowths. (B) is a close-up of these small (2-10 μm) euhedral overgrowths. Sample # NH-3-11. Tic mark = 10 μm.
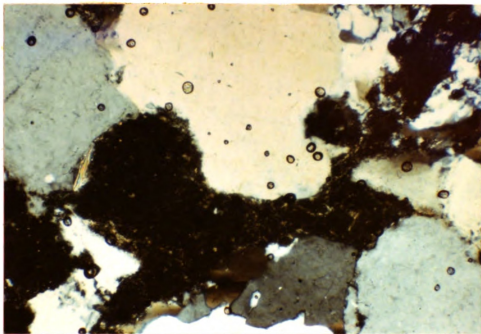
Figure 18 Complex assemblage of sericite, illite and chlorite pore-fillings. sample # NH-3-22. (Frame dim.: 1.0 mm x 1.5 mm)
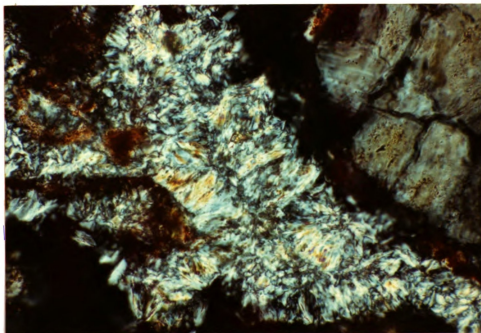
Figure 19 Radial authigenic pore-lining clay (illite-smectite ?) crust. Sample # NH-3-1. (Frame dim.: 0.4 mm x 0.6 mm)
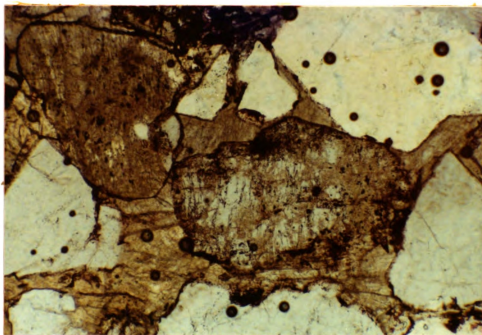
(A)
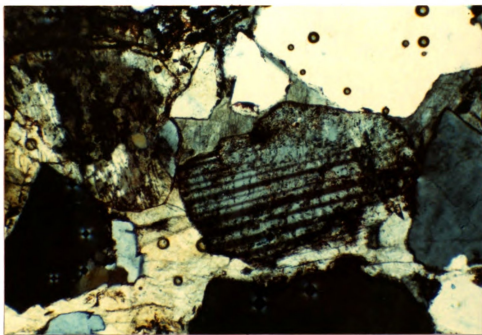
(B)

Figure 20 A) Laumontite as a pore-filling and
replacement (arrows) of plagioclase
feldspar. B) is a cross polar of A.
Sample # NH-3-10.
(Frame dim.: 1.0 mm x 1.5 mm)

part of the section. Considerable zeolite occurs in the arkoses in Hampden and northern New Haven but is uncommon in other areas (Heald, 1956).

Stop 2

The New Haven Arkose exposed at this outcrop consists of medium- to coarse-grained, angular to subangular, poorly sorted, pebbly, arkosic pale red sandstone and conglomerates with red sandy mudstone interbeds. They range in size between 0.4 and 0.6mm.

This arkose contains an average of about 36% monocrystalline quartz, 8% polycrystalline quartz, 17% microcline, 10% plagioclase, 1% opaques (mainly hematite cement), 4% muscovite and biotite, and 2% detrital chlorite (Table 1).

Albitization of potassium feldspars (Chapter 5) as well as fracturing of feldspars are prominent in most of the samples, but diminish near the top of the section.

Multiple generations of calcite occur as an interstitial filling, fracture filling, and as a replacement of feldspars (Figure 21). Feldspars were partially or completely replaced by calcite, as indicated by a ring of hematite within the calcite (Figure 22). In some specimens a few grains are completely replaced and the remaining grains are unaltered. Pervasive calcite cements were observed in the arkoses of this stop, whereas no calcite cement was observed at the other stops of the New Haven Arkose. The calcite is undeformed; yet
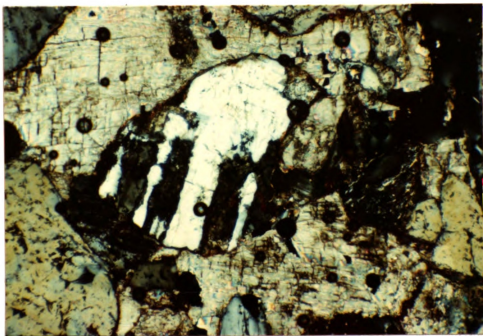
Figure 21 Calcite replacement along twinning planes
of plagioclase feldspar. Notice the
pore-filling calcite cement. Sample #
NH-2-14. (Frame dim.: 1.0 mm x 1.5 mm)
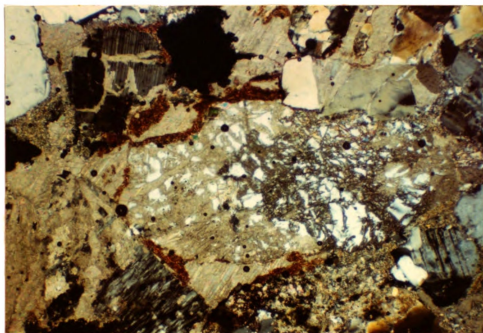
Figure 22 Calcite pseudomorph (P) with ring of hematite which represents the original coatings on the replaced feldspar grain. Sample # NH-2-19. (Frame dim.: 2.5 mm x 3.8 mm)
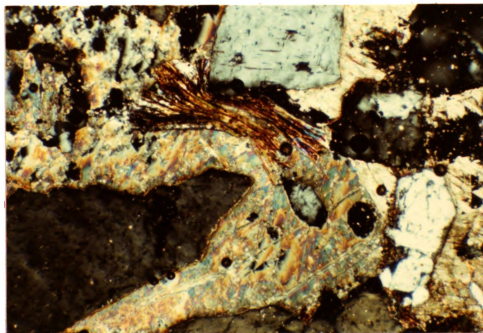
Figure 23 Deformed mica (biotite) surrounded by pore-filling calcite cement. Sample # NH-2-14. (Frame dim.: 1.0 mm x 1.5 mm)

surrounds bent mica and fractured feldspars (Figure 23).

Light-green pleochroic detrital chlorite occurs in many arkoses, particularly abundant in specimens near the bottom of the section. Minor amounts of authigenic pore-filling chlorites are present in most of the samples. No quartz- or feldspar-overgrowths have been recorded in the arkoses of this outcrop.

Laumontite was detected in only four samples (NH-2-1 through NH-2-4) near the base of the section. Similar to stop 3, laumontite is present as a pore-filling cement and partially replaces detrital feldspar.

EAST BERLIN FORMATION

The fluvial and lacustrine sandstones of the East Berlin Formation (stop 1) are arkoses (Figure 7a). The proportion of quartz and feldspar among the grains are similar in both environments, as are the authigenic mineral cements and their proportions.

Stop 1

The East Berlin sandstones are medium- to coarse-grained, angular to subangular, moderately to poorly sorted arkoses. Their size ranges between 0.35 and 0.55mm. They consist of about 31% quartz, 8% plagioclase, 6% microcline, 12% calcite cement, 17% hematite-stained clay matrix, 8% dolomite, 6% muscovite and biotite (Table 2).

Table 2. Petrographic point counts of the East Berlin Formation.

Stop	Sample	Totalt Qz	Dolt Qz	Detrital Feldspar Micr.	Orth.	Plag.	Rock Frag.	Opaqt	Mica	Chlorite Det.	G.C.	P.L.	Calcite Cem.	Rep.	Port	P.S.t	Overgrowth Qz	Feld	Fract	Albt
	EB-1-28	42	-	4	-	13	4	17	11	8	-	-	9	-	-	-	-	-	-	2
	EB-1-27	40	-	9	-	17	3	2	1	-	-	-	8	-	-	-	-	-	-	-
	EB-1-26	41	-	17	-	10	4	21	2	-	-	-	4	-	-	-	-	-	-	1
	EB-1-25	32	-	8	-	10	3	4	-	-	4	22	12	-	-	-	1	-	-	4
	EB-1-24	20	27	2	-	5	1	14	12	2	1	-	16	-	-	-	-	-	-	-
	EB-1-23	24	20	1	-	2	-	38	-	5	-	-	10	-	-	-	-	-	-	-
	EB-1-22	37	10	-	2	-	20	20	5	-	-	10	-	-	-	-	-	4	-	1
	EB-1-21	20	25	6	-	8	-	22	11	-	-	-	8	-	-	-	-	-	-	-
	EB-1-20	27	33	10	-	7	2	1	-	1	-	-	19	1	-	-	-	-	-	-
	EB-1-19	12	33	-	-	1	4	12	23	-	-	-	14	-	-	-	-	-	-	1
	EB-1-18	14	29	3	-	2	1	30	9	-	-	-	11	-	-	-	-	-	-	-
	EB-1-17	19	10	3	-	19	8	15	-	-	4	-	22	-	-	-	-	-	-	2
	EB-1-16	40	1	4	-	7	-	22	14	-	-	-	10	-	-	-	-	-	-	-
	EB-1-15	33	9	5	-	2	-	33	10	-	-	-	4	4	4	-	-	-	-	-
	EB-1-14	34	7	7	-	10	8	12	-	3	1	-	15	2	-	-	-	-	-	1
	EB-1-13	37	1	5	-	12	4	20	-	-	-	16	-	-	-	-	-	-	-	2
	EB-1-12	26	1	4	-	5	8	11	-	-	3	-	-	20	1	14	-	3	-	4
	EB-1-11	23	3	2	-	11	4	5	18	-	4	-	11	4	-	11	-	2	-	2
	EB-1-10	20	1	5	-	14	-	20	-	8	4	-	22	2	-	5	1	-	-	1
	EB-1-9	32	-	5	-	4	4	17	-	3	1	-	8	5	-	10	-	1	-	2
	EB-1-8	39	-	2	-	1	4	16	11	3	1	-	9	9	-	-	-	5	-	-
	EB-1-7	38	-	10	-	8	8	25	-	-	-	-	11	-	-	-	-	-	-	-
1	EB-1-6	43	4	5	-	15	4	14	-	-	-	-	15	-	-	-	-	-	-	-
	EB-1-5	40	3	5	-	4	5	18	21	-	-	-	4	-	-	-	-	-	-	-

Table 2 (cont'd.)

stop	sample	Total Qz	Polt Qz	Detrital Feldspar			Rock Frag.	Opaqt	Mica	Chlorite			Calcite		Port	P.S.t	Overgrowth		Fract	Albt
				Micr.	Orth.	Plag.				Det.	G.C.	P.L.	Cem.	Rep.			Qz	Feldt		
	EB-1-4	30	2	9	-	4	9	16	10	-	-	-	20	-	-	-	-	-	-	-
	EB-1-3	40	6	9	-	5	5	14	11	-	-	-	10	-	-	-	-	-	-	-
	EB-1-2	32	-	8	-	20	7	22	-	-	-	-	9	-	-	-	-	-	-	2
1	EB-1-1	40	-	5	-	10	9	20	1	5	-	-	2	4	-	-	2	-	-	2

In the fluvial pale red sandstones, quartz overgrowths are less common than albite overgrowths. Both overgrowths are superposed on hematite-stained clay that rims the detrital grains (Figure 24). The hematite formed by post-depositional aging of limonite (Hubert and Reed, 1978). In the lacustrine gray sandstone, the quartz and albite cements are superposed on clay rims unstained by hematite, because limonite was dissolved in the reducing lake water, evidently as organic-ferrous iron complexes (Hubert and Reed, 1978).

Calcite is more common as cement than as replacement of feldspars. Dolomite cements are confined to the lacustrine cycle. It is believed that the dolomite was precipitated by partial evaporation of the perennial lake (Hubert et al., 1978).

Few samples, near the base of the section, show evidence of pressure solution. Conspicuously sutured grain contacts (Figure 25) and closely spaced microstylolite seams are prevalent (Figure 26). This indicates that mechanical compaction has initiated quartz pressure solution (Adams, 1964; Pettijohn et al., 1987). Pressure solution diminished considerably near the contact with the overlying Hampden Basalt, but was relatively high near the underlying Holyoke Basalt (Heald, 1956). Compared with the fractured grains of the New Haven Arkose, the absence of fracturing of framework grains in the sandstones of the East Berlin Formation is overwhelming. This may be due to the high abundance of
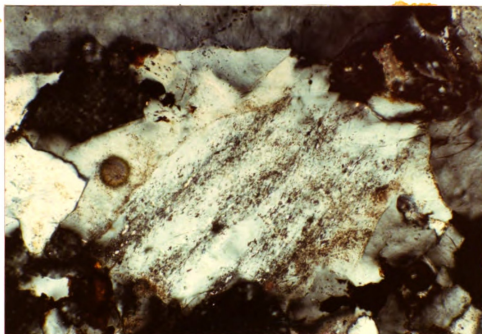
Figure 24 Hematite-stained clay (H) coats detrital feldspar in fluvial sandstone of the East Berlin Formation. Sample # EB-1-10. (Frame dim.: 0.4 mm x 0.6 mm)
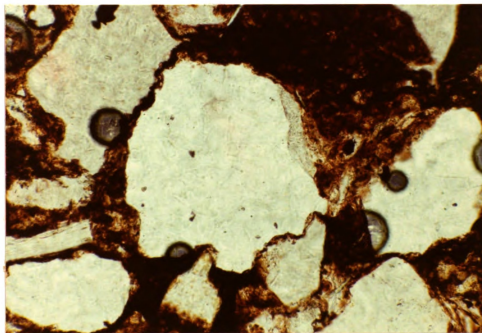
Figure 25 Sutured contact between quartz grains caused by pressure solution. Sample # EB-1-10. (Frame dim.: 0.4 mm x 0.6 mm)
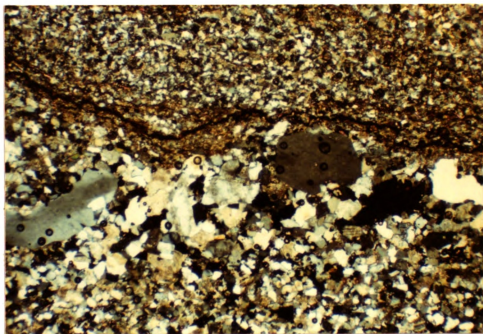
Figure 26 A microstylolitic solution seam near
contact surface between coarse- and fine-
grained sandstone in the East Berlin
Formation. Sample # EB-1-11.
(Frame dim.: 2.5 mm x 3.8 mm)

hematite-stained clay that minimizes the effect of mechanical compaction on the quartz and feldspar grains as they are floating in the clay.

A different variety of zeolite, analcime, is also present in two gray mudstone samples (EB-1-25 and -26). The presence of analcime was initially established by XRD, however, analcime could not subsequently be identified in thin-section or with the aid of the SEM. A detailed discussion of zeolites will be addressed in chapter 7.

DISTRIBUTION AND GENESIS OF THE BULK ROCK MINERALOGY

The variety of major minerals is limited in the sedimentary sequences of Connecticut Valley. Ubiquitous occurrences of quartz, most of which is detrital, were observed in the different stops. To a lesser extent, quartz occurs as one of a number of authigenic cements, forming overgrowths on detrital quartz grains.

Feldspar is the second most abundant mineral observed in these rocks. It occurs in all samples but samples collected from the caliche red mudstones of the New Haven Arkose (stop 2). Plagioclase and microcline are the most abundant feldspars, occurring as detrital grains. Syntaxial authigenic plagioclase overgrowths are common among the New Haven Arkose rocks. April (1978), after Reed (1976), reported that the range in compositions of detrital plagioclase grains in the East Berlin Formation is An_0 to An_{29} while authigenic overgrowths are nearly pure albite. Detrital orthoclase

appears more frequently in the lacustrine deposits of the East Berlin Formation, but is not restricted to these rocks.

Calcite and dolomite are the major carbonate minerals observed in the Hartford basin's rocks. Both are primary cementing agents, yet dolomite occurs also as concretions and isolated rhombs. Dolomite is restricted to the East Berlin Formation, and was not observed in the New Haven Arkose. Both minerals occur together in fewer than 28% of the East Berlin formation samples. On the other hand, calcite cement occurs in both formations, but is more abundant in the New Haven Arkose. Apparently, during and after deposition of the sediments in New Haven time (Late Triassic), the sedimentary environment remained deficient in magnesium such that dolomitization did not take place. This is unlike the condition reported by Hubert et al, (1976, 1978) for the Lower Jurassic East Berlin Formation in which calcite and Mg-calcite were extensively dolomitized early after burial by magnesium-rich pore waters. The abundance of calcite in the New Haven results in part from the numerous caliche paleosol horizons reported by Hubert (1977) and Hubert et al., (1978). They attributed the development of these horizons to semi-arid climatic conditions and to an influx of Ca^{++} from weathering in the source area and possibly from $CaCO_3$ dust derived from Lower Paleozoic carbonate rocks to the west.

Hematite occurs pervasively as coatings or stains on detrital grains in the red beds of all formations. It is easily identifiable in thin sections as the source of the red

color in most samples. Hubert and Reed's (1978) four suggested modes of origin for hematite in the East Berlin Formation were summarized in chapter 1.

Authigenic pyrite, in cubic and framboidal form, occurs only in the black shale and lacustrine gray mudstone and siltstone of the East Berlin Formation. Hubert et al., (1976) point out that reducing conditions must have been present during deposition of the lacustrine black shale and gray beds for authigenic pyrite to form. H_2S, derived from the decomposition of organic matter, combined with ferrous iron brought into solution by the reduction of detrital iron oxide-hydroxide grain coatings. The high organic content, color and undisturbed carbonate laminae of both rock types as well as the presence of unaltered magnetite grains (Hubert and Reed, 1978) and abundant articulated fish fossils in the black shales (Hubert et al., 1978) are further evidence for reducing anoxic sulphidic conditions (Berner, 1981) during and after sediment deposition.

Laumontite occurs only in about 40% of the New Haven Arkose samples at stop 3 and 11% at stop 2, but no laumontite was observed in stop 4. The presence of laumontite in stop 3 and 2 was initially established by thin section petrography, and confirmed by XRD, SEM and EDS. Heald (1956) reported the presence of laumontite in some samples of the New Haven Arkose in Hamden and northern New Haven, Connecticut. He noted that laumontite fills pore spaces and partly replaces the feldspar, especially potash-feldspars, in contact zones near intrusives.

The fact that laumontite occupies cracks in fractured detrital grains and surrounds deformed mica indicates that it formed after at least initial compaction of the sediments (Heald, 1956). Although laumontite may result from alteration of original feldspar in sediments (Hay, 1966), part of the material for the laumontite in the Triassic may have been introduced because much of it occurs as interstitial filling. The introduced material may be of igneous origin, for laumontite is present in some of the diabases and in the contact zone at Pine Rock in Hampden, Connecticut (Heald, 1956).

April (1978) reported the presence of analcime in the gray mudstone and black shale of the East Berlin Formation. In this study analcime occurs in only two (about 7%) of the twenty-eight samples of the East Berlin Formation. It was only detected by XRD, as it could not be identified in thin section or with the aid of SEM. This suggests that analcime exists as a well dispersed cement and may have formed as a direct precipitate from concentrated alkaline solutions or as a syngenetic alteration product of a zeolite or clay mineral precursor (Hay, 1966). In either case, its presence in the gray mudstones indicates a depositional or early diagenetic sedimentary environment influenced by sodium-rich alkaline solutions (Iijima and Utada, 1966).

Muscovite occur as flakes visible in hand specimen and usually along with chlorite constitutes the bulk of the matrix surrounding detrital grains in most of the red siltstones and

sandstones.

Brown biotite flakes occur in between detrital framework grains. Partial to nearly complete oxidized biotite (dark reddish brown), sometimes bent due to compactional deformation are also noted. Intrastratal solution of Fe-silicate grains (biotite) was pervasive in the fluvial and lacustrine sandstones and believed to be the source of iron for hematite (Hubert and Reed, 1978).

Sedimentary and metasedimentary lithic fragments, including chert, quartzite and schist, are the main rock fragment types in the Hartford Basin sandstone. Some fragments show partial alteration to clay minerals (smectite ?) and calcite replacement. The composition of the rock fragments reflect partial derivation from sedimentary cover or metamorphic envelopes that partly mask or shield basement gneiss and granites.

PROVENANCE AND EVOLUTION OF THE ARKOSIC SANDSTONES

Sandstone provenance refers to the group of factors that influenced the sand production in its source area (Pettijohn et al., 1987). Sandstone compositions are influenced by the character of sedimentary provenance, the nature of the sedimentary processes within the depositional basin, and the kind of dispersal paths that link provenance to basin that are governed by plate tectonics (Dickinson and Suczek, 1979). Therefore, plate tectonics ultimately controls the distribution of the different types of sandstones.

Krynine (1950) believed that the necessary condition for production of arkosic sands was high relief with consequent rapid erosion rather than unfavorable climatic conditions. Distinguishing between these possibilities in an ancient arkose is difficult, but on the whole, it seems more likely that high relief is more important than rigorous climate in arkose formation (Pettijohn et al., 1987).

Dickinson and Suczek (1979) found that the detrital framework modes of sandstone suites from different kinds of basins are a function of provenance types governed by plate tectonics. They utilized triangular diagrams that show that framework proportions of quartz, the two feldspars (plagioclase and K-feldspar), polycrystalline quartzose lithics, and unstable volcanic and sedimentary lithic fragments successfully distinguish the key provenance types. In this study, the main detrital framework components (quartz, feldspars, and rock fragments) were plotted on a QFR ternary diagram (Figure 7a) and then compared to Dickinson and Suczek's diagrams. The comparison shows clearly that the detrital arkosic Hartford Basin sandstones were derived from the continental block (uplifted basement) provenance. Sands shed by rapid erosion from fault-bounded uplifts of pre-Triassic continental basement rocks accumulated in the nearby Hartford Basin without much transport, giving rise typically to quartzo-feldspathic sands of arkosic character. The percent-average QFR diagram (Figure 7b) shows that the composition of the East Berlin and the New Haven arkoses are

very similar with a slight increase in the rock fragment (sedimentary and metamorphic) content in the East Berlin Formation. QPK plot (Figure 7c) shows a high concentration of points in the direction of quartzose end which reflects increasing maturity or stability for detritus derived from continental block provence (Dickinson and Suczek, 1979).

Several studies discussed the relation between sand composition and paleoclimate (Mack and Suttner, 1977; Walker, 1978). These studies used thin-section petrography in order to compare the abundance of unstable constituents (feldspars and rock fragments) in ancient and modern sands under different paleoclimates. As mentioned in chapter 1, the Late Triassic climate was warm and dry, changing in Early Jurassic time to relatively cooler and probably wetter conditions (Hubert et al., 1978, Suchecki et al., 1988). Velbel and Saad (1991) studied the Triassic Chatham Group sandstones of the Deep River basin (another Mesozoic rift-valley; #1 in figure 1), North Carolina, where the ancient sediments were produced under more arid conditions than the modern wet climate. They found that these subarkose to sublitharenite sediments have higher unstable grain contents ($Q_{50-90}F_{0-50}L_{0-50}$) than modern sands derived from similar source rocks but under a humid climate. This indicates that weathering is more important than diagenesis in determining the modal framework composition of the Chatham Group sandstones, as diagenesis tends to destroy unstable rock fragments, whereas weathering under arid climate causes preservation of rock fragments in the absence of

diagenetic effects. Compaction and cementation, without extensive replacement of the framework grains, were the main diagenetic signature in the Chatham Group sandstones. In contrast, in the Hartford Basin, unstable detrital framework grain abundances were modified by intense diagenetic processes, especially replacement of detrital grains by different authigenic minerals. Velbel and Saad (1991) concluded that diagenesis did not destroy lithic fragments in the Chatham Group. Rock fragments were modified by diagenesis in the Hartford Basin. This might explain the lower unstable grain contents ($Q_{40-90}F_{5-45}L_{0-20}$) in the sediments of the Hartford Basin than those of the Chatham Group sandstones. However, a more likely explanation for the difference in the lithic fragment content between the Chatham Group and the Hartford Basin sediments is probably due to differences in the source rock of both basins. The Chatham group sublitharenites-subarkoses were derived from pre-Triassic metamorphic rocks of the adjacent Appalachian Piedmont (McCarn and Mansfield, 1986), whereas the source of the arkoses of the Hartford Basin is the uplifted pre-Triassic crystalline basement rocks. This suggests that detailed study of early diagenetic minerals in addition to detrital minerals, is helpful for reconstructing paleoclimatic conditions, along with studies of the framework grain response to the various factors affecting these sediments.

PARAGENETIC SEQUENCE OF THE HARTFORD BASIN SANDSTONES

The paragenetic sequence in the basin's sandstones varies stratigraphically from the New Haven Arkose to the East Berlin Formation. It varies slightly within the New Haven Arkose from one stop to another. Figures 27-30 summarize the diagenetic sequence in the four stops based on the relative timing of the precipitation of authigenic material after deposition as evident from the petrographic examination.

In general, the paragenetic sequence in both formations begins with mechanical compaction of the sediments. Compaction in the New Haven Arkose was much more extensive than in the East Berlin Formation as evident by the absence of fracturing of detrital grains in the latter. The greater amount of compaction in the New Haven Arkose is related to additional sediment deposition on this formation as it was buried deeper than the East Berlin Formation. Hematite coatings formed after compaction as evident by coating all detrital grains and along their contacts. Hematite precipitation continued after quartz-overgrowth as evident by the presence of double hematite lines (Figure 15).

Formation of chlorite grain coatings (stop 1) and pore-linings (stop 4) took place after the hematite coating as hematite separates detrital grains from chlorite cement. The highest chlorite content was seen in the New Haven Formation (stop 4).

Authigenic syntaxial feldspar and quartz overgrowths were formed after the coatings. In most samples the overgrowths

PARAGENESIS OF THE NEW HAVEN ARKOSE (STOP 4)

	OLD		YOUNG
Compaction	├────────────┤		
Fractures	├────────────┤		
Hematite coating	├────────────┤		
Pore-lining chlorite	├────────────┤		
Pore-filling chlorite			├────────────┤
Quartz overgrowth		├────────────┤	
Albitization		├────────────┤	
Clay minerals (illite)		├──────── ─ ─ ─ ─?	
Calcite replacement and cement	├──────────────── ─ ─ ─ ─ ─ ─ ─ ─ ─?		
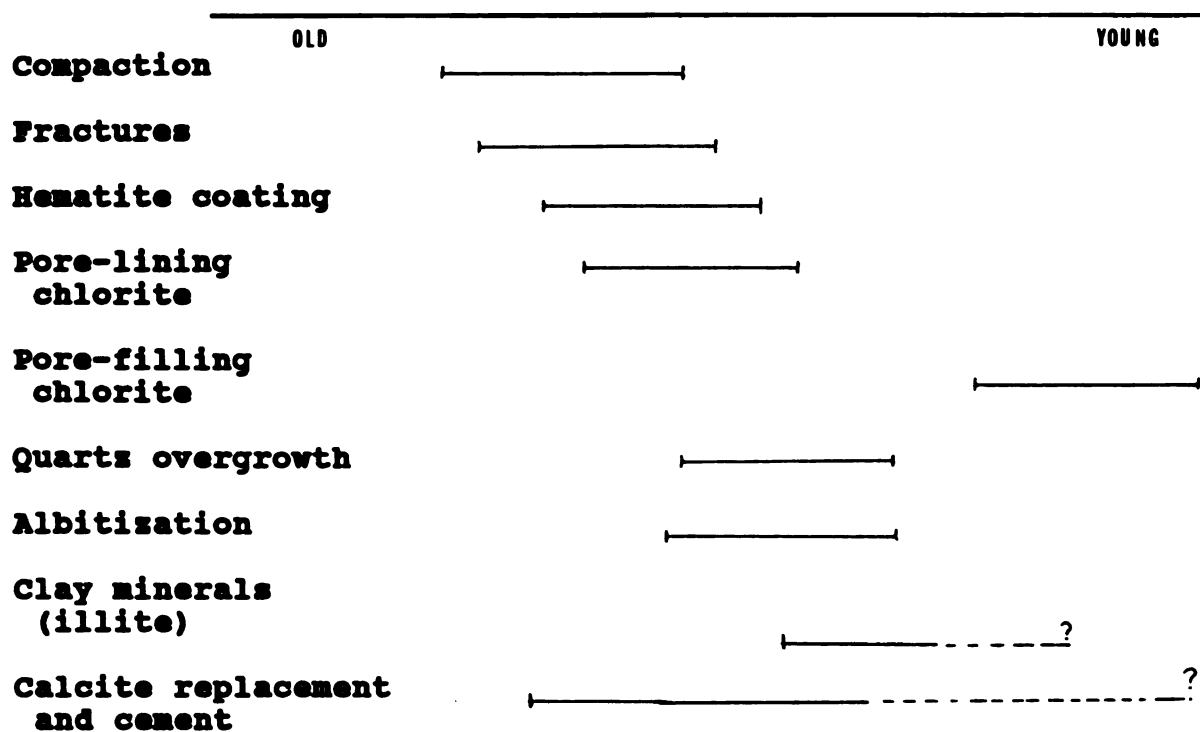
Figure 27 Summary of the paragenetic sequence in
the New Haven Arkose (stop 4)

PARAGENESIS OF THE NEW HAVEN ARKOSE (STOP 3)

	OLD		YOUNG

Compaction   ├───────────┤

Fractures   ├───────────┤

Chlorite pore-   ├──?....
  filling (minor)

Hematite coating   ├─────────┤

Quartz overgrowth   ├──────────────┤

Feldspar overgrowth   ├────────────┤

Albitization   ├──────────┤

Sericite?   ├─────────┤

Clay minerals   ├─────────┤
  (illite/sm.?)

Zeolite   ├───────...?
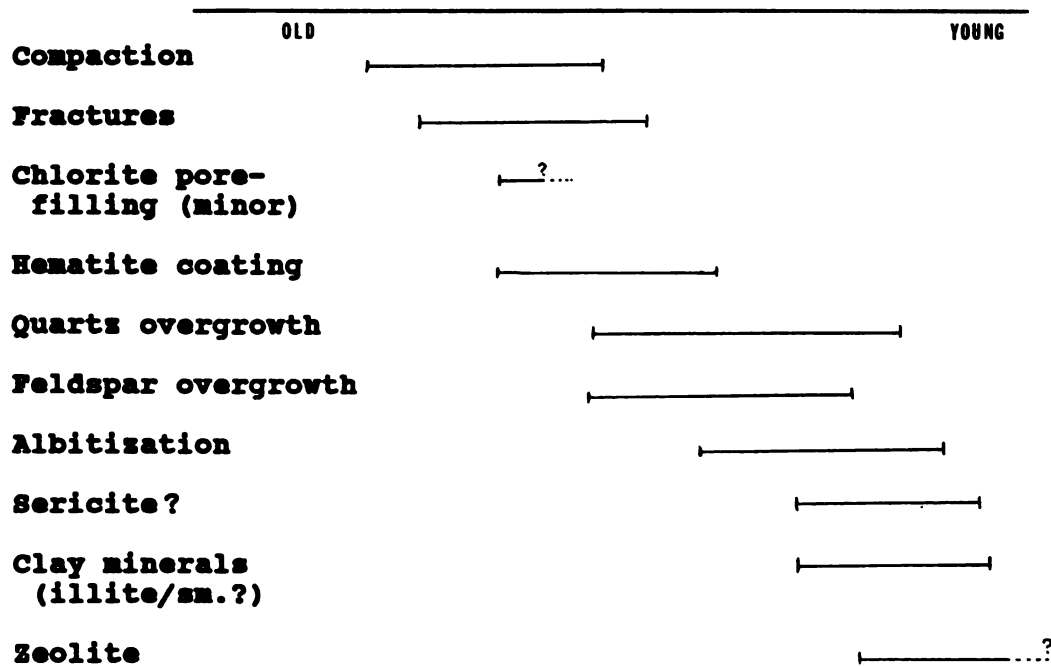
Figure 28 Summary of the paragenetic sequence in
         the New Haven Arkose (stop 3)

PARAGENESIS OF THE NEW HAVEN ARKOSE (STOP 2)

	OLD		YOUNG

Compaction

Fractures

Hematite coating

Chlorite pore-
  filling

Albitisation

Sericite?

Clay minerals
  (illite/sm.?)

Calcite replacement
and cement

Zeolite
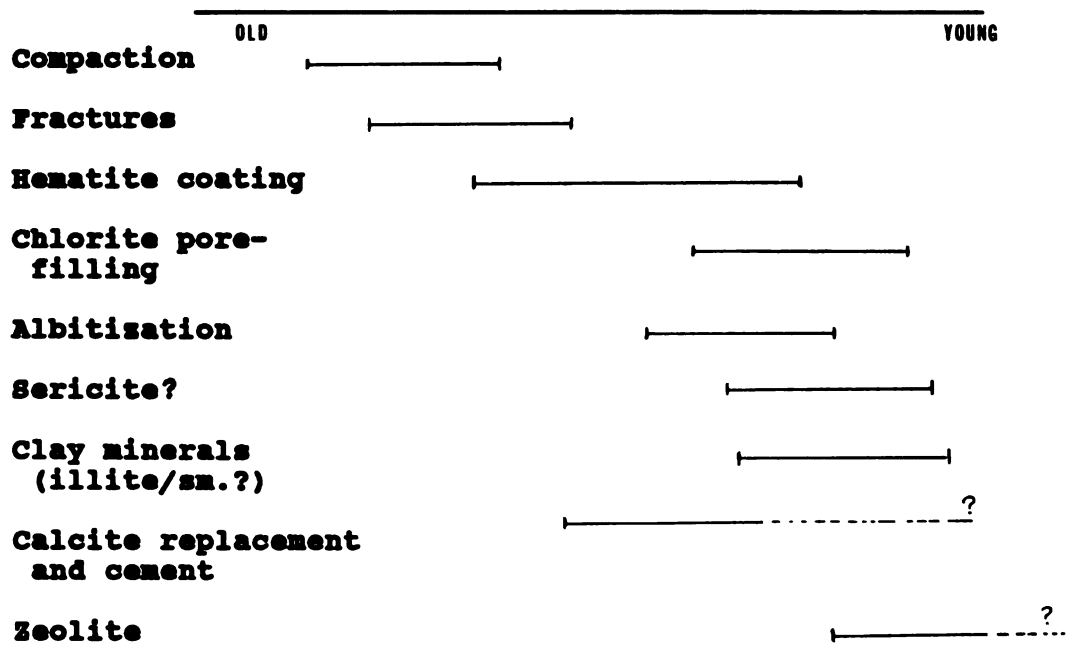
Figure 29 Summary of the paragenetic sequence in
         the New Haven Arkose (stop 2)

PARAGENESIS OF THE EAST BERLIN FORMATION (STOP 1)

	OLD	YOUNG
Compaction	|——————————————|	
Hematite coating	|——————————————|	
Chlorite coating	|—————————|	
Quartz overgrowth	|——————————|	
Feldspar overgrowth	|——————————|	
Albitization	|————————|	
Clay minerals (illite & sm.?)	|———————————————|	
Calcite replacement and cement	|——————————————————— ?	
Pressure solution	|———————— — — — —	
Dolomite cement	. |———————————————————————?	
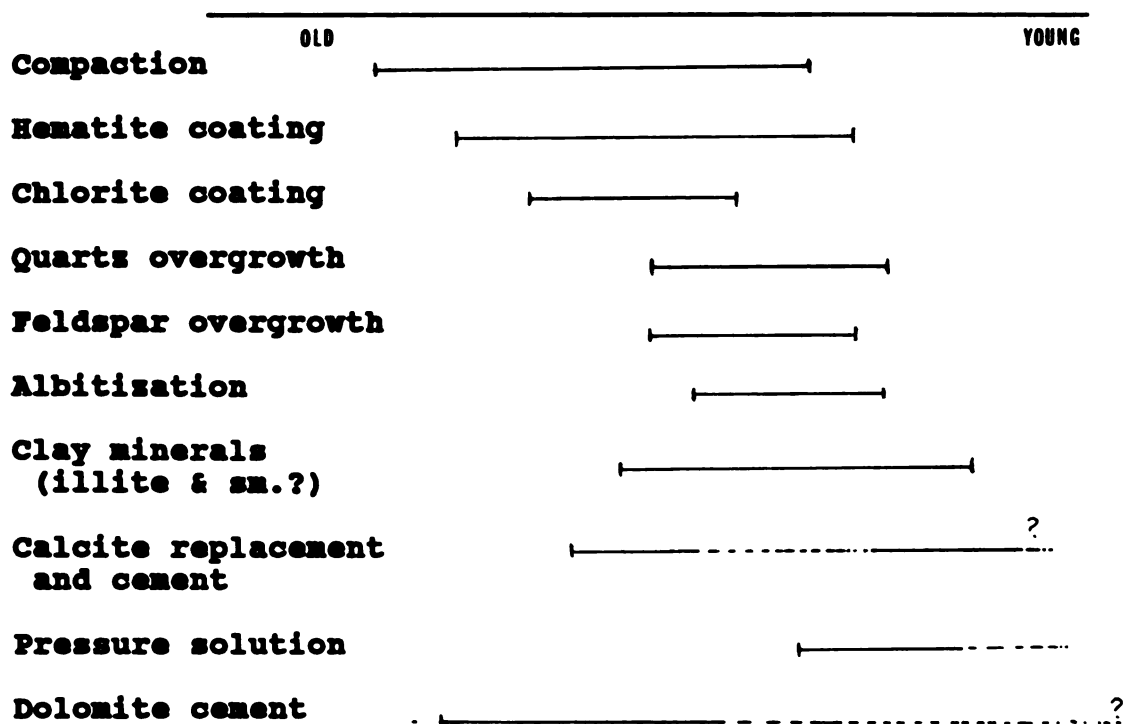
Figure 30 Summary of the paragenetic sequence in the East Berlin Formation (stop 1).

are euhedral formed on detrital grains. Quartz overgrowths
formed either contemporaneously with feldspar overgrowths or
shortly after them. Petrographically it is hard to tell which
phase began forming first, but thin section evidence clearly
shows that the quartz overgrowths continued to form after the
feldspar overgrowths. The ubiquitous presence of these
overgrowths suggests that the pore fluids had a high
concentration of sodium and silica, and that dissolved
aluminum was present. Pressure solution can be another source
of silica, but only in the sandstones of the East Berlin
Formation. Additional sodium was required for albitization
of potassium feldspars.

Petrographic evidence does not clearly indicate when
authigenic sericite and clay minerals formed in the New Haven
sequence; however, they probably formed after the feldspar
overgrowths and albitization. In the East Berlin Formation
clay-mineral formation occurred before the feldspar
overgrowths, as seen by a clay rim that separates overgrowths
from the detrital feldspar grain.

Diagenetic pore-filling chlorite cement could have
precipitated either long after or immediately after the
overgrowths and albitization.

Calcite formed early in the New Haven Arkose as evident
by its filling fractures in feldspar grains; this can be due
to redistribution of carbonate in these caliche-rich rocks.
Calcite replacement of feldspar could have formed earlier than
the pore-filling cement, which formed later in the diagenetic

sequence, possibly as a result of deep burial and albitization of feldspars. There is a possibility that the pore-filling calcite is late in the sequence, but that its optical continuity with the rest of the fracture filling type (Figure 11) could easily be the result of many generations of calcite all being recrystallized at the end. Evidence of multiple generations of calcite was observed in the New Haven Arkoses (Figure 21). Under cathodoluminescence of sample NH-2-14 in figure 21, scattered parts of the calcite pore-filling are non-luminescent (dark red), whereas calcite replacement of feldspar grain which is in a different crystallographic orientation shows bright red luminescence suggesting multiple generations of calcite. This evidence supports the idea of recrystallization (neomorphism) of calcite. The above discussion shows how complicated the paragenesis of calcite may be; i.e. complex history of caliche, calcite fracture filling, and recrystallization optically continuous with pore-fillings. A detailed genetic investigation of the different types of carbonates in these sediments is suggested for future studies.

Zeolite replacement of feldspar and pore-filling cement are considered to be the latest formed diagenetic phase in the New Haven Formation (stop 2 and 3) as evident by the absence of the calcite cement in the zeolite rich samples.

Early dolomite cement is restricted to the alkaline lacustrine cycle of the East Berlin Formation. It is believed that its formation is due to evaporation of the magnesium-

rich lake water.

A detailed discussion of some of the above mentioned diagenetic features (albitization, chloritization, and zeolites) and their proposed origin, supported by SEM, EDS, EMP, and BSEM evidences, will be addressed in the following chapters.

CHAPTER 4

CLAY MINERALOGY

The clay minerals identified in the New Haven Arkose and East Berlin Formation are illite, chlorite, smectite, vermiculite, kaolinite, expandable chlorite, mixed-layered illite-smectite, mixed-layered chlorite-smectite, and mixed-layered chlorite-vermiculite. The following is a presentation of the clay mineralogy of each formation as interpreted from their characteristic XRD reflections.

CLAY MINERAL IDENTIFICATION

The clay minerals were identified by their characteristic basal X-ray diffraction reflections. As described in chapter 2, various chemical and thermal treatments as well as peaks from non-basal planes (random mounts) were used to distinguish between clay mineral groups (e.g., smectite vs. vermiculite, dioctahedral vs. trioctahedral) and to identify mineral species within groups (e.g., chlorite polytypes). No attempt was made in this study to determine quantitatively relative clay mineral abundances, except in a general way.

Illite. A basal sequence of 10, 5, and 3.33 Angstroms that remained unmodified after glycolation was identified as illite. Heat treatment to 300°C and 550°C for 1 hour also caused no significant changes in d-spacings.

Chlorite. Basal reflections at (approximately) 14, 7, 4.7 and 3.5 Angstroms not affected by glycolation represent the chlorite phase. Heat treatment to 300°C and 550°C for 1 hour reinforces the 14 Angstrom (001) peak, whereas higher order reflections weaken or disappear. In some instances glycerol solvation causes a 14.2-14.5 Angstrom peak to broaden and shift to 15 Angstrom. Heat treatment at 550°C displaces the peak to 13.8-14.1 Angstroms. This behavior seems to be indicative of expandable or swelling-chlorite type layers. Brindley (in Brown 1961) suggested that imperfections or "discontinuities" in the interlayer brucite sheets of swelling chlorite may allow organic molecules to enter and cause limited expansion to occur. It is possible that some random mixed-layering of chlorite and swelling chlorite layers does exist; however, in the absence of any low-order superlattice peak characteristic of ordered mixed-layering, this clay phase will herein be referred to as expandable chlorite.

Chlorite polytypes were identified by h0l reflections (Hayes, 1970; Brown and Brindley, 1980). Results of chlorite polytype analyses are given in chapter 6.

Smectite. Clays of the smectite group were recognized by an (001) 14-15 Angstrom reflection expanding to 18 Angstroms upon magnesium saturation and glycerol solvation and collapsing to 10 Angstroms with heat treatment at 300°C and 550°C. The glycerol treatment confirmed smectite rather than a low charge vermiculite as the clay mineral (Walker, in Brown 1961). K-

saturation of the smectites in some cases caused contraction of the lattice to 12 Angstroms, but also frequently resulted in a diffuse range of reflections or complete collapse down to 10 Angstrom. Changes in relative humidity can easily cause K-saturated smectites to exhibit a range of hydration states such that the d(001) gradually shifts from 10 Angstroms (dry) to 12.5 Angstroms (wet) (Eslinger and Pevear, 1988). Therefore, K-saturation was not employed as a definitive test to distinguish smectites from vermiculites (12 Angstroms vs. 10 Angstroms collapse respectively) or as an indicator of the layer charge on the smectite.

Vermiculite. Vermiculites, depending upon their layer charge, may or may not expand with glycerol-solvation (Walker, in Brown 1961). Vermiculites were recognized and distinguished from smectites in this study by their inability to expand upon magnesium saturation and glycerol solvation. The (001) 14-14.5 Angstrom peak contracts to 10 Angstroms upon both K-saturation and heat treatment to 300°C and 550°C. Although vermiculite and chlorite reflections may be juxtaposed and unresolved in a diffractogram, the higher order (001) reflections of vermiculite are normally weaker than those of chlorite. K-saturation and heat treatment, however, are the definitive tests used to discriminate between the two minerals.

Kaolinite. Kaolinite was identified by its basal reflections at 7.15 and 3.58 Angstroms. However, in the presence of chlorite this is not diagnostic. The disappearance of the (001) 7.13-7.15 Angstrom peak upon heating to 550°C for 1 hour distinguishes kaolinite from chlorite. The resolution of the (004) chlorite peak at 3.55 Angstrom from the (002) kaolinite peak at 3.58 Angstrom in some samples aided in the discrimination of these two minerals. Kaolinite was identified in only two samples from the East Berlin Formation.

Mixed-layer minerals. Mixed layered illite-smectite was recognized using the criteria of Reynolds (1980), and Eslinger and Pevear (1988). Shifts in the position of (001) reflections between air-dried and glycerol-solvated samples as well as the symmetry of the major basal peaks were used to characterize the nature of the interlayering (random vs. ordered) and in some instances the approximate relative abundance of each component.

Both 1:1 regularly interstratified chlorite-smectite and chlorite-vermiculite were recognized by superlattice reflections at 28.5-29 Angstroms and a series of rational higher order reflections at 14.3-14.7, 9.7, 7.2, and 4.78 Angstrom. Upon glycerol-solvation, the superlattice peaks of both shift to ~31-32 Angstrom with corresponding shifts of the (002) peaks to ~15.5-15.9 Angstrom. The two minerals are best distinguished by their behavior upon magnesium saturation and glycerol solvation; the chlorite-vermiculite showing no shift

s

i

A

po

ar

re

dio

Hav

for

refl

of t

in d-spacings relative to air-dried positions and the chlorite-smectite exhibiting a shift of the superlattice peak to 32 Angstrom corresponding to expansion of the smectite layers from ~15 to 18 Angstrom. Both K-saturation and heat treatment at 550°C for 1 hour result in peaks at 23-24 Angstrom and 11.8 to 12 Angstrom for the (001) and (002) reflections respectively.

NEW HAVEN ARKOSE

The <2 micron fraction of 60 samples from the New Haven Arkose was examined (Table 3). X-ray diffraction analysis demonstrates that illite is the dominant clay mineral in all samples, along with subordinate amounts of smectite. Slight shifts and asymmetries of the 10 Angstrom reflection between air-dried and glycerol-solvated XRD patterns suggest that in some samples the illite may be mixed-layered illite-smectite, in most cases revealed by a diffuse peak between 10 and 12 Angstroms in the air-dried state, which is not affected by potassium saturation but disappears with glycerol-solvation and heat treatment (Figure 31). In some samples, a d(060) reflection at 1.50-1.51 Angstroms indicates the mineral to be dioctahedral.

Chlorite is present in the different stops of the New Haven Arkose. It was identified in 48 of the 60 samples and for some of the samples it displays a weak and diffuse reflection, probably poorly crystallized, whereas in the rest of the samples it shows a strong reflection at 14.3-14.4

Table 3. Clay mineralogy of the New Haven Arkose

STOP NO	SAMPLE	ILL.	CHL.	SM.	OTHER
	NH-4-6	A	A	-	-
	NH-4-5	A	A	-	-
4	NH-4-4	A	A	-	-
	NH-4-3	M	A	-	-
	NH-4-2	M	A	-	-
	NH-4-1	M	A	-	I/S
	NH-3-35	A	-	A	-
	NH-3-34	A	-	-	-
	NH-3-33	A	-	M	-
	NH-3-32	A	M	M	-
	NH-3-31	M	M	M	-
	NH-3-30	A	M	-	-
	NH-3-29	A	-	tr	
	NH-3-27	A	-	tr	-
3	NH-3-25	A	-	-	-
	NH-3-24	A	-	M	M
	NH-3-23	A	-	M	I/S
	NH-3-22	A	-	A	I/S
	NH-3-21	A	-	A	I/S
	NH-3-20	A	-	A	I/S
	NH-3-19	A	-	-	-
	NH-3-18	A	-	-	-
	NH-3-17	A	-	-	-
	NH-3-16	A	-	M	-

Table 3 (Cont'd.)

STOP NO	SAMPLE	ILL.	CHL.	SM.	IL/SM
	NH-3-14	A	-	M	-
	NH-3-13	A	-	-	-
	NH-3-12	A	-	-	I/S
	NH-3-10	A	-	M	-
	NH-3-8	A	-	A	I/S
3	NH-3-7	A	-	A	I/S
	NH-3-6	A	-	M	-
	NH-3-5	A	-	M	-
	NH-3-4	M	-	M	-
	NH-3-3	A	-	-	-
	NH-3-2	A	-	-	-
	NH-3-1	A	-	-	-

STOP NO	SAMPLE	ILL.	CHL.	SM.	IL/SM
	NH-2-33	A	-	tr	tr
	NH-2-30	A	-	-	-
	NH-2-29	A	tr	-	-
	NH-2-28	A	-	-	tr
	NH-2-26	A	-	tr	tr
	NH-2-25	A	M	tr	tr
2	NH-2-22	A	M	tr	tr
	NH-2-21	A	-	-	tr
	NH-2-20	A	-	A	M
	NH-2-16	A	tr	A	M
	NH-2-15	A	M	M	M
	NH-2-14	M	M	M	M
	NH-2-13	M	tr	A	A

Table 3 (Cont'd.)

	NH-2-12	A	M	A	A
	NH-2-11	A	M	tr	M
	NH-2-10	A	M	tr	M
	NH-2-9	A	A	-	tr
	NH-2-7	A	A	-	tr
2	NH-2-6	A	tr	-	tr
	NH-2-5	A	tr	-	tr
	NH-2-4	A	-	A	-
	NH-2-3	A	tr	-	-
	NH-2-2	A	A	M	-
	NH-2-1	A	A	M	-

A = Abundant   tr = Trace   M = Minor   - = None
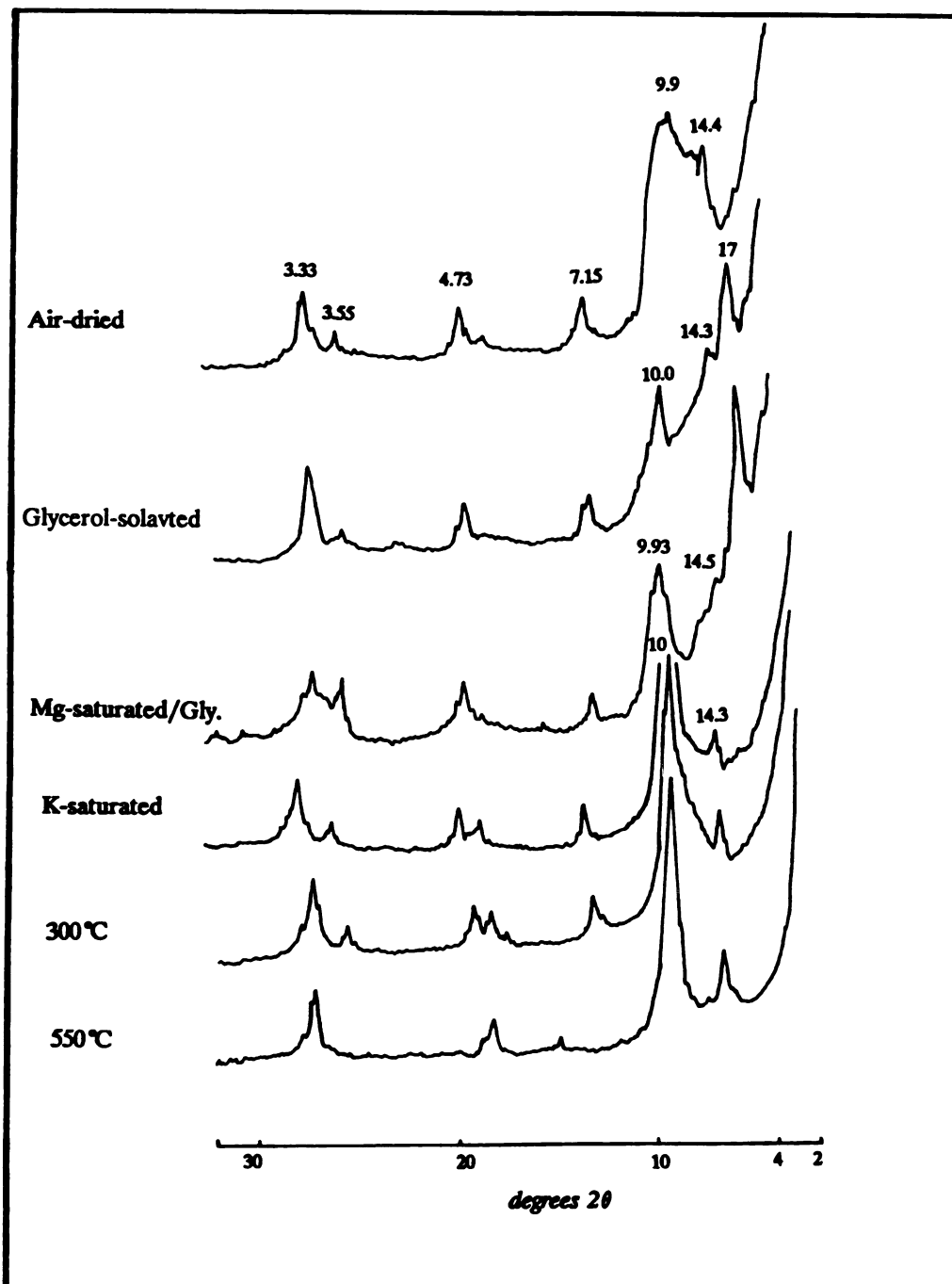
Figure 31 X-ray diffraction traces of the <2 μm fraction of New Haven Arkose. Sample NH-4-6 shows chlorite and illite-smectite patterns.

Angstroms (Figure 31). Samples collected from stop 4, stratigraphically located in the lower portion of the New Haven Arkose, (Chapter 1, Figure 4) show the predominance of chlorite in all samples. A minor amount of mixed-layered illite-smectite is also present in only one sample at stop 4, and discret smectite is absent.

Samples collected from mudstones and sandstones from stops 3 (near the Hampden basalt intrusion) and 2 (caliche-rich paleosol horizons), situated stratigraphically higher in the New Haven sequence, are mainly composed of illite, smectite, and mixed-layer illite-smectite. In some samples, a strong d(060) reflection occurring at about 1.502 Angstroms suggests a dioctahedral illite type. A weaker, yet distinct reflection at approximately 1.53 Angstroms indicates a trioctahedral smectite type. Chlorite occurs in portions of these outcrops.

EAST BERLIN FORMATION

The East Berlin Formation (stop 1) contains a varied clay mineral assemblage. Clay minerals identified in the 25 samples examined are illite, chlorite, smectite, vermiculite, swelling chlorite, kaolinite, and a number of interstratified minerals including illite-smectite, chlorite-smectite and chlorite-vermiculite (Table 4). Figure (32) shows randomly interstratified illite-smectite, where a small 18 Angstrom peak appears by glycolation (Eslinger and Pevear, 1988). Generally, these rocks are illitic with most containing subordinate amounts of chlorite.

Table 4. Clay mineralogy of the East Berlin Formation

STOP	SAMPLE	ILL.	CHL.	SM.	VERM.	CHL/SM	CHL/VER	OTHER
	EB-1-28	tr	-	-	-	M	A	-
	EB-1-25	A	A	M	-	-	A	-
	EB-1-24	A	-	tr	M	tr	M	-
	EB-1-23	tr	-	A	M	tr	A	Kao.tr
	EB-1-20	tr	tr	A	-	A	M	-
	EB-1-19	A	-	A	-	A	tr	-
	EB-1-18	A	M	-	tr	A	tr	-
	EB-1-17	tr	-	-	tr	M	-	-
	EB-1-15	M	-	A	-	-	-	Exp.chl
	EB-1-14	A	-	-	-	-	-	-
1	EB-1-13	A	M	tr	-	-	-	Exp.chl
	EB-1-12	M	tr	tr	-	-	-	Exp.chl
	EB-1-11	M	tr	A	-	-	-	-
	EB-1-10	M	-	-	-	-	-	-
	EB-1-9	M	-	A	-	-	-	-
	EB-1-8	A	-	-	-	-	-	-
	EB-1-7	A	-	-	-	-	-	-
	EB-1-6	M	-	-	-	-	-	-
	EB-1-5	M	-	-	-	-	-	-
	EB-1-4	M	-	tr	M	-	-	Kao.tr
	EB-1-3	A	-	M	-	-	-	-
	EB-1-2	A	-	A	-	-	-	-
	EB-1-1	M	-	A	-	-	-	-

A = Abundant   tr = Trace   M = Minor   - = None
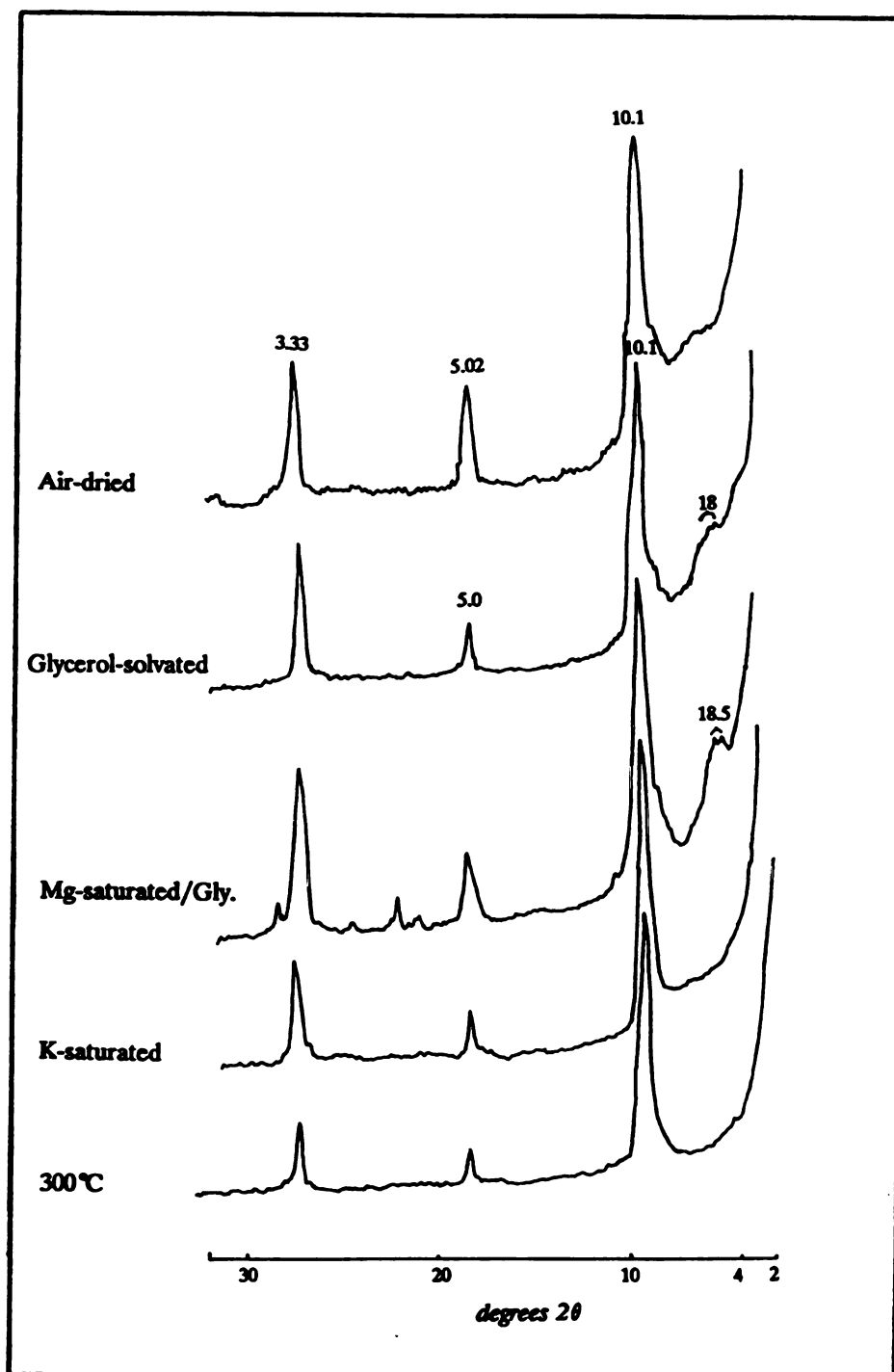
Figure 32 X-ray diffraction patterns of the <2 μm
fraction of the New Haven Arkose. Sample
NH-3-20 shows illite-smectite interlayer.

disti

et al

rock

syst

oxid

syst

repr

1- F

crys

(Tal

is

ref

1.5

pre

in

<1

chl

for

ide

amo

muc

of

34

co

The various lithologies in the East Berlin Formation are distinguished by distinct clay mineral assemblages. Hubert et al., (1976) assigned two major depositional systems for the rock units in the East Berlin Formation: 1) the flood plain system consists of stream channel, floodplain and shallow oxidizing temporal lake sediments, and; 2) the perennial lake system contains gray siltstone-mudstone and black shale representing shallow and deeper lakes respectively.

1- Floodplain System

Floodplain system red beds are characterized by well-crystallized illite and abundant to minor amounts of chlorite (Table 4 and Figure 33). Illite is dioctahedral and chlorite is trioctahedral in character as indicated by d(060) reflections occurring at 1.502-1.506 Angstroms and 1.544-1.546 Angstroms respectively. April (1978) reported the predominance of the (high temperature) 2M polytype of illite in these rocks, ranging in abundance from 65 to 100% 2M in the <1 micron fraction. In this study, the presence of type Ib chlorite in these sediments that suggests an authigenic origin for this mineral (refer to Chapter 6 for the method of identification and diagnostic peaks of this polytype). Minor amounts of vermiculite were detected in the floodplain red mudstone samples # EB-1-4, EB-1-24 and EB-1-25. Minor amount of kaolinite and illite are observed in these rocks (Figure 34).

Samples collected near the Hampden Basalt-red mudstone contact contain abundant well crystallized 1:1 interstratified
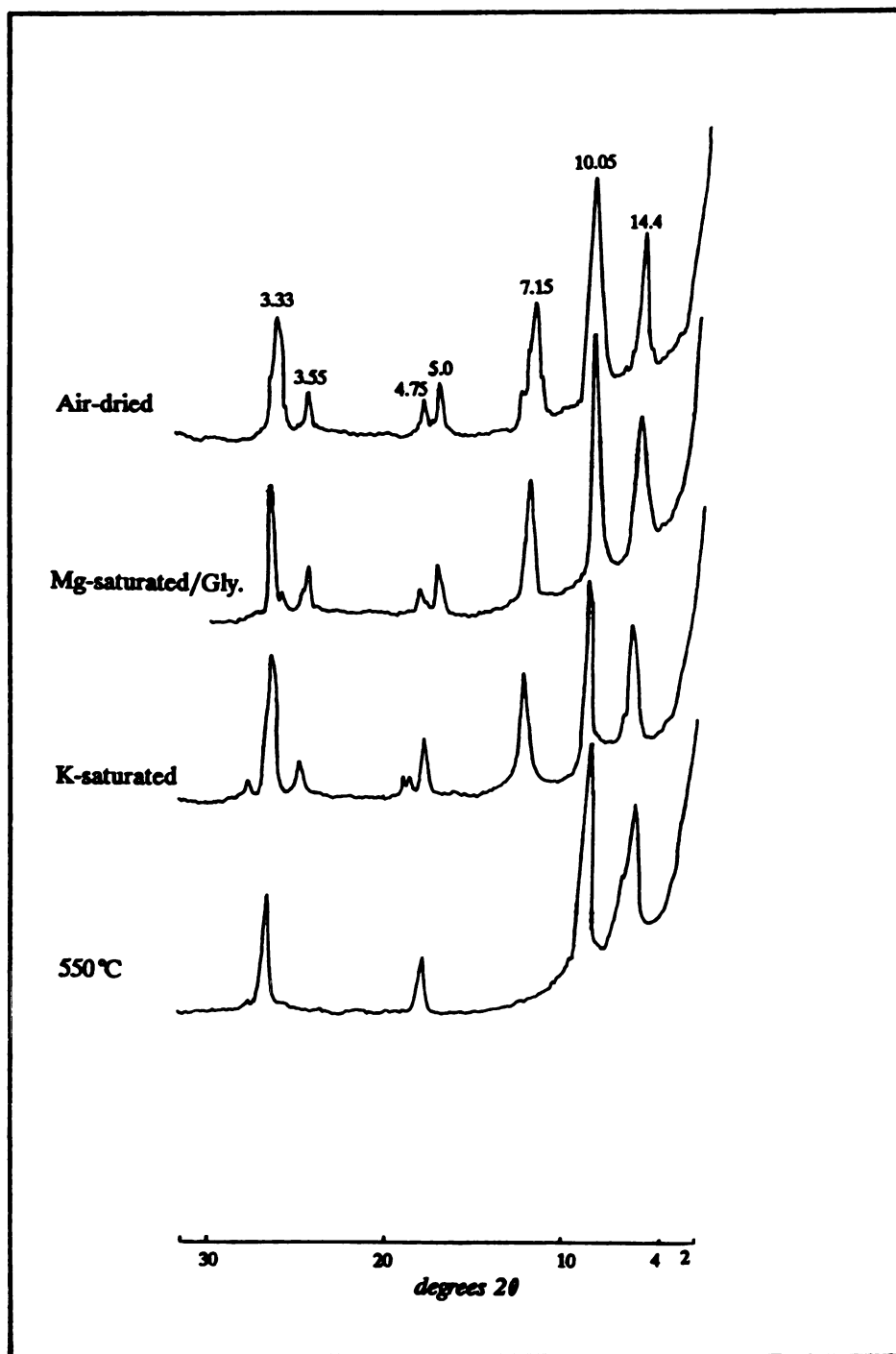
Figure 33 XRD pattern of the <2 μm of sample EB-1-
2, a floodplain red sandstone in the East
Berlin Formation. Sample contains illite
and chlorite.
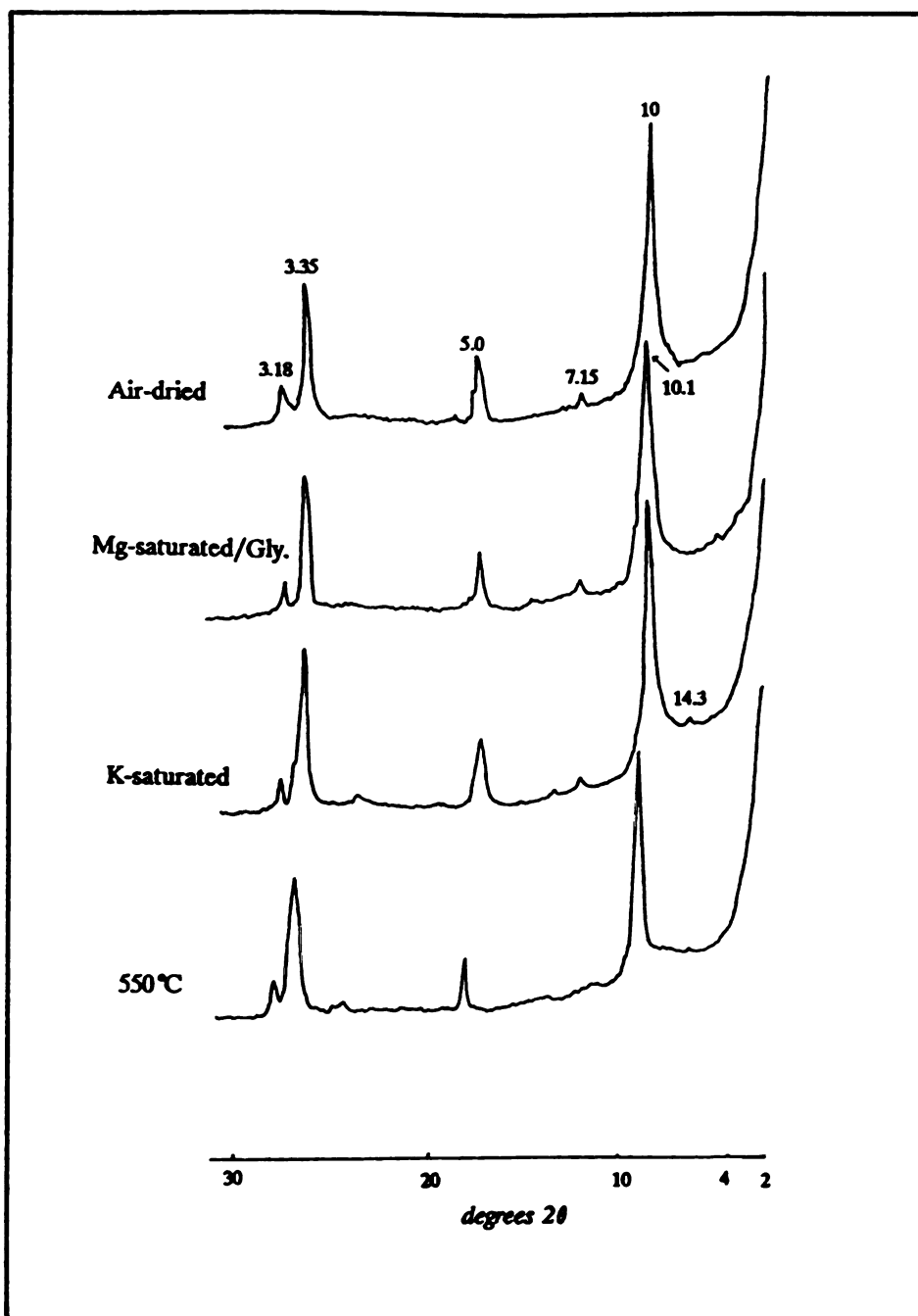
Figure 34 XRD pattern of the <2 μm of sample EB-1-
        2 of the East Berlin Formation. Sample
        contains illite and minor amount of
        kaolinite.

chlor

occur

in th

Basal

a gr

mine

defi

is

int

per

sup

for

(F

2)

dc

s

d

s

e

chlorite-vermiculite (Figure 35). April (1980) reported the occurrence of regularly interstratified chlorite-vermiculite in these floodplain red mudstones directly beneath the Hampden Basalt. Samples obtained further away from the contact show a gradual decrease in the abundance of the mixed-layered mineral. The trend is noted by observing changes in the definition of the superlattice peak. This basal reflection is a sensitive indicator of the degree of ordering for these interstratified clays. A well developed superlattice suggests perfect to near perfect 1:1 ordering, whereas a poorly defined superlattice reflections implies a random interstratification, for the mixed-layered chlorite-vermiculite (Millot, 1970), (Figure 35).

2) Perennial lake system

The clay mineralogy of the lacustrine gray beds is dominated by illite, chlorite and/or interstratified chlorite-smectite (Table 4). Minor amounts of swelling chlorite and/or discrete smectite are also present in nearly 1/3 of the samples (Figure 36). Illite is present to some extent in every sample. April (1978) characterized the illite to be 100% 1Md mica and highly crystalline as evidenced by a sharp basal reflections. An illite d(060) reflection at 1.50-1.51 Angstroms indicates a dioctahedral nature for this mineral.

Chlorite was identified in only five samples. It is trioctahedral as indicated by strong intensity d(060) reflections at approximately 1.54 Angstroms in samples containing only the dioctahedral illite-chlorite assemblage.
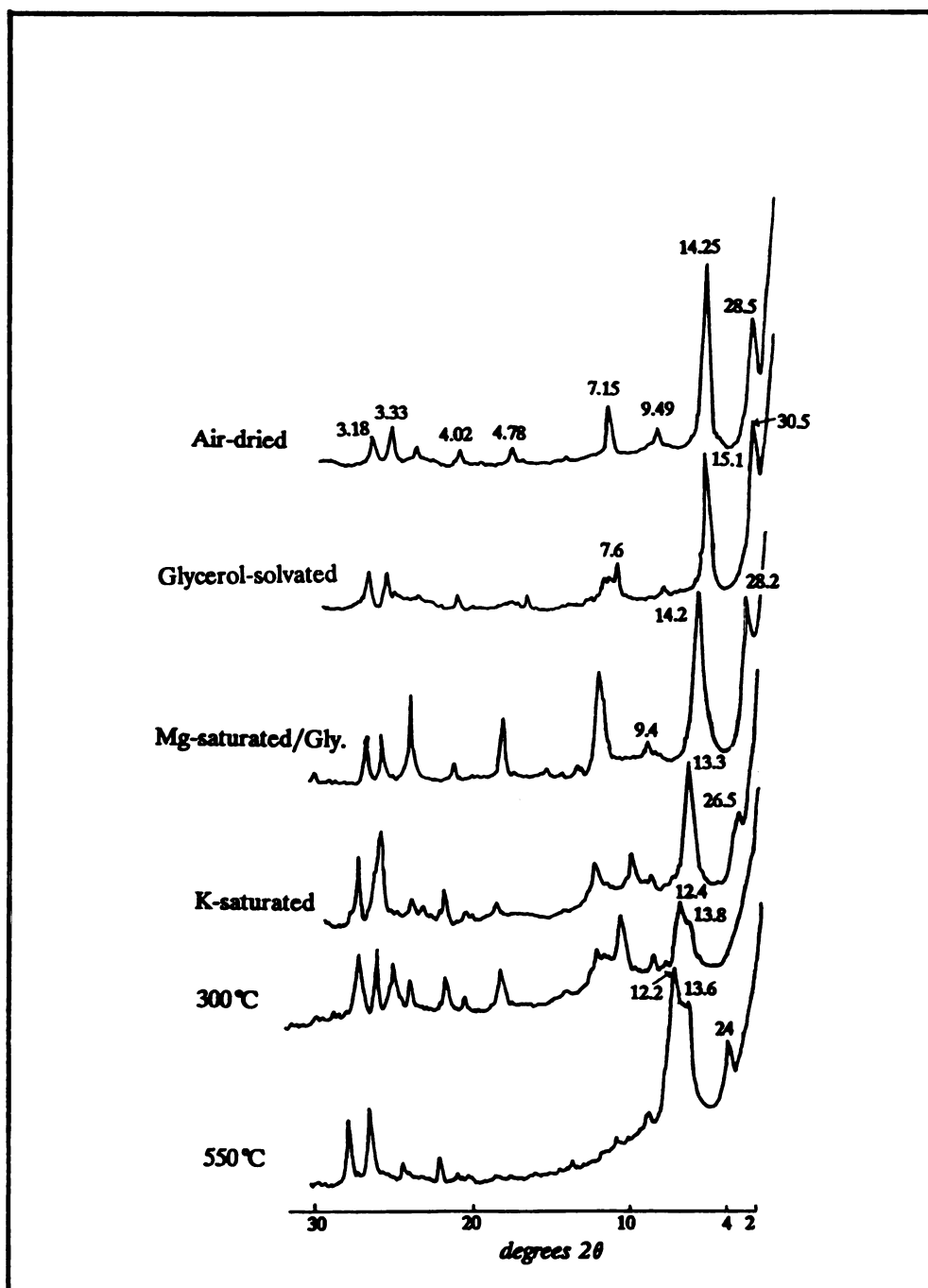
Figure 35 XRD pattern of the <2 μm fraction of sample EB-1-25, East Berlin Formation. Sample contains chlorite-vermiculite interlayers.
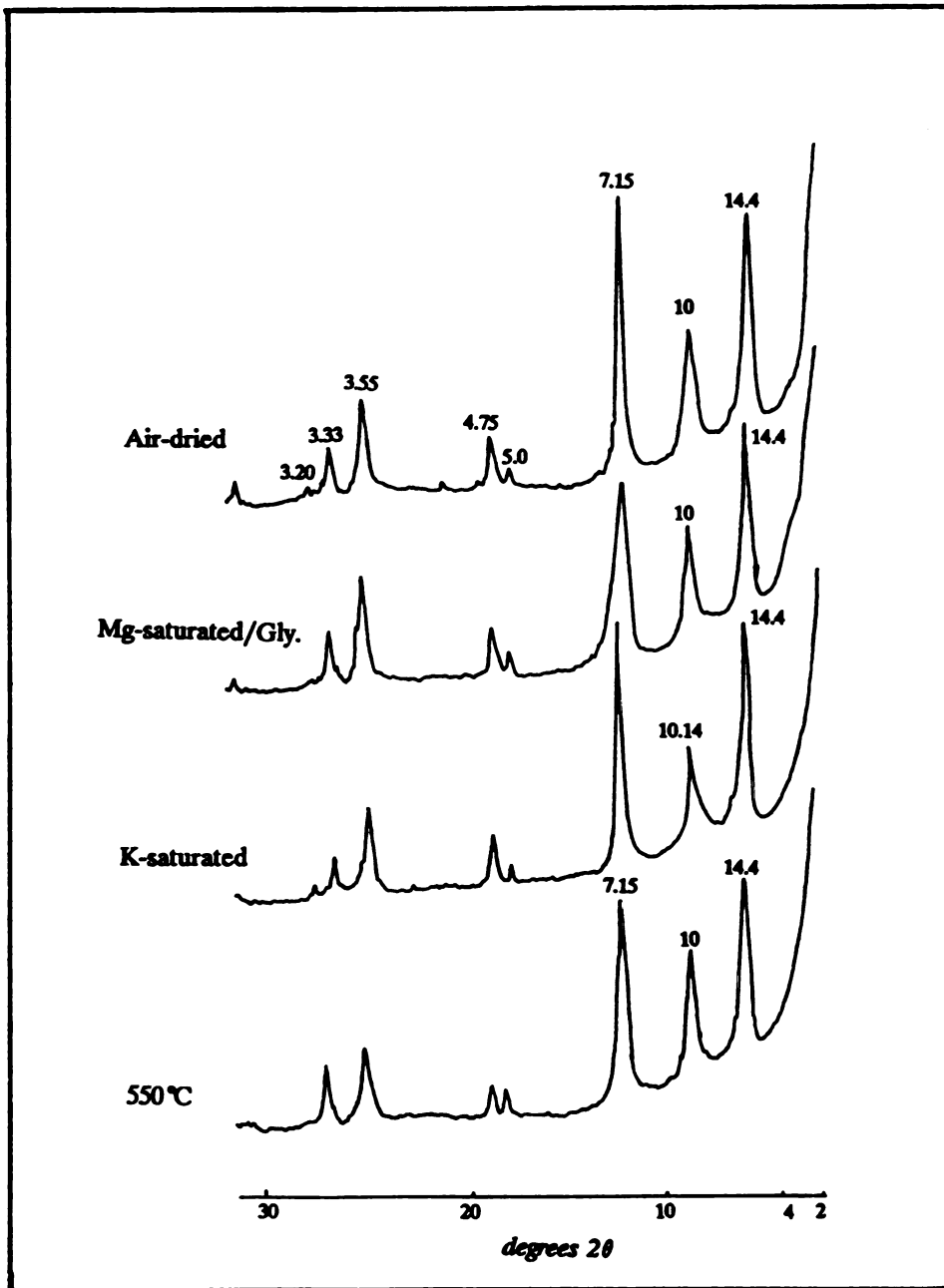
Figure 36 XRD pattern of the <2 μm of sample EB-1-13, East Berlin Formation. Sample contains well-crystallized illite and chlorite.

The i

as th

of th

to be

varie

many

chara

refle

Angst

trea

550·

shif

12 A

that

dioc

laye

1.5(

samp

to

for

38)

occ

New

ch

int

The intensities of the sequence of basal reflections as well as the position of the d(001) imply a high magnesian content of the chlorite (Brindley, in Brown 1961). Chlorite was found to be IIb polytype which is characteristically a detrital variety (Chapter 6).

A mixed-layered chlorite-smectite occurs abundantly in many of the gray mudstones and siltstones. The mineral is characterized by a distinct superlattice d(001) basal reflection at 29 Angstroms which shifts to 32 Angstroms (14 Angstroms chlorite-18 Angstroms smectite) upon glycerol treatment after magnesium saturation (Figure 37). Heating to 550°C for 1 hour induces structural contraction causing a shift in the d(001) to 24 Angstroms with a d(002) spacing at 12 Angstroms. A strong 1.536 Angstrom reflection indicates that the mineral is trioctahedral. A small amount of dioctahedral illite is probably associated with the mixed-layered mineral as indicated by a weak d(060) reflection at 1.506 Angstroms.

Swelling chlorite occurs to a minor extent in some samples. It is identified by a 14 Angstrom peak that broadens to 14.5-15 Angstroms after glycolation and by heating to 550°C for 1 hour, after which it remains at 14 Angstroms (Figure 38). Suchecki et al., (1977) described a similar mineral occurring in the rocks of the Cow Head klippe, western Newfoundland, and characterized it as a mixed-layered chlorite-expandable layer clay with random interstratification. April (1978) believes that the
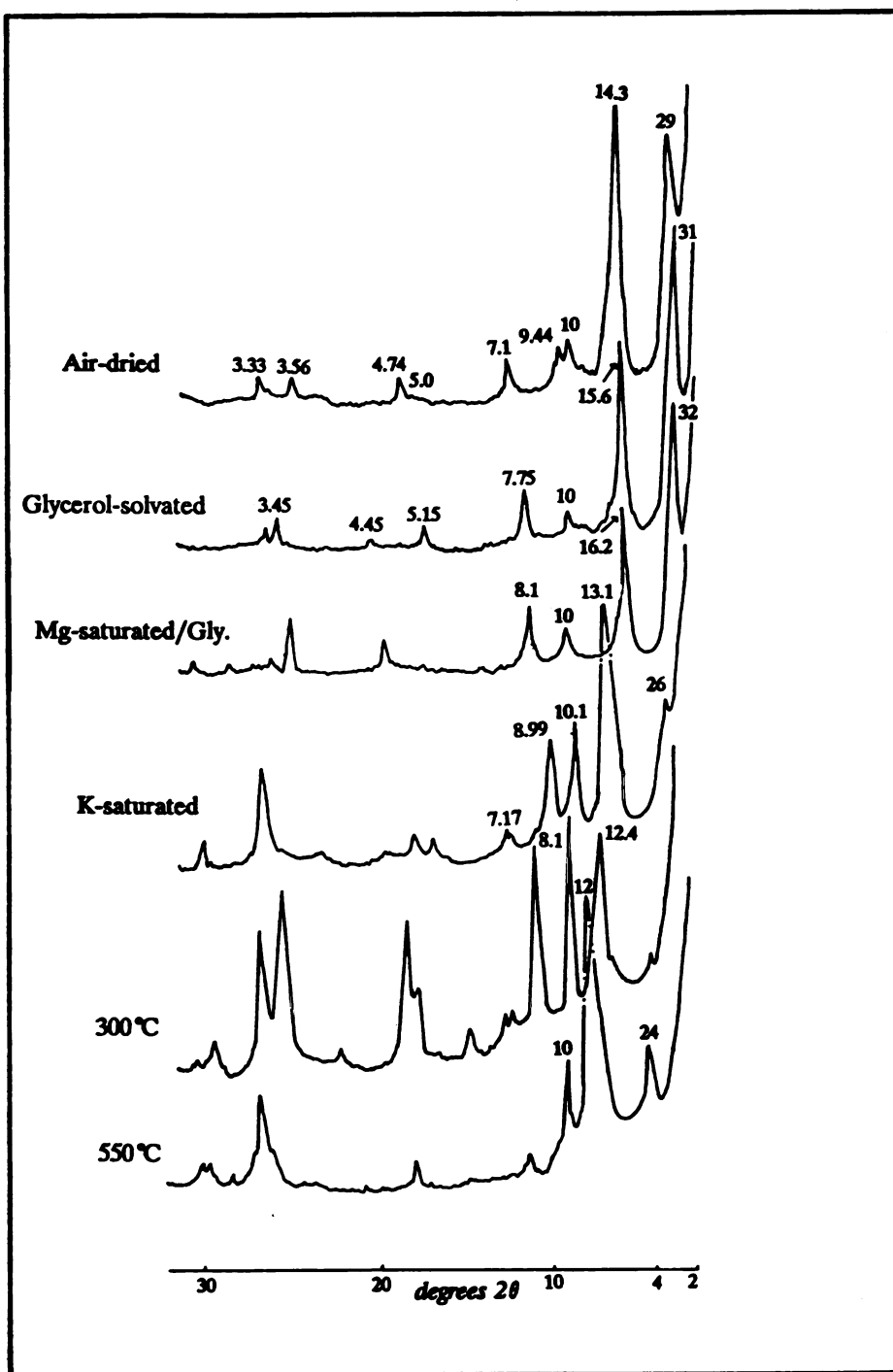
Figure 37 XRD traces of the <2 μm of sample EB-1-
19, East Berlin Formation. It contains
chlorite-smectite interlayer.
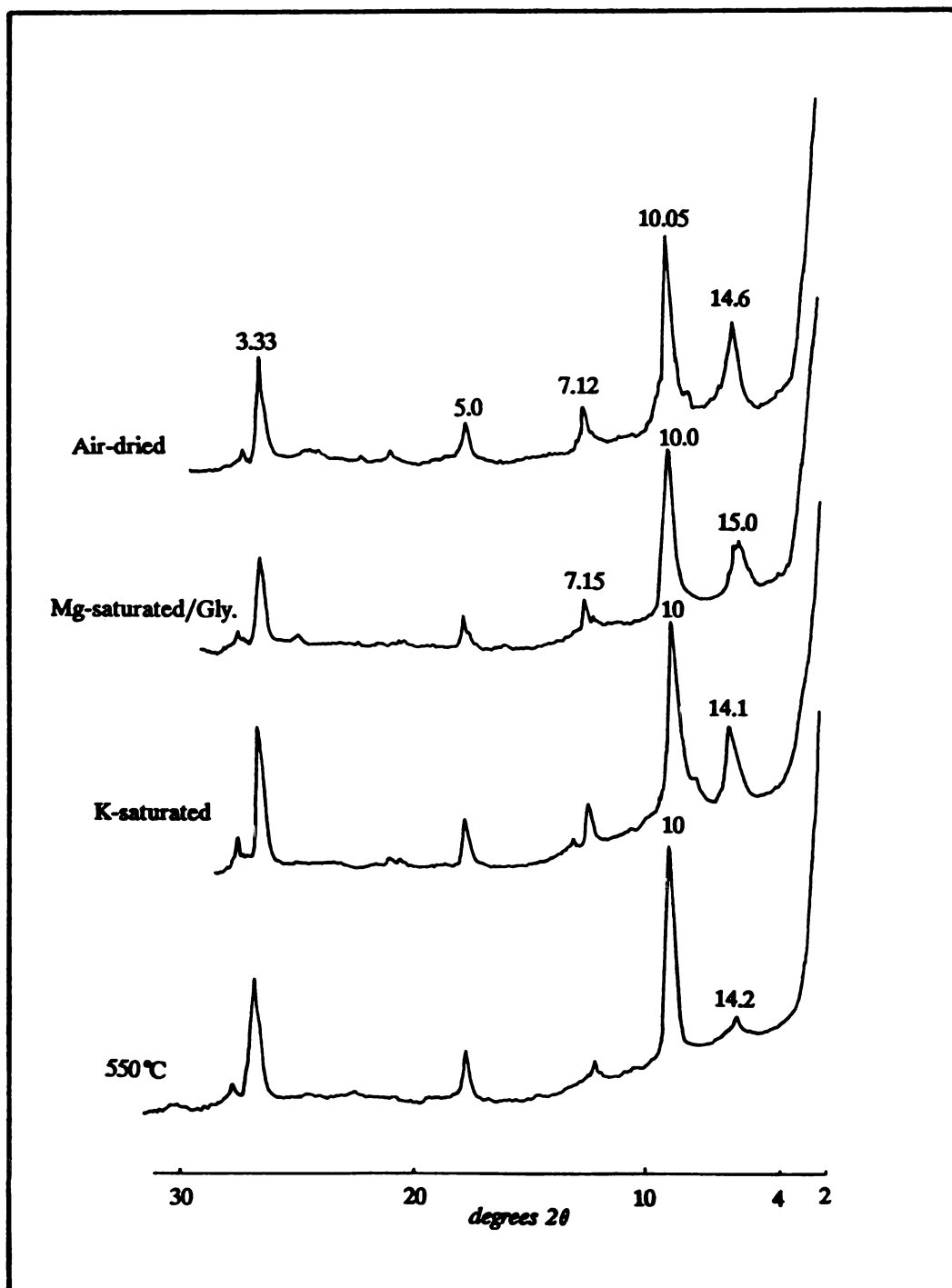
Figure 38 XRD pattern for the <2 µm of sample EB-
1-15, East Berlin Formation. Sample
contains illite and expandable chlorite
phases.

expandable layer might well in itself be an expandable or swelling chlorite.

The black shales of the lacustrine sequence contain major amounts of discrete smectite and illite, some interstratified illite-smectite and minor amounts of chlorite (Figure 39). Dioctahedral illite and trioctahedral smectite are present as evidenced by d(060) reflections occurring at 1.50 and 1.52 Angstroms respectively.

Interstratified illite-smectite occurs in many samples of the black shales. Identifications were made by observing shifts in the position of the first order reflection toward the low angle (higher d-spacing) side.

ORIGIN AND DISTRIBUTION OF THE CLAY MINERALS

The Hartford Basin is characterized by terrestrial sedimentation; however, the clay-mineral assemblages in many areas of the basin are similar. The distribution of clay minerals in the Triassic-Jurassic deposits of the Connecticut Valley resembles the general scheme proposed by Millot (1970).

Clay minerals in sedimentary rocks may originate in a number of ways. Generally, three principal processes account for their genesis: 1) detrital inheritance; 2) transformation; and 3) neoformation (Millot, 1970). Mechanical or detrital inheritance implies that the clays in the depositional environment are derived from the source area and remain unaltered during burial. Whether or not the clay lattice will be modified is determined by the clay mineral's stability and
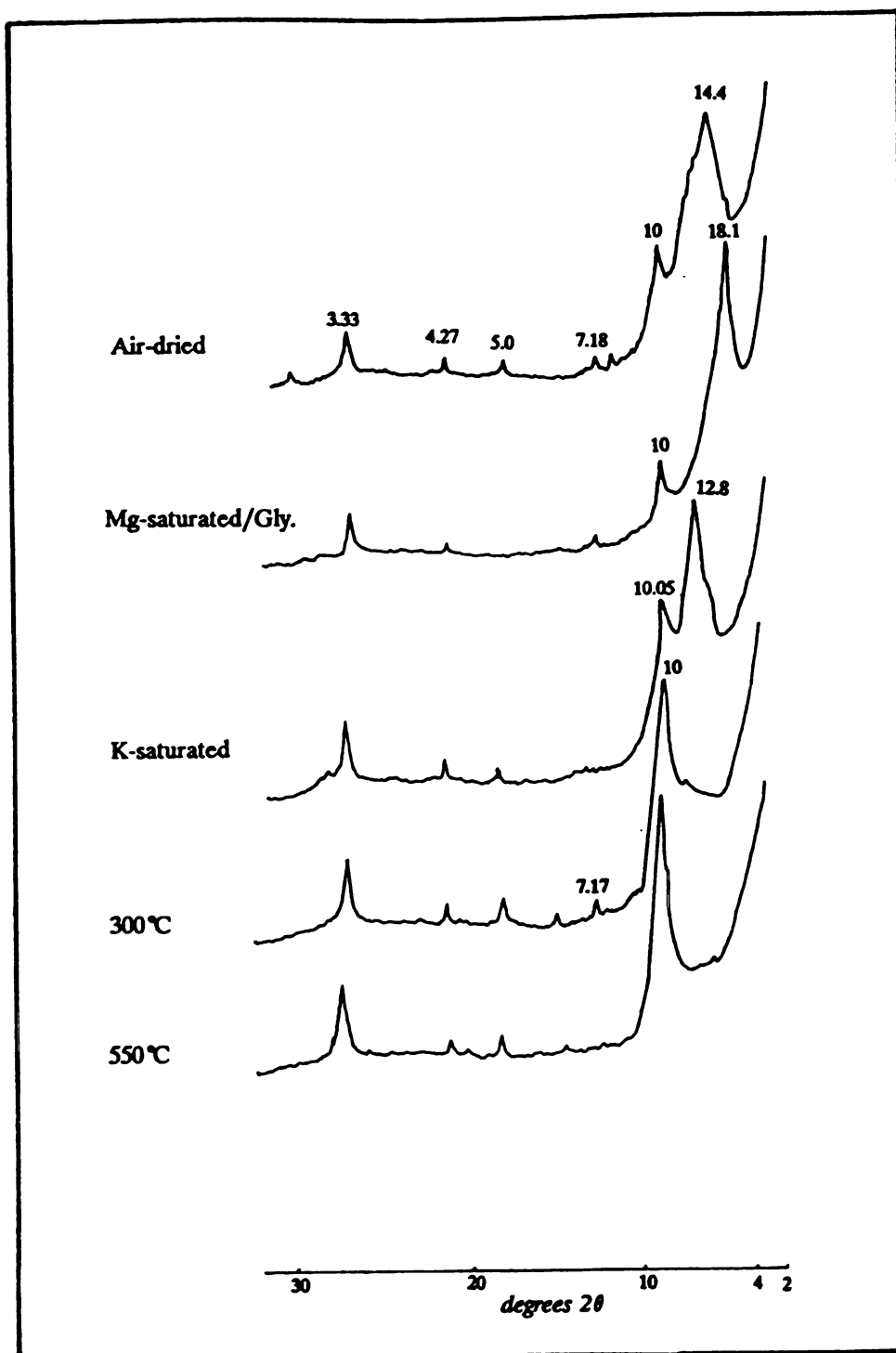
Figure 39 XRD pattern of the <2 μm fraction. Black shale of the East Berlin Formation. Sample contains illite, smectite, and traces of kaolinite.

the chemical nature of the sedimentary environment.

Clay mineral transformation may take place during weathering, sedimentation or diagenesis (burial metamorphism). This may occur by either aggradation or degradation processes (Millot, 1970). These processes are illustrated by reactions such as: chlorite → vermiculite; illite → vermiculite; chlorite → mixed-layered chlorite-smectite.

Finally, neoformation or authigenesis is the process by which clay minerals are newly synthesized in the sedimentary environment. Reactions involving existing clay minerals, non-clay minerals, pore waters and gels may produce neoformed clay minerals under innumerable physicochemical conditions (Millot, 1970). Although these processes are well documented in the literature, criteria for determining the genesis of clay minerals in sedimentary rocks are few in number. The origin of some of the clay-mineral assemblages seems clear in the light of the sedimentologic and mineralogic evidences, yet the genesis of others is problematic and open to several interpretations.

Generally, the distribution of clay minerals in the Triassic-Jurassic beds of the Connecticut Valley can be described in terms of clay-mineral occurrences in lithologies that represent three major depositional environments namely: 1) floodplain environment (red beds); 2) shallow lacustrine environment (gray beds); 3) deep lacustrine environment (black shale) (Krynine, 1950; Hubert et al., 1976; Hubert, 1977; Hubert et al., 1978). April (1978) summarized the clay

mineral distribution in the three major depositional environments in the basin as follows:

a) <u>Red beds of floodplain environment</u> - containing abundant 2M illite of detrital origin with subordinate amounts of chlorite, smectite and interstratified illite-smectite and rare occurrences of vermiculite and kaolinite.

b) <u>Gray beds of shallow lacustrine environment</u> - containing the assemblage 1Md illite + chlorite with subordinate amounts of interstratified chlorite-smectite, discrete smectite and expandable chlorite. This clay mineral assemblage indicates much authigenic mineral formation and less detrital influence (April, 1978).

c) <u>Black shales of deep lacustrine environment</u> - characterized by 1Md illite + trioctahedral smectite assemblage with minor amounts of chlorite and mixed-layered illite-smectite.

The following is an attempt to depict the possible origin of the clay mineral assemblages in the study area.

<u>Illite</u>

Illite is believed to have originated primarily, in the shallow buried East Berlin Formation, as a detrital phase inherited from the mechanical and chemical breakdown of micas in the crystalline metamorphic and igneous rocks in the source highlands. In X-ray diffractograms, illite d(001) reflections are often sharp and intense indicating the presence of a well crystallized material.

Subjected to weathering during soil development in the source area and/or during transportation and reworking in the basin, it is not unlikely that some, if not much, of the detrital illite suffered some degree of chemical/structural degradation. Broad and weak reflections in diffractograms indicate that illite is present mainly in degraded form. The occurrence of well-crystallized illite does not necessarily imply that they were deposited as such. Millot (1970) stated that the degree of crystallinity may reflect subsequent rejuvenation (recrystallization) during burial. Therefore, the well-crystallized illite could indicate a relatively higher diagenetic stage (Gottfried and Kotra, 1988), assuming that the minerals were affected only by burial during diagenesis.

Illite in the deeply buried (> 3 km, burial temperature about 110°-150°C) New Haven Arkose is believed to have originated diagenetically. Extensive illitization of illite-smectite mixed-layer is believed to be the source of illite in these rocks. This is demonstrated by the down-section increase of illite and decrease of smectite (Tables 3 and 4).

Chlorite

Chlorite occurs in any particular sample in one or more of the following forms: 1) discrete chlorite; 2) expandable chlorite; 3) interstratified chlorite-smectite; and 4) interstratified chlorite-vermiculite. According to Millot (1970) and Dunoyer De Segonzac (1970), the three phases could

represent various stages in the diagenetic transformation of a degraded 2:1 clay mineral (smectite ?) by magnesium-rich waters in the order from interstratified form to a discrete form. In X-ray diffractograms, chlorite d(001) reflections are often sharp and intense indicating the presence of a well-crystallized material. Identification of the chlorite polytypes suggest the presence of a detrital IIb type variety mainly in the East Berlin Formation and parts of stop 2 of the New Haven Arkose (Chapter 6). Authigenic chlorite cement (Ib polytype; Chapter 6) is present in the other stops of the New Haven Arkose. Chlorite is either absent or shows weak reflections in diffractograms in samples from the East Berlin Formation. That suggests that chlorite suffered some degree of physical or chemical degradation due to diagenesis, or it was never there. A detailed discussion on the distribution, texture and origin of chlorite will be presented in chapter 6.

Smectite

Authigenic precipitation of smectite in the pores of the red muds is favored, although it is possible that some smectite may have been inherited from the detrital load (April, 1978). Hubert et al., (1978) stated that the floodplain environment of the East Berlin Formation experienced numerous wet and dry periods. This is evidenced by the occurrence of abundant mudcracks, short-lived shallow oxidizing lakes, dinosaur footprints, raindrop impressions,

trails, etc. It seems reasonable to infer that during periods of protracted dryness in the poorly drained floodplain lowlands, ions in solution became concentrated in both surface and pore waters (April, 1978). Under such conditions the authigenic smectite is favored (Millot, 1970; Dunoyer de Segonzac, 1970; Keller, 1970). With smectite forming in the floodplain during times of drought, it is not difficult to visualize sediment redistribution with the onset of heavy winds, rain or flood (April, 1978). This might account for the apparent lack of correlation between clay-mineral assemblages and depositional subenvironment. Also, diluted by large volumes of detrital illite and chlorite, smectite would remain a minor constituent in the sediments.

Vermiculite

Few samples contain minor amounts of vermiculite. It may have been derived as a detrital component from the chemically weathered source area or from the degradation of illite and chlorite in soil horizons developing on the floodplain (April, 1978). Before burial, vermiculite was probably a much more abundant constituent in the floodplain sediments. Aggradation to illite and/or chlorite following adsorption of magnesium and potassium during burial eventually reduced vermiculite to minor importance in the sedimentary sequence.

Interstratified illite-smectite

Samples collected from the upper part of the New Haven

Arkose contain the clay mineral assemblage illite + smectite. Hower et al., (1976) proposed the following equation for the conversion of smectite to illite in Gulf Coast sediments:

smectite + K-feldspar (+ mica ?) → illite + quartz + chlorite. (1)
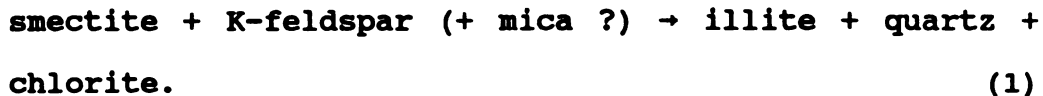
Assuming the original clay-mineral assemblage of the upper New Haven sediments was dominantly illite + smectite, conversion of some smectite to illite-smectite would produce the observed assemblage of illite + chlorite + illite-smectite + discrete smectite.

The persistence of the assemblage illite + smectite indicates that maximum temperatures in the upper part of the sequence did not exceed those attributed to the upper limit of smectite stability (Hower et al., 1976; Velde, 1977). Velde (1977) gave this temperature as about 100°C. Ramseyer and Boles (1986) reported the occurrence of smectite and illite-smectite interlayers at a burial temperature of about 120°C to 140°C. Palynological data of Cornet and Traverse (1975) shows spore color and reflectance to indicate that the rocks of the Shuttle Meadow Formation (located just above the New Haven Formation) have not been subjected to temperatures above 200°C. The absence of discrete smectite in the lower part of the New Haven Arkose indicates that the temperature ceiling for smectite stability was exceeded in the lower part of the sequence during the conversion of smectite to illite-smectite, and ultimately to illite (stop 4, Table 3). Pratt et al. (1988) studied the thermal history of the Hartford

Basin and proposed a regional pattern of thermal maturation increases down the stratigraphic section, i.e. increases with depth of burial. They reported a low level of thermal maturity in the Portland Formation (uppermost formation in the succession) and suggest that these rocks did not reach burial temperatures above 90°C. The East Berlin and Shuttle Meadow sediments (thermally mature) reached burial temperatures of 90 to 110°C. Samples from the Triassic New Haven Arkose were not analyzed, but their equivalent in the Newark Basin (the Passaic Formation) were thermally overmature with respect to petroleum generation. Therefore, the New Haven Arkose probably reached a burial temperature >110°C, as it is the deepest formation in the stratigraphic section.

Additional evidence in support of this inference comes from the observation that K-feldspar is abundant in the chlorite-deficient rocks, yet present in minor amounts or almost absent from the chlorite bearing rocks. Figure 40 is a plot of the percent chlorite versus the percent K-feldspars of some New Haven Arkose samples (Table 1); it shows an inverse relationship between the two minerals. Note that in the New Haven Arkose, the greatest depletion of K-feldspar, and the greatest abundance of authigenic chlorite, occur in the deepest samples (stop 4). Equation (1) shows that K-feldspar is one possible source of potassium for the formation of illite-smectite and eventually illite from smectite, and that chlorite is one of the products, so the inverse relationship between K-feldspar and chlorite is consistent
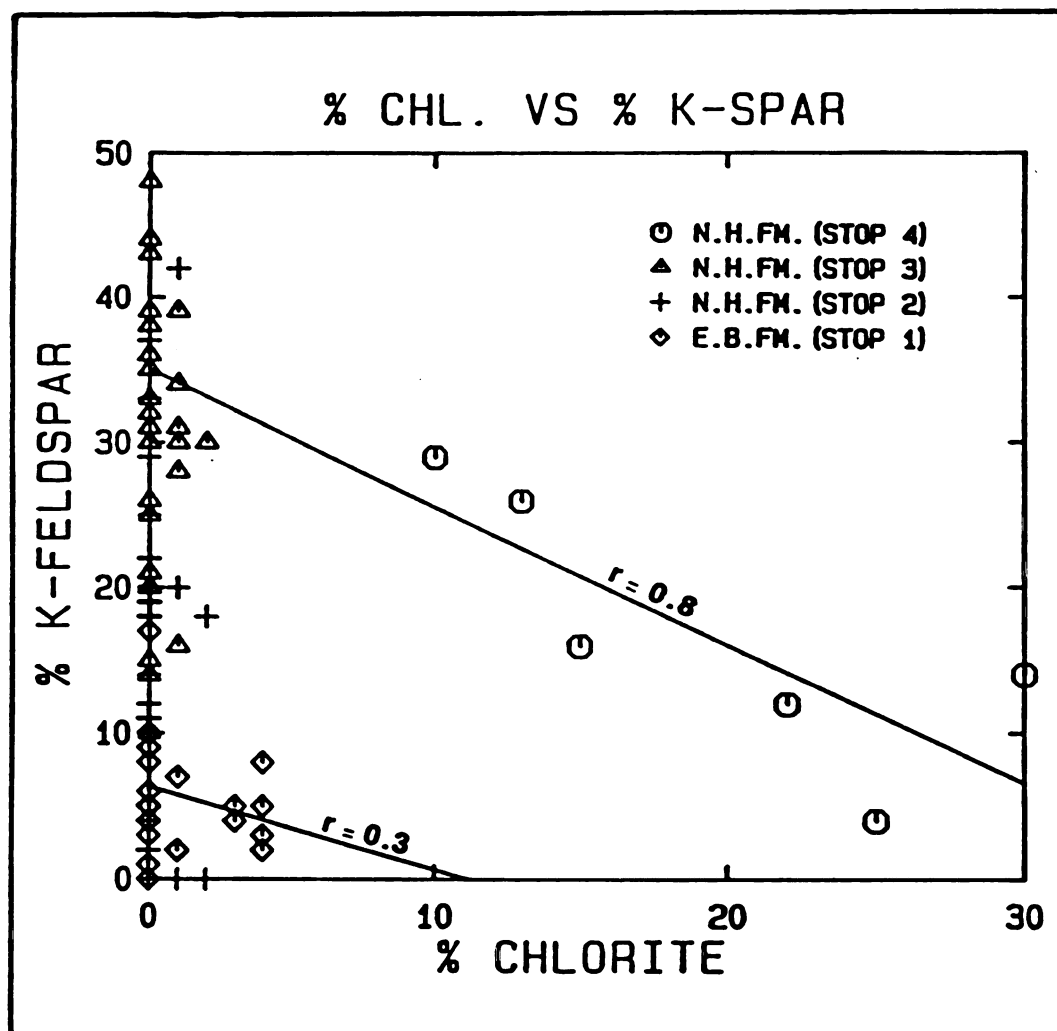
Figure 40 Plot of the % chlorite vs. % K-feldspar
for the three stops of the New Haven
Formation.

with reaction (1).

Corrensite

The term corrensite was originally proposed by Lippman (1956) to describe a mixed-layered clay mineral with regularly alternating layers of chlorite and swelling chlorite. Since that time, the terms corrensite, corrensitic-material and corrensite-like have been used to describe a variety of similar mixed-layered clay minerals in a spectrum of lithologies and modes of origin. These clays result from the regular, or near-regular, interstratification of chlorite with swelling chlorite, smectite or vermiculite (Early et al., 1956; Bradley and Weaver, 1956; Lippman, 1956; Peterson, 1961; Johnson, 1964; Dunoyer de Segonzac, 1970; Blatter et al., 1973; Post and Janke, 1974; Ross and Kodama, 1976; April, 1980 and 1981; Vergo and April, 1982).

Brown (1961) suggested that a specific name be furnished to a mixed-layered clay for which "the interstratification is regular and the nature of the layers is established". Martin-Vivaldi and MacEwan (1960) attempted to clarify the nomenclature of mixed-layered clays. They concluded that there is much confusion over the meaning of the term corrensite. For the sake of concision, and not to confuse the matter further, the term corrensite will be used to describe an ordered 1:1 interstratified chlorite-swelling layer clay mineral.

Mechanisms controlling corrensite formation are not yet fully understood; this mineral forms under a wide variety of conditions. Two distinct, rather general models for corrensite formation that are related to this study will be focused on. Millot (1970) used the term aggrading and degrading to describe these models.

The aggrading model was synthesized using information from Weaver and Pollard (1975), Carstea et al., (1970) and Dunoyer de Segonzac (1970). They assumed that the initial material is some 2:1 layer silicate such as smectite or vermiculite. By exposing it to a diagenetic or metasomatic environment rich in magnesium, the mineral may begin aggrading by random fixation between tetrahedral sheets of Mg-hydroxy (brucite) interlayers. The development of asymmetric structural charge distributions on the lattice causes fixation to become more ordered and results in regular alternations of 2:2 (chlorite) and 2:1 (smectite or vermiculite) sheets.

The degrading model differs from the above mentioned one in that the parent material from which the corrensite forms is usually a chlorite (Bradley and Weaver, 1956; Johnson, 1964; Post and Janke, 1973; Ross and Kodama, 1976). Structural disruption of interlayer brucite sheets by weathering or oxidation can cause selective removal of alternate interlayers. This may result from asymmetries in the structural charge distribution within the 2:1 layers (April, 1978). Ross and Kodama (1976) have shown that for chlorites, those with intermediate Fe^{+2} contents (brunsvigites)

are most likely to alter to a regularly interstratified chlorite-vermiculite. It should be noted that this model seems to be more directed toward explaining the genesis of interstratified chlorite-vermiculite rather than chlorite-smectite.

The following is a discussion of the origin and occurrences of corrensite in the East Berlin Formation. As mentioned earlier in this chapter no corrensite was detected in the New Haven Arkoses. This discussion is based on XRD analysis, more discussion of the distribution and origin of corrensite based on petrographic, SEM, and polytype analyses in Chapter 6.

Origin and Occurrence of the Chlorite-smectite Interlayers- Diffractograms of samples from the upper parts of the East Berlin Formation show well- to poorly ordered mixed-layer chlorite/smectite. The behavior of corrensite to different treatments is illustrated in Figure 37. The air-dried and glycerol-solvated samples display a peak at about 28.5 Angstroms and about 31 Angstrom respectively. Upon Mg-saturation and glycerol treatment, a well defined peak at 32 Angstroms appears as the result of regularly alternating 14 and 18 Angstrom layers. The swelling layers partially collapse to 12.5 Angstrom with potassium saturation and totally collapse upon heating to 300°C and 550°C; the 24 Angstrom superlattice peak is now the result of the regular interstratification of 10 Angstrom collapsed swelling layers

and 14 Angstrom chlorite. The behavior of the swelling layers is characteristic of smectite rather than vermiculite.

The author believes that the mixed-layered chlorite-smectite in the East Berlin sedimentary sequence is formed by the alteration (chloritization) of a precursor smectite. Smectite occurs in minor amounts in the gray mudstones and is also the predominant clay mineral in the black shale of the lake cycle sequence. It is clearly absent to rare in the corrensite-rich upper parts of the East Berlin Formation, implying that the original smectite altered to corrensite.

According to Hubert et al. (1976), structures including ripple marks, dolomite concretions, mudcracks and dinosaur footprints indicate deposition of the upper lake cycle in shallow water. The authors also stated that the combined mineral assemblage of the black shale and gray mudstone suggests alkaline, hard water lakes with abundant Mg^{++}, Ca^{++}, Na^{+} cations and HCO_3^{-} and $SO_4^{=}$ anions. Under these conditions authigenic smectite is favored (Weaver et al., 1975). However, with extended evaporation of the lake waters conditions would shift to favor corrensite over smectite. With the increased evaporation dolomite would begin to precipitate. As a result, pH would rise in the increasingly alkaline lake water which would favor the precipitation of analcime (Hay, 1966).

Corrensite formation likely began in the depositional environment and continued during burial as alkaline, magnesium-rich pore-waters continued to react with the

sediment.

Origin and Occurrence of the Chlorite-vermiculite Interlayers-
Samples collected from the East Berlin Formation near the
contact with the overlying Hampden Basalt contain a well
ordered corrensite. With increasing distance from the contact
a more poorly ordered corrensite plus relatively greater
amounts of illite are predominant.

Figure 35 is a series of diffractograms illustrating the
behavior of corrensite with different treatments. The
diffraction pattern for the air-dried sample clearly shows the
presence of a superlattice peak at approximately 28.5
Angstroms that expands upon glycolation giving a d(001)
reflection at about 30.5 Angstroms. These data indicate a
well ordered 1:1 interstratification of a 14-14.5 Angstrom
peak which swells to 16.5-17 Angstrom with glycol solvation.
Failure of the swelling layers which expanded with glycerol
to do the same upon Mg-saturation and treatment with glycerol
suggests a character more related to vermiculite rather than
smectite.

The restricted occurrence of the 1:1 regularly
interstratified chlorite-vermiculite to the East Berlin
floodplain red mudstone adjacent to the lowest Hampden lava
flow prevents an origin strictly by inheritance. Rather, it
is almost certain that the corrensite is an alteration product
formed as a direct result of the physicochemical conditions
brought about by emplacement of the lava flow. As reported

previously, corrensite occurs below the basalt. The occurrence of 1:1 regularly interstratified mixed-layered minerals as the result of hydrothermal alteration has been previously reported by a number of authors (Velde, 1977; April, 1978 and 1980).

The clay mineral composition of the East Berlin Formation grades from expanding chlorite, to chlorite-smectite, and finally to chlorite-vermiculite (Table 4) as you get closer to the basalt (Figure 6). That suggests that the corrensite originated mostly by aggrading transformation of a smectite precursor.

Sources of magnesium are believed to be related to contact with the Hampden basalt, as noticed by the concentration of corrensite near the lava. Near the contact, hydrothermal fluids originating from the lava and from the synchronous alteration of basalt fragments by superheated pore waters provided a source of magnesium. Further from the contact, magnesium was primarily derived from the thermal dissociation of dolomite (April, 1980).

SUMMARY OF THE CLAY MINERALOGY

This study of the clay mineralogy of the Triassic-Jurassic rocks of the Hartford Basin has led to the identification of the following clay minerals: illite, chlorite, smectite, vermiculite, expandable chlorite, mixed-layered illite-smectite, chlorite-smectite and chlorite-

vermiculite.

The floodplain sediments of the New Haven Arkose contain illite, chlorite, smectite, and interstratified illite-smectite and rare occurrences of vermiculite. The lacustrine sediments of the East Berlin Formation contain illite, smectite, subordinate amounts of chlorite, and corrensite.

The distribution of chlorite and mixed-layered illite-smectite in the New Haven Arkose indicates that maximum temperatures in the upper sedimentary sequence of the Hartford Basin did not exceed those attributed to the upper limit of smectite stability (100-150°C). The absence of smectite in the basal New Haven Arkose, the abundance of authigenic chlorite, and the decreased K-feldspar abundance all indicate more extensive illitization, and possibly temperatures above smectite stability, at the base of the section.

Thermal dedolomitization in the red mudstones beneath basalt flows resulted in the transfer of magnesium from carbonates to silicates and the formation of a 1:1 regularly interstratified chlorite-vermiculite (April, 1980).

Uptake of magnesium by precursor smectite resulted in the formation of an expandable chlorite followed by a 1:1 regularly interstratified chlorite-smectite in the upper gray mudstone of the perennial lake cycles. This mineral was further altered to regular interstratified chlorite-vermiculite near the overlying basalt.

CHAPTER 5

DIAGENETIC ALBITIZATION OF FELDSPARS

Diagenetic albitization of potassium feldspars has been recognized in the various formations of the Hartford Basin. Petrographic, SEM, and BSEM investigations revealed that albitization is prominent in the New Haven Arkose, whereas it is uncommon in the East Berlin Formation. The following is an attempt to describe and characterize the texture and origin of the albitized feldspar in the Hartford Basin rocks.

Albitization of K-feldspars in igneous and metamorphic rocks has long been known (Anderson, 1937; Starkey, 1959; Smith, 1974), but analogous albitization in sandstones during burial diagenesis has not been as well documented. Middleton (1972) reported that K-feldspar present in Charny sandstones (Quebec) has been albitized during diagenesis. Lajoie (1973) questioned Middleton's conclusion, suggesting a detrital rather than diagenetic origin of the albites. Recently, diagenetic albitization of K-feldspars has been recognized by a few more workers (Ogunyomi et al., 1981; Walker, 1984; and Saigal et al., 1988) in sandstones from different parts of the world.

Albitization of plagioclase in sedimentary rocks has been recorded by several workers from different parts of the world (Iijima and Utada, 1972; Surdam, 1973; Merino, 1975; Land and Milliken, 1981; Boles, 1982). Therefore, albitization of detrital feldspars is a widespread and important process which

can significantly alter the original sandstone framework composition, form several byproducts (e.g., illite, kaolinite, and calcite; Saigal et al., 1988), and modify pore size and geometry (Boles, 1982). These changes can influence reservoir properties; therefore it is important to recognize diagenetic albitization.

In this study, the author believes that albitization has occurred in situ, during burial diagenesis as seen by the pervasive albitization observed in the Upper Triassic New Haven Arkose (deeply buried) compared to the minor amounts present in the Lower Jurassic East Berlin Formation (shallow buried). The following is a presentation of a comprehensive description of textures of diagenetically albitized K-feldspar grains as revealed by optical microscopy, SEM, EDS and BSEM, and a shorter discussion of albitization of plagioclase.

PETROLOGY AND TEXTURES OF ALBITIZED K-FELDSPAR

Standard optical microscopy revealed that the albitized feldspar grains are characteristically untwinned and mostly riddled with abundant minute brownish inclusions (Figure 41). A wide range of variation from only slight to complete pseudomorphic replacement of K-feldspar by albite has been observed in the different stops of the New Haven Arkose. Generally, albitization in the New Haven Arkose tends to be incomplete and patchy high in the section, while nearly complete pseudomorphic replacement is more common lower in the section (Table 1). Saigal et al. (1988), in their study of
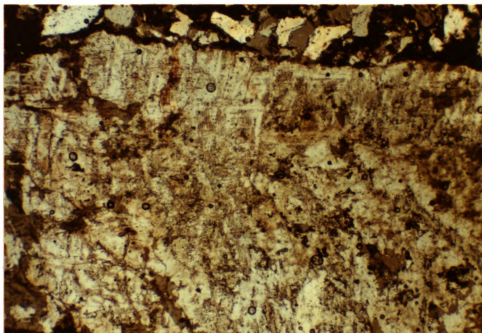
Figure 41 Thin-section photomicrograph of partly
albitized K-feldspar grain riddled with
abundant inclusions. Sample # NH-3-16.
(Frame dim.: 2.5 mm x 3.8 mm)

the Jurassic clastic reservoir rocks from offshore Norway, found that albitization occurs at depths ranging between 3.0 km to >3.5 km for the shallow and deep depths respectively. Morad et al., (1990) in their study of the Triassic sandstones from the Snorre Field, Norwegian North Sea, reported that albitization of K-feldspar would increase at greater burial depths and at higher temperatures (>3 km and higher than 100°C).

The albitized patches may be irregular or planar lamellar in shape. The planar lamellar structure resembles perthitic texture and is similar to those structures described by Middleton (1972), and Ogunyomi et al. (1981). Partially altered grains with irregular and tabular patches of albite characteristically show a blocky to tabular sector extinction pattern (usually resembling textures of chessboard albite), while complete albite pseudomorphs generally show uniform extinction (Figures 42 and 43). Similar blocky to tabular sector extinction patterns have recently been reported by Gold (1987) in partially albitized plagioclase grains. Backscattered electron images and EDS patterns clearly reveal that the grains with sector-extinction patterns are chemically inhomogeneous (Figure 44). Domains of albite are represented by darker shades of gray, while relict K-feldspar domains are represented by lighter shades of gray (Figure 45). The compositional contrast illustrated by backscattered images was confirmed by EDS and electron microprobe analyses (Figure 46, and Appendix A). This compositional inhomogeneity causes
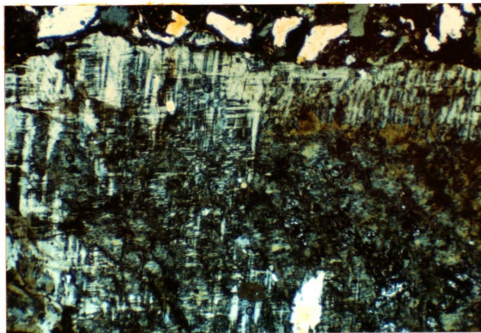
Figure 42 Photomicrograph of albitized K-feldspar grain showing blocky to tabular sector extension (chessboard albite) patterns. Sample # NH-3-16. (Frame dim.: 2.5 mm x 3.8 mm)
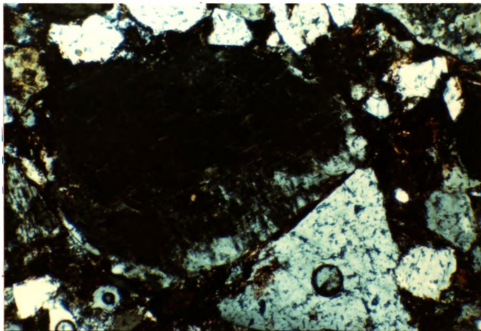
Figure 43 Photomicrograph showing uniform extinction of albitized K-feldspar grain. Surrounding grains are mostly of quartz. Sample # NH-3-16. (Frame dim.: 1.0 mm x 1.5 mm)
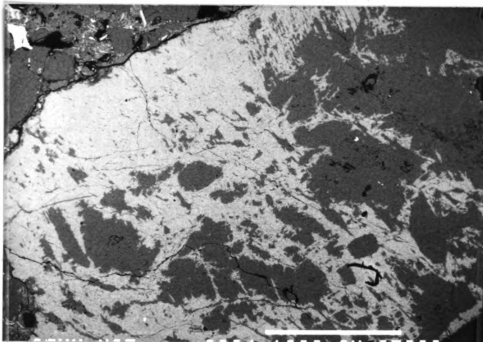
(A)
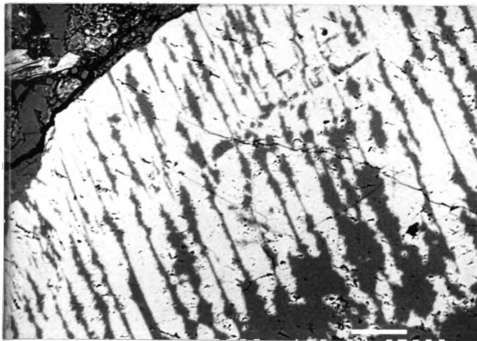
(B)

Figure 44 Corresponding BSEI (A and B) of the albitized grain in Figure (42) revealing albitization features more clearly due to chemical inhomogeneity. B) is the enlarged image of (A). Sample # NH-3-16. Bar scale= 1000 μm and 100 μm for A and B respectively.
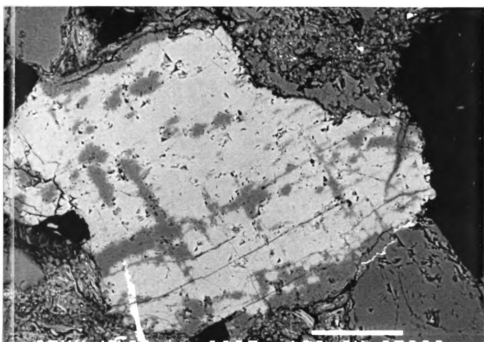
Figure 45 Backscattered electron image of albitized
K-feldspar. Notice that albite is dark
gray and K-feldspar is light gray.
Surrounding grains showing uniform dark
gray shades are quartz. Sample # NH-3-
19. Bar scale = 100 μm.

119
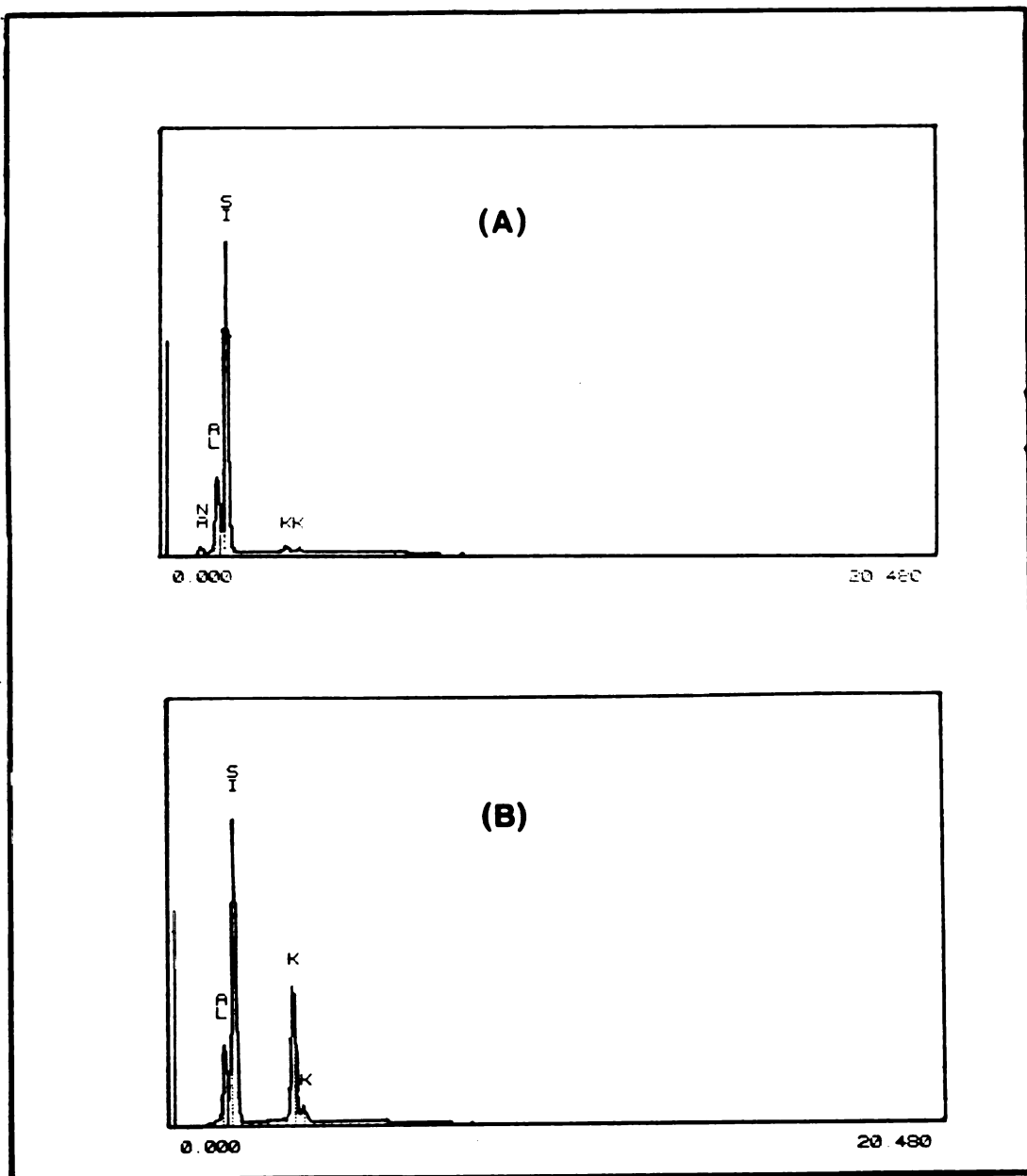
Figure 46 EDS pattern showing the elemental
chemical composition of the albitized
grain in figure (45). A) EDS pattern of
albite (dark gray) and for K-feldspar
(light gray), (B). Sample # NH-3-19.

blocky to tabular sector extinction patterns in the partly albitized grains which often resemble textures of chessboard albite (Figure 47). The characteristic minute brownish inclusions (Figure 41) are useful in finding untwinned albitized grains and have been reported by several workers (Middleton, 1972; Ogunyomi et al., 1981; Boles, 1984; Walker, 1984). These "dusty" or cloudy inclusions are believed to be composed of submicroscopic fluid inclusions and/or hematite (Walker, 1984).

Under SEM and BSEM, the albites reveal two main varieties of textures: 1) Numerous tiny euhedral albite crystals growing within leached K-feldspar grains; 2) blocky, euhedral albite crystals forming pseudomorphs of detrital K-feldspar and lacking any dissolution porosity.

Type 1- This type of albitization is common in the upper parts of the New Haven and parts of the East Berlin Formations. Saigal et al., (1988) found this type of albitization to be common at depths between 2.2 and 3 km (65 degrees to 90 degrees celsius). Albitized feldspar of this type shows few to numerous euhedral albite crystals growing within leached K-feldspar grains of a delicate skeletal structure (Figure 48). The albite crystals vary in size from about 2 to 25 microns and show sharp edges and corners. The crystal faces are smooth and most of the albite crystals show growth parallel to the cleavage planes of the parent feldspar grain and, accordingly, are preferentially oriented (Figure 49). Scattered growth of only a few tiny albite crystals within a
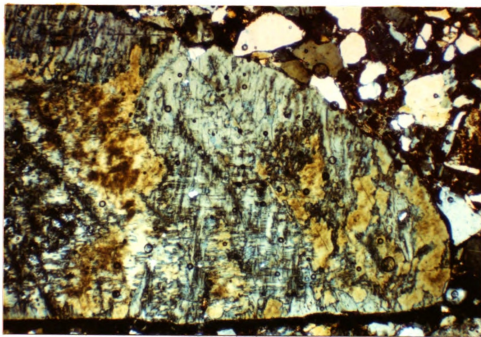
Figure 47 Photomicrograph showing albitized K-feldspar grain resembling chessboard albite. Blocky and tabular dark gray patches are albite (Alb) while light gray-yellow areas represent relict K-feldspar (Ksp). Sample # NH-3-15. (Frame dim.: 2.5 mm x 3.8 mm)
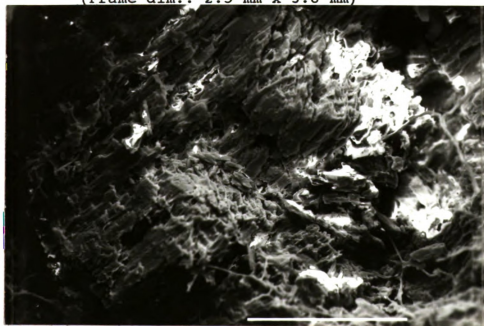
Figure 48 SEM photomicrograph of type 1 albite showing delicate skeletal structures of a leached K-feldspar grains. Sample # EB-1-12. Bar scale = 100 μm.
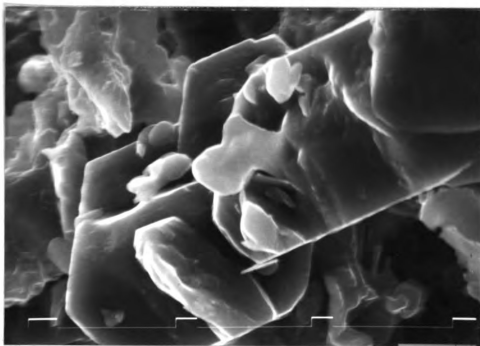
Figure 49 Enlarged SEM view showing parallel oriented albite crystals (arrows) within K-feldspar host. Sample # NH-3-36. Tic mark = 10 μm.
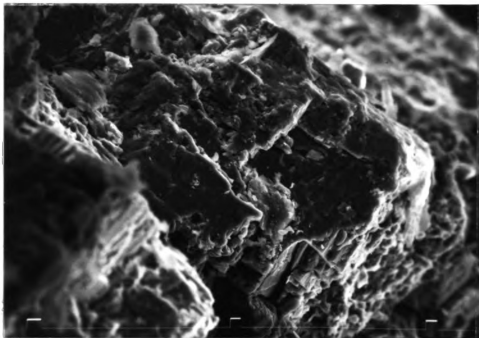
Figure 50 SEM photomicrograph of type 2 albitization showing no intracrystalline dissolution porosity. Sample # NH-4-2. Tic mark = 100 μm.

significantly leached K-feldspar grain is also common. Such leached K-feldspar grains retain their delicate skeletal structure, suggesting that their dissolution has occurred in situ after early burial compaction. Boles (1982), Gold (1987) and Saigal et al. (1988) reported similar dissolution textures in partly albitized plagioclase grains in sandstones from the Gulf Coast and offshore Norway. The tiny albite crystals in notably leached K-feldspar grains can easily be overlooked in a rapid SEM examination, particularly when viewed under low magnification.

Type 2- Pseudomorphic replacement of detrital K-feldspars by blocky albite crystals is usually seen in samples from the lower parts of the New Haven Arkose, particularly the basal unit that overlies the Milford Chlorite Schist (stop 4). Albite crystals are generally less numerous but bigger and more massive in appearance than those in type 1. Like type 1, albite crystals show typical smooth surfaces and sharp edges and corners. There is very little or no intracrystalline dissolution (Figure 50). Boles (1982) observed a lack of dissolution textures in completely albitized plagioclases. Close SEM examination reveals that albite starts growing simultaneously at several places in a preferred direction, along cleavage planes of the parent grain (Figure 51). With continuous growth, coalescence of individual albite crystals takes place, and eventually, a pseudomorph of detrital feldspar is formed (Figure 52). Partial to complete stages of albitization can be seen within
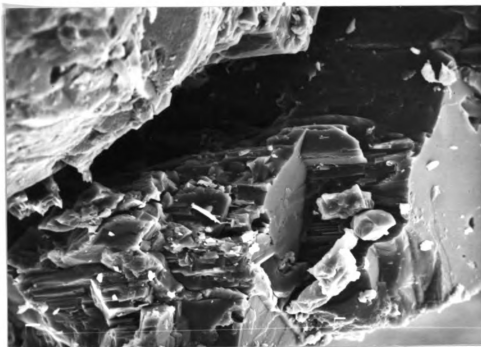
Figure 51 SEM photomicrograph showing pseudomorphic replacement of K-feldspar by blocky albite crystals. Notice the preferred orientation of albite along cleavage planes of parent K-feldspar. Sample # NH-2-6. Tic mark = 100 μm.
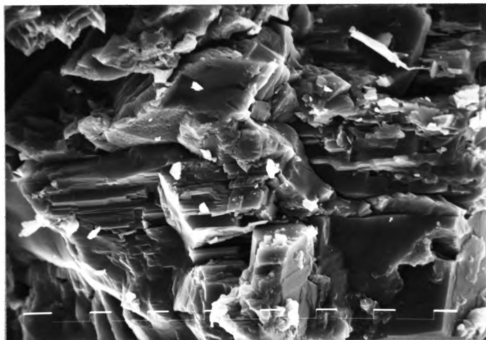
Figure 52 SEM photomicrograph showing detrital feldspar pseudomorph formed by continuous growth of individual albites. Sample # NH-2-6. Tic mark = 10 μm.

a single thin-section.

ALBITIZATION OF DETRITAL PLAGIOCLASE

Albitization of plagioclase is not quite so obvious as albitization of K-feldspar. Several grains were examined and show partial albitization. Random examination of contrast-mottled grain under BSEM imaging reveal that albitized plagioclase is not as common as albitized K-feldspar.

In the few grains investigated in this study, most of the plagioclases are twinned, although absence of albite twinning is common for albitized feldspars of diagenetic and igneous or metamorphic origins (Boles, 1982). However, individual albite crystals in diagenetic pseudomorphs may display twinning (Morad et al., 1990). Albitization of plagioclase starts preferentially along microfractures (Figure 53). The diagenetic albite is optically clear and in many samples, optical orientation of the albite follows the orientations of the two sets of twin lamellae in the plagioclase. Morad et al. (1990) mentioned that without careful microscopic examination, these albite pseudomorphs can easily be misinterpreted as unaltered detrital plagioclase. SEM and BSEM studies shows different tones of gray color, detrital plagioclase is light gray and albitization is dark gray (Figure 53), due to the variation in the average atomic number between detrital and albitized parts.
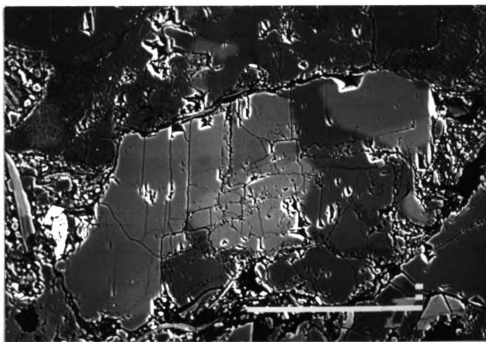
Figure 53 BSE image showing a detrital plagioclase grain
(light gray) replaced by albite (dark gray).
Notice the different range of gray tones within the
grain. Also, notice that albitization starts along
microfractures in the detrital plagioclase.
Sample # NH-3-16. Bar scale = 100 μm.

ELECTRON MICROPROBE ANALYSIS

Figures 54a, b, and c summarize the different feldspar compositions in the Hartford Basin sediments. Microprobe analysis of detrital K-feldspar show composition of a nearly pure orthoclase end member (Figure 54c).

Probe analysis of albitized K-feldspar (e.g., sample NH-3-16; stop 3) indicate that the diagenetic albite is pure (Ab = 94 to 99%), (Appendix A). However, diagenetic albite deviates somewhat from formula of ideal albite, particularly by having high total sum of K^+ + Ca^{++} ($Ab_{94.0}Or_{5.0}An_{1.0}$).

Analysis performed on the remnants of detrital plagioclase and the albitized part of it, shows An composition higher than the albitized part ($Ab_{81.5}Or_{1.7}An_{16.8}$), (Appendix B). This suggests a gradual decrease in An towards the domains of pure albite composition (Appendix A and B; sample NH-3-16), therefore suggests that albite has been formed by replacement of the plagioclase rather than by simple void filling (Boles, 1982; Pittman, 1988). This is supported by the presence of remnants of plagioclase within the domains of diagenetic albite (Figure 53).

ORIGIN OF ALBITIZED K-FELDSPARS

Diagenetic versus detrital origin of the albitized grains in sandstones has been the topic of considerable discussion (Lajoie, 1973; Walker, 1984) since the publication of Middleton's (1972) paper on albite of secondary origin in the Charny sandstones of Quebec. Detrital albite grains as well

Or

☉ N.H.FM. (STOP 4)
▲ N.H.FM. (STOP 3)
+ N.H.FM. (STOP 2)
◇ E.B.FM. (STOP 1)

90
80
70
60
50
40
30
20
10

10 20 30 40 50 60 70 80 90

Ab

An
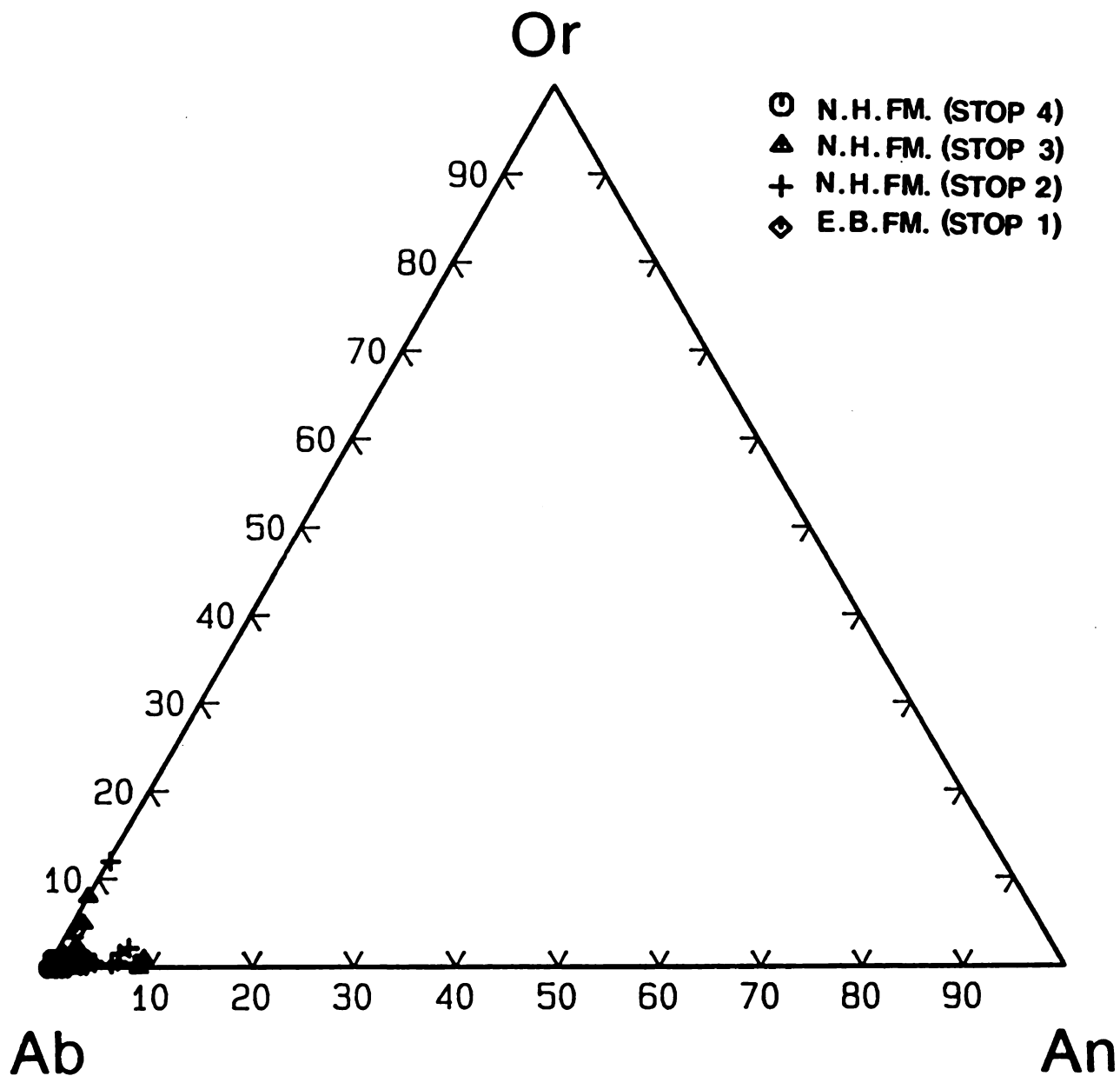
Figure 54a. Ab Or An ternary plot showing the compositional variation of microprobe analyses (Appendix A) of albitized K-feldspar in the Hartford Basin (modified after Deer, Howie, and Zussman; 1963).
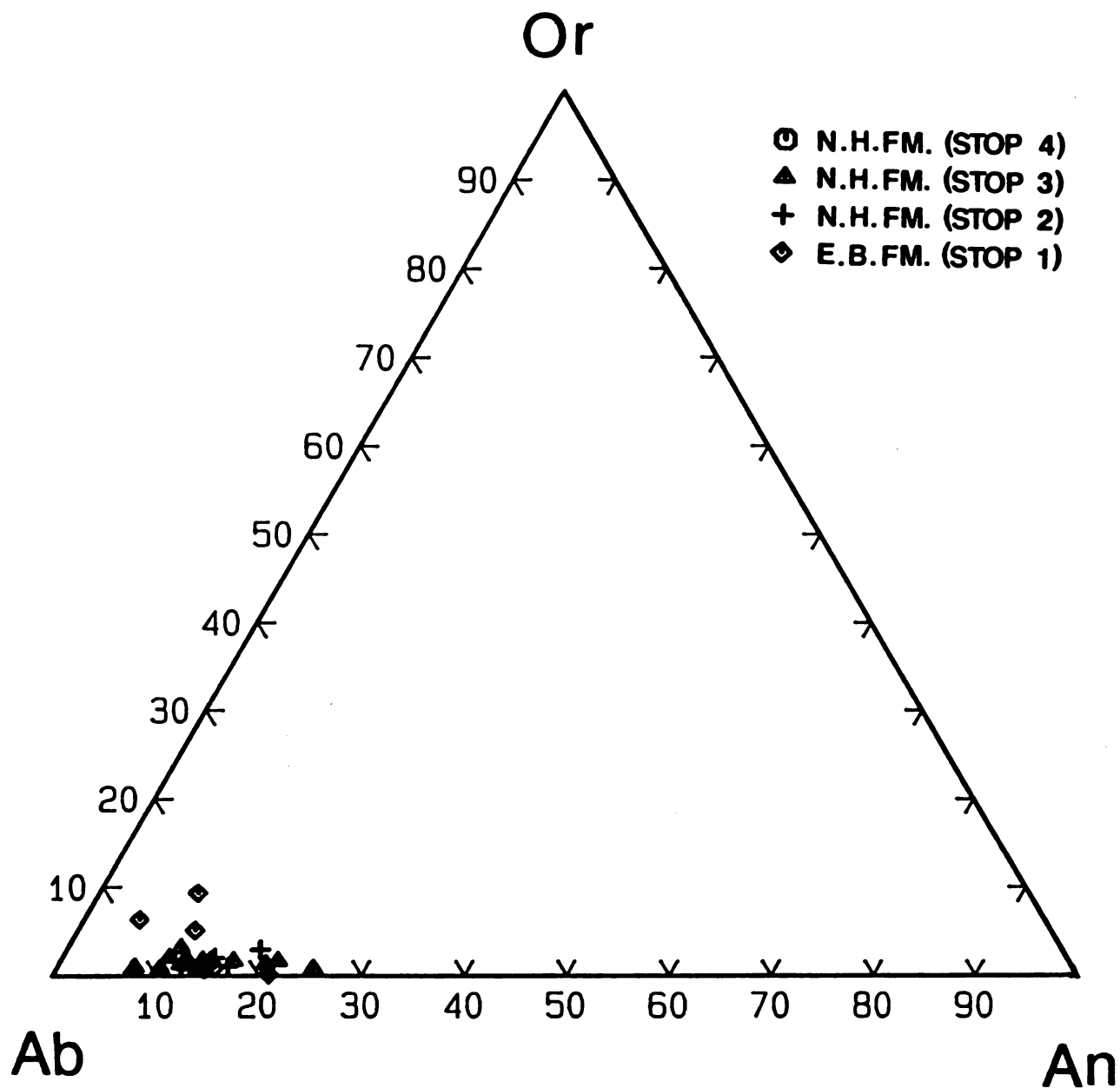
Figure 54b.   Or Ab An ternary plot showing compositional
               variations of the microprobe analyses
               (Appendix B) of detrital plagioclase feldspar
               in the Hartford Basin.
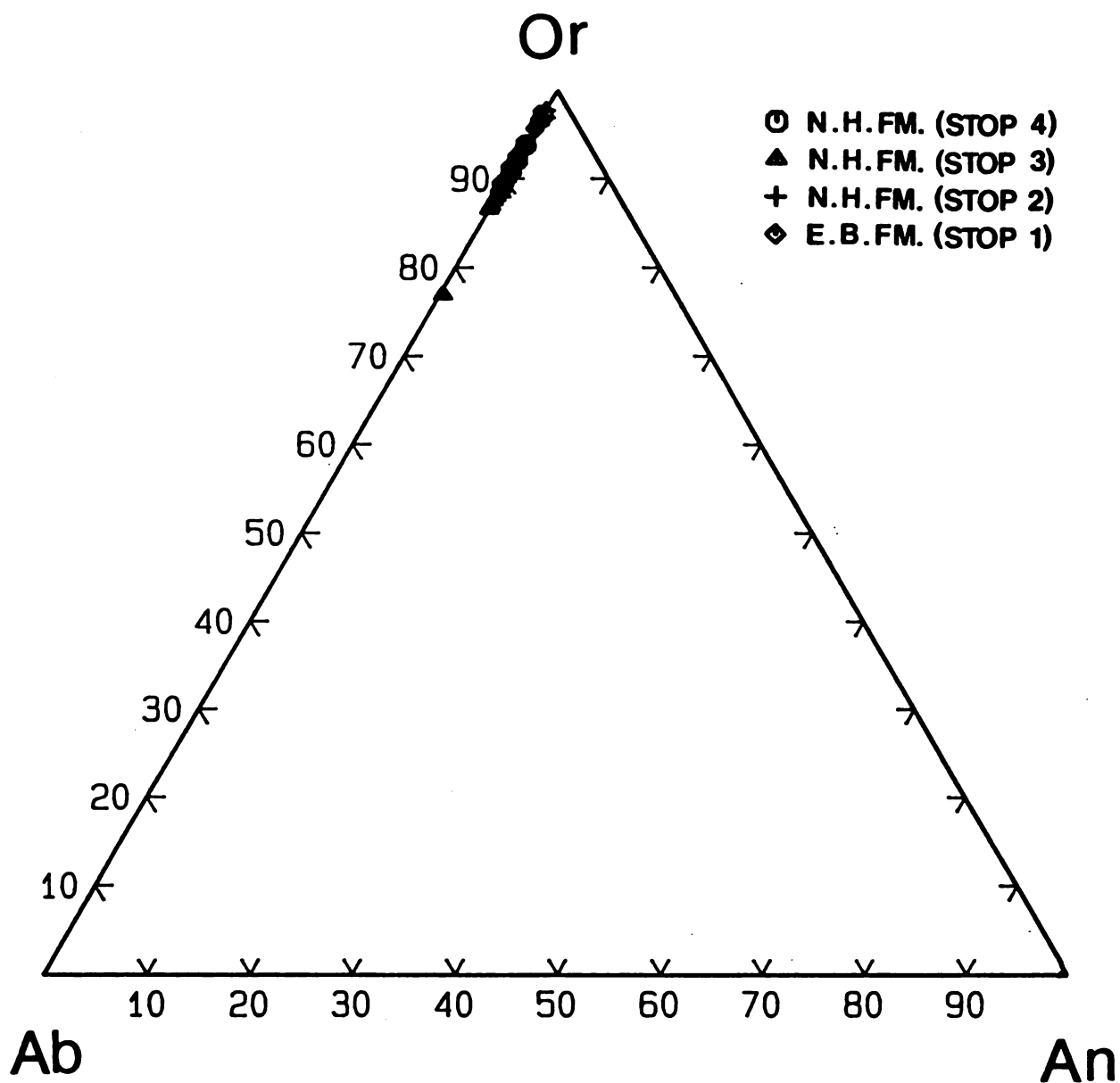
Figure 54c.   Or   Ab   An   ternary   plot   showing   the compositional   variations   of   probe   analyses (Appendix C) of relict K-feldspar in the Hartford Basin.

as authigenic albitized K-feldspar were observed in the studied formations of the Hartford Basin. Saigal et al., (1988) established a combination of petrological and chemical characteristics to prove that albitization has occurred in situ during burial diagenesis. Many of their criteria fit perfectly the Hartford Basin albites. The evidence is as follows:

1) Crystal Morphology

SEM studies reveals that albite crystals in both of the albite textural types are nearly euhedral with sharp edges and corners and smooth crystal faces. If this albite had formed in the source area, the crystals would have subjected to some chemical and physical alteration during weathering in the source area, and transportation. Also, albitized K-feldspar grains show delicate skeletal structures that suggest that dissolution has occurred in situ. Particularly, sharp crystal edges and corners, having the highest free energy, are the most susceptible to dissolution. Also, crystal edges and corners are expected to be rounded during transportation of the albitized grain from the metamorphic source rock area.

2) Twinning

All of the albitized grains are untwinned. Absence of twinning is considered an important feature of diagenetic albite (Kastner, 1971; Kastner and Siever, 1979; Saigal et al., 1988). As revealed by SEM studies, albite nucleates at several places on the parent K-feldspar grain and eventually individual albite crystals grow and converge to form untwinned

albite pseudomorphs (Walker, 1984).

The partially albitized grains resembling chessboard albite reveal on close examination that the checkered pattern is caused by compositional inhomogeneity and not because of albite twinning (as described earlier). Lack of chessboard twinning in albite pseudomorphs also confirms that the checkered pattern in partially albitized grains is not due to typical chessboard twinning. Texturally, the classic chessboard albite shows more regular, uniformly thick, parallel, and sharper extinction patterns than those described by the partially albitized grains (Starkey, 1959; Walker, 1984; Gold, 1987; Saigal et al., 1988). Moreover, most studies suggest that the chessboard albite forms by the replacement of K-feldspar involving the combination of external and internal stresses and inherited characteristics of the potash feldspar lattice in the replacing albite (Starkey, 1959). In contrast, the albite replacement in the Hartford Basin sandstones is clearly a low-temperature, dissolution-reprecipitation process, not a high-temperature metamorphic recrystallization, which is discussed later in this chapter.

3) Composition

Microprobe analyses show that albite is almost pure (Ab = 96.1 to >99.8%), irrespective of textural type (Appendix A; Figure 54a). This chemical purity also suggests a diagenetic origin for the albite (Kastner, 1971; Kastner and Siever, 1979; Boles, 1982 and 1984; Walker, 1984; Morad 1986).

Microprobe data show that replacement albite and albite overgrowth are similar in composition (Ab = 99.1 to 99.9%), (Appendix A; Figure 54a). Detrital plagioclase has a different composition ($Ab_{81.5}An_{1.7}Or_{16.8}$), (Appendix B; Figure 54b). This similarity in composition between albite overgrowth and replacement albite provides good evidence that albitization has occurred during burial diagenesis and is not a feature inherited from the clastic grains.

4) Inclusions

The presence of abundant minute dusty inclusions is another characteristic of albitized grains (Ogunyomi et al., 1981; Boles, 1982; Walker, 1984; Saigal et al., 1988). Petrographically, their grayish white appearance under reflected light suggests that are only vacuoles.

5) Change in Albitization with Depth

A plot of point counting data of % albitized K-feldspar versus depth (Figure 55) shows that albitization starts near 1.5 km (lower parts of the East Berlin Formation) and reaches a maximum by 3.5 km, where nearly complete pseudomorphic replacement is more common. This increase of the percentage and degree (partial to complete) of albitized K-feldspar with depth also suggests that albitization has taken place during burial diagenesis. The less abundant albitization in the basal New Haven Arkose (stop 4), which was most deeply buried (> 3.5 km), suggests that burial depth alone is not the only factor that controls albitization.

Figure 55 Plot of the percent albitized K-feldspar grains
(from point counts data) versus depth in the New
Haven and the East Berlin Formations. Trend
showing increase in albitization with increase in
depth.
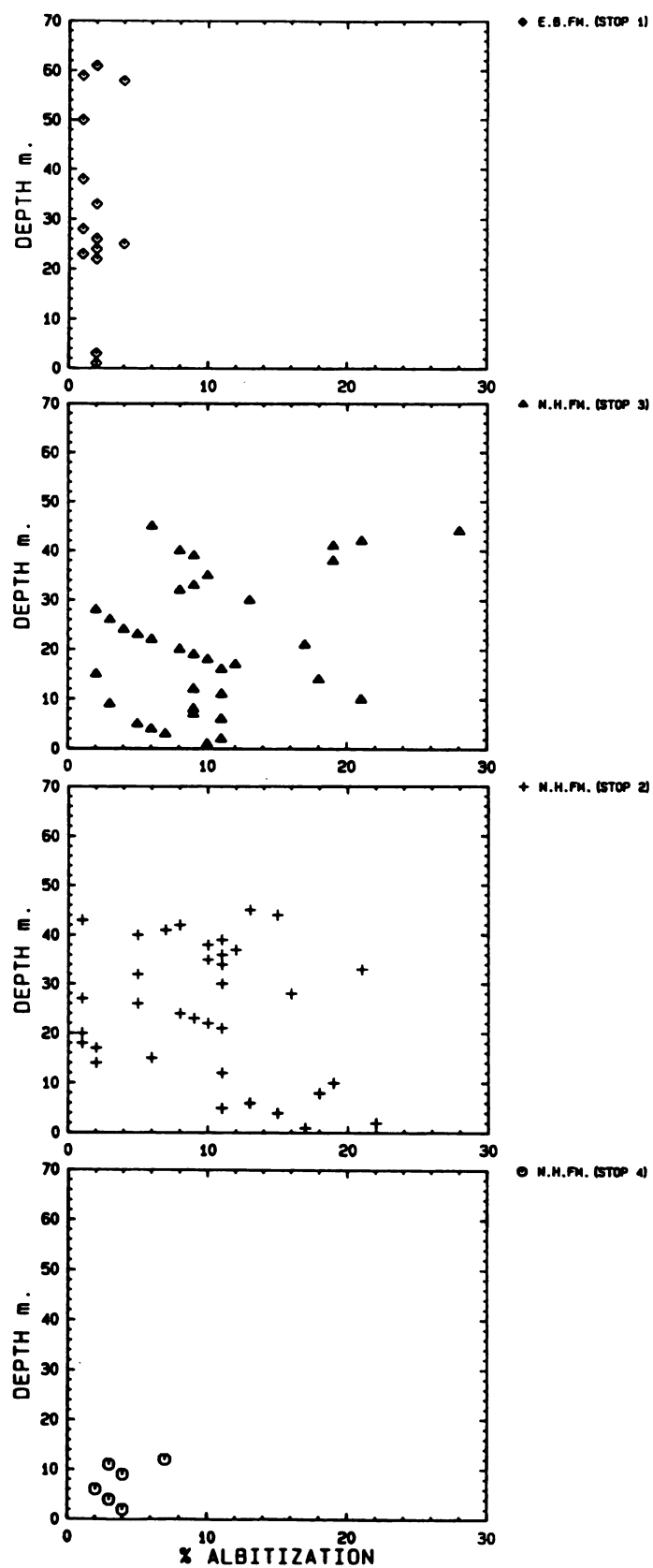
Figure 55

Process of albitization in the studied Formations

SEM examination of albitized grains clearly shows that albite nucleates at several sites on the parent K-feldspar grain (Figure 50). Eventually, these individual crystals grow and coalesce to produce albite pseudomorphs (Figure 51). The sharp contacts between relict K-feldspar and pure albite crystals support the suggestion of Boles (1982) that albitization proceeds by a dissolution-precipitation mechanism. The fact that albitized grains of the New Haven Arkose at greater depths (> 3.5 km) lack dissolution textures, while at shallower depths (< 2 km) the albites of the East Berlin Formation show abundant dissolution textures, suggests that the rate of K-feldspar dissolution versus albite precipitation may be responsible for the resulting albite type. It is believed that K-feldspar dissolution has been more rapid than albite precipitation during the formation of type 1 albite, while a balance between the two would favor the formation of type 2 albite. Saigal et al. (1988) suggested that the rate of albite precipitation increases at greater depths due to higher temperatures and replacement of K-feldspars by pseudomorphic albite (type 2) is favored at greater burial depths (> 3.5 km). Aagaard et al. (1990) supported the view of Saigal et al. (1988), that albitization of K-feldspar is going on these sandstones at burial temperatures between 65 and 125°C. However, rates of dissolution also increase with temperature and the existing data indicates that both K-feldspars and albite have the same

activation energy. Therefore Saigal's explanation is probably not favorable.

Albitization of plagioclase at an earlier burial stage than for K-feldspar has been observed by Kaiser (1984) and Milliken (1989) in the Oligocene Frio Formation of Texas Gulf Coast. Land and Milliken (1981) found that the zone of K-feldspar disappearance is between 3,600 m and 4,200 m (130-150°C) in the Frio Formation. Gold (1987) observed that in sandstones from Louisiana Gulf Coast the K-feldspar is unaltered at depths shallower than 4,800m (125°C), whereas the plagioclase is albitized. Morad et al. (1990) reported that albitization of detrital plagioclase has been accomplished by dissolution-precipitation processes at about 75-100°C. Thus, there is a similarity in the diagenesis behavior of detrital feldspars between some of the Gulf Coast sandstones and those of the Hartford Basin where minor albitization of K-feldspars were observed in the East Berlin Formation (<120°C) (Pratt et al., 1988). As depth increased more K-feldspar albitization were noted (Figure 55), except in the basal part of the section.

A mechanism for the removal of potassium and supply of sodium is required for the dissolution of K-feldspar and precipitation of albite. If albite precipitation was homogeneous on K-feldspar grain surfaces, then replacement of K-feldspar will take place only on grain surfaces forming thin rims of albite. Such rims will act as shields and preserve the remaining part of the clastic K-feldspar grain.

Microporosity observed between authigenic albite crystals may have acted as pathways for the outward diffusion of K^+ from the K-feldspar core and inward diffusion of Na^+ to form albite. Accordingly, during the deep burial of the New Haven Arkose, these micropores may have mended to produce a tight authigenic Na-feldspar.

Replacement of K-feldspar by albite can be expressed by the following reaction:

$$KAlSi_3O_8 + Na^+ \rightarrow NaAlSi_3O_8 + K^+ \qquad (1)$$

This reaction is believed to be essential in producing type 2 albitization where byproducts and dissolution textures are absent. Middleton (1972) and Walker (1984) suggested a similar direct replacement mechanism.

The presence of intracrystalline dissolution textures associated with type 1 albite (Figure 48) in the East Berlin Formation suggests that replacement of detrital K-feldspar in the East Berlin Formation is not by equal volume. Part of the dissolution texture may have formed during feldspar leaching by meteoric water (i.e., before albitization), while some could be due to albitization. Some of the Al and K released during albitization can be incorporated into illite.

Alteration of smectite to illite consumes K^+ produced from reaction (1), and releases Na^+ that is likely to contribute towards albitization. The growth of albite crystals along the K-feldspar cleavage planes suggests that the replacement is guided by cleavage planes. Perhaps cleavage surfaces have greater free energy or higher

dissolution rates. Also, albitization is enhanced along grain fractures where fluid can easily infiltrate. Boles (1982) and Milliken et al., (1985) mentioned that surface dissolution kinetics, lattice defects, and plutonic versus volcanic origin of K-feldspar are other factors that could be critical for the albitization process.

The fact that albitization is more pronounced lower in the section (> 3.0 km) suggests that higher temperatures are favored. Type 2 albitization of the New Haven Arkose, forming complete pseudomorphs with no dissolution textures, is likely to occur under faster rates of nucleation and crystal growth of albite. The higher the temperature the faster would be the rates nucleation and crystal growth. This may account for the dominant occurrence of type 2 albites at greater depths (> 3.0 km).

The absence of prominant albitization at stop 4 is a puzzling question because the QFR data (Figure 7a) show that the total feldspar is the same at stop 4 as at stops 2 and 3. Also the percent K-feldspar decreases with the increase of chlorite at stop 4 (Figure 40). But this does not mean that the feldspar at stop 4 is mainly unalbitized plagioclase, as evident by the low content of plagioclase at stop 4 (Table 1 and Figure 7c), i.e. the decrease of K-feldspar relative to the increase of chlorite does not mean the plagioclase content should be higher than K-feldspar, but it means that K-feldspar was altered to mica (illite) or that K moved out of the system.

More than one reaction can be written to express albitization of plagioclase. Due to low mobility, Al^{3+} might be conserved in these reactions. Land (1984) suggested the following reaction:

Anorthite + $2Na^+$ + $4H_4SiO_4$ → 2Albite + Ca^+ + $8H_2O$ (2)
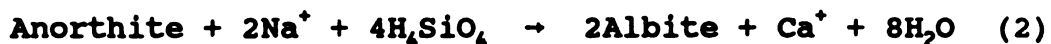
According to this reaction, the volume of albite produced upon albitization of plagioclase is twice the volume of anorthite component. The presence of albite overgrowths formed in the Hartford Basin sandstones, the lack of microporosity in the albitized plagioclase, and the presence of zeolite in the New Haven Arkose indicate that this reaction might be important.

Another explanation is that kaolinite was formed as a byproduct of the albitization reaction proposed by Morad et al. (1990):

Anorthite + HCO_3 + H^+ + H_2O → Kaolinite + Calcite (3)
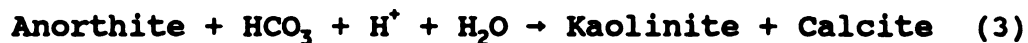
K^+ released from albitization of K-feldspar is used in the illitization of kaolinite:

2 K-feldspar + 2.5 Kaolinite + Na^+
→ Albite + 2 Illite + 2 Quartz + 2.5 H_2O + H^+ (4)

The small amounts of kaolinite formed in these sandstones indicate that reactions 3 and 4 may not have been important.

Sources of sodium

The sources of sodium needed for albitization in the Newark Supergroup are not clear (Oshchudlak and Hubert, 1988). Generally, high sodium concentrations are not necessary for albitization (Schwartz and Longstaffe, 1988). Several

possible sources of sodium are proposed for the sandstones of the Hartford Basin. Perhaps much of the sodium was provided by mobile pore fluids with substantial flow rates that carried sodium from outside the basin (Hubert and Meriney, 1988). In this model, heated water rose through the basin fill, transporting dissolved sodium obtained from crystalline rocks beneath the basin. Again, the near absence of albitization at stop 4 could be due to the rapid filling of the basin with sediments that the albitization reaction never had enough time to be completed.

The East Berlin Formation shows little evidence for albitization and authigenic albite, whereas the New Haven Arkose is dominated by both. A satisfactory explanation might be that the New Haven Arkose was more deeply buried than the overlying East Berlin Formation and that explains why it has the highest proportion of highly altered plagioclase grains and the most albitized K-feldspar and authigenic albite. The plagioclase grains are altered, but not cavernous or skeletal, so it is likely that dissolution of plagioclase grains was volumetrically a minor source of the sodium needed for albitization.

Also, some sodium may have been released during conversion of smectite and interlayered smectite/illite to illite (reaction 1, Chapter 4; Hower et al., 1976).

My data show that samples of the New Haven Arkose (stop 3; Figure 5b) from within several meters of the dolerite dike are slightly more albitized than those away from the dike near

the bottom of the section. The thermal gradient created by the dike may have promoted migration of sodium ions towards the higher temperatures. Van Houten (1965), in his study of the Lockatong Formation in the Newark Basin, estimated this temperature to be between 350 and 700°C. Another possibility is that some sodium may have moved in hydrothermal solutions associated with emplacement of the sill in a manner similar to that suggested for arkoses in the Hartford Basin by Heald (1956).

CHAPTER 6

CHLORITES

This chapter is focused on the discrimination of different types of chloritic clays in the fluvial and lacustrine rocks of the New Haven and East Berlin Formations, Hartford Basin. This includes the identification and distribution of detrital and authigenic chlorite, polytype analyses, diagenetic history versus burial depth, and origin of the various types of chlorite.

The New Haven Arkose contains abundant chlorite of both authigenic and detrital origin, whereas the East Berlin Formation is dominated by detrital chlorite (Chapter 3 and 4). Flakes of detrital chlorite generally occur in discrete laminae, often aligned along bedding planes, as matrix, or as reworked mudstone clasts. The authigenic chlorite occurs as thin isopachous coatings around detrital grains, as a pore-filling cement, and occasionally as a pore-lining cement that is absent at grain contacts.

As mentioned earlier, the petrographic studies show the presence of a number of cements in addition to chlorite, including quartz overgrowth, feldspar overgrowth, calcite, dolomite, and local zeolite cement. In the East Berlin Formation, there is an inverse relationship between the amount of dolomite and the minor amount of chlorite cement (Figure 56). Textural evidence suggests that the grain-coating (chlorite-vermiculite) and pore-lining chlorite formed very

Figure 56 Variation in the dolomite versus chlorite in the sediments of the East Berlin Formation.

early in the diagenetic sequence (Chapter 3). This would imply according to Hower et al. (1976), that it was formed during or after significant illitization of smectite. The more widely occurring pore-filling chlorite which occurs only in the New Haven Arkose relates to a later event during burial (Chapter 3). This may account for the near absence of chlorite cement in the shallow sediments of the East Berlin Formation.

The following is a detailed description of the morphology of the different authigenic chlorite textures as shown by petrographic, SEM, BSEM and EDS techniques. This will be followed by XRD and polytype study of different types of chlorite as an attempt to interpret their mode of origin.

MORPHOLOGY OF AUTHIGENIC CHLORITE

Three main varieties of authigenic chlorite were encountered in the basin: grain-coating, pore-lining and pore-filling cements partially cementing in between detrital feldspar grains. In thin-section all forms of chlorite are pale green in color under transmitted light and show gray-yellow birefringence colors in polarized light. Distinction between grain coating and pore-lining chlorite is based upon the presence or absence of chlorite at grain contacts (Wilson and Pittman, 1977). Microscopic investigation shows that grain-coating is present on and between grain contacts (Figure 57), whereas pore-lining chlorite is absent at grain contacts (Figure 58).
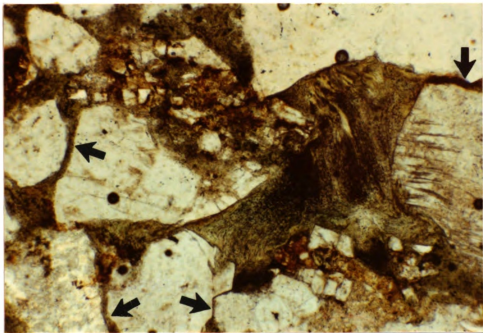
Figure 57 Grain-coating chlorite rimming around detrital grains and in between grain contact (arrows). Notice a later generation of chlorite cement within the voids. Sample # EB-1-25. (Frame dim.: 1.0 mm x 1.5 mm)
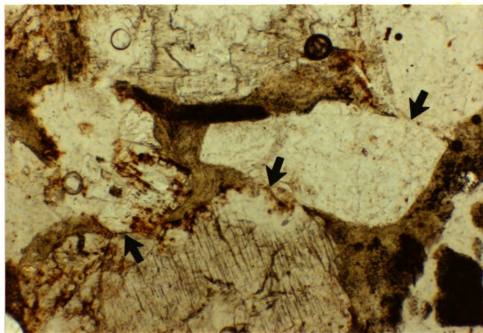
Figure 58 Pore-lining chlorite covering different detrital grains, but absent at grain contacts (arrows). Sample # NH-4-6. (Frame dim.: 1.0 mm x 1.5 mm)

Grain-coating chlorite-vermiculite

This form of chlorite-vermiculite mixed layer (corrensite) is very distinctive and it is only observed at stop 1 of the East Berlin Formation. The corrensite crystals have grown perpendicularly onto the host grains forming an isopachous rim of cement. Under the electron microscope, the enveloping corrensite typically shows slightly curved or crenulated plates (Figure 59), arranged in a cellular or honeycomb pattern. Individual crystal plates may not always be resolved. In this form, chlorite resembles the crinkly morphology of mixed-layer chlorite/vermiculite (corrensite) that probably formed from a chlorite-smectite precursor (Tompkins, 1981; Helmold and Van de Kamp, 1984; Humphreys et al., 1989), but a non-swelling chlorite structure can be confirmed by XRD (sample # EB-1-11, Table 4).

Pore-lining authigenic chlorite

This form of chlorite is confined to few samples from stop 4 of the New Haven Arkose. Generally, this chlorite consists of idiomorphic chlorite platelets arranged in a rosette-like pattern on a plagioclase feldspar grain (Figure 60), typically 3-8 microns in maximum dimension as evidenced by SEM. Petrographic examination revealed the presence of two generations of superposed pore-lining chlorites. Pale green chlorite fringes grow perpendicular to the substrate grains and line the pores, in contact with a finer green chlorite filled with dark inclusions (Figure 61).
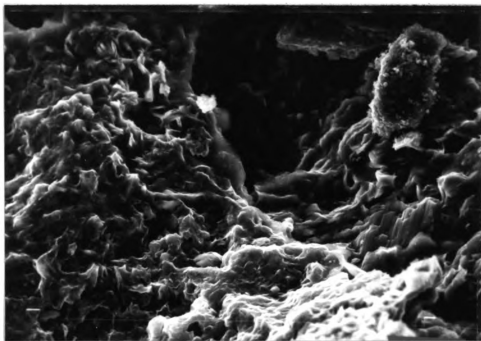
Figure 59 SEM photomicrograph showing crenulated plates of chlorite-vermiculite grain-coatings of detrital framework. Sample # EB-1-25. Tic mark = 100 μm.

Figure 60 SEM photomicrograph showing euhedral rosette-like platelets lined on a detrital plagioclase feldspar grain and growing towards the pore. Sample # NH-4-2. Tic mark = 10 μm.
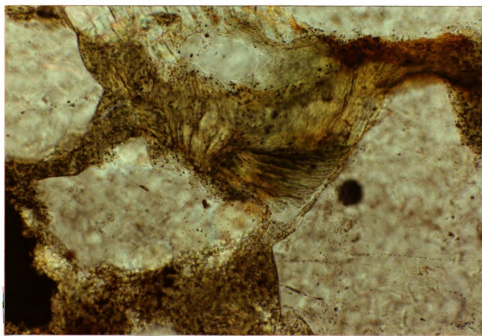
Figure 61 Photomicrograph of multiple pore-lining chlorite superposed one on top of the other. Sample # NH-4-1. (Frame dim.: 0.4 mm x 0.6 mm)

Pore-filling authigenic chlorite

This form of chlorite usually consists of subhedral to euhedral crystal plates arranged in a haphazard face-to-edge cardhouse arrangement. Some pores are totally occluded, whereas adjacent pores may remain empty (Figure 62). Sometimes the cement forms fan-shaped clusters of crystals (rosettes) up to 10 microns in diameter. Samples from stop 4 are dominated by this type of cement, however a few samples from stop 3 of the New Haven Arkose show its presence.

X-RAY DIFFRACTION

Some chlorite-rich specimens are recognizable petrographically, but most are only revealed by X-ray analysis of clay mineral suites. XRD analyses were taken on the <2 micron fraction of both sandstones and mudstones from the four stops of the studied formations. Throughout the succession the mudstones record a detrital clay assemblage of chlorite and illite with variable amounts of mixed-layer chlorite-smectite and chlorite-vermiculite (other clay minerals are discussed in Chapter 4). EDS analysis shows that the detrital chlorite is mainly Mg-chlorite (clinochlore species) (Figure 63).

The authigenic chlorite was found to have weak and broad (001) 14 Angstroms and (003) 4.7 Angstroms reflections, but the (002) 7 Angstroms reflection and the (004) 3.55 Angstroms reflection were very sharp and intense (Figure 64). The small broad (001) reflection was largely unaffected by glycerol-
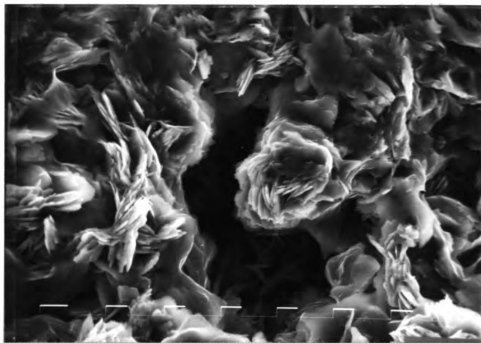
Figure 62 SEM photomicrograph showing pore-filling chlorite cement. Sample # NH-4-1. Tic mark = 10 μm.
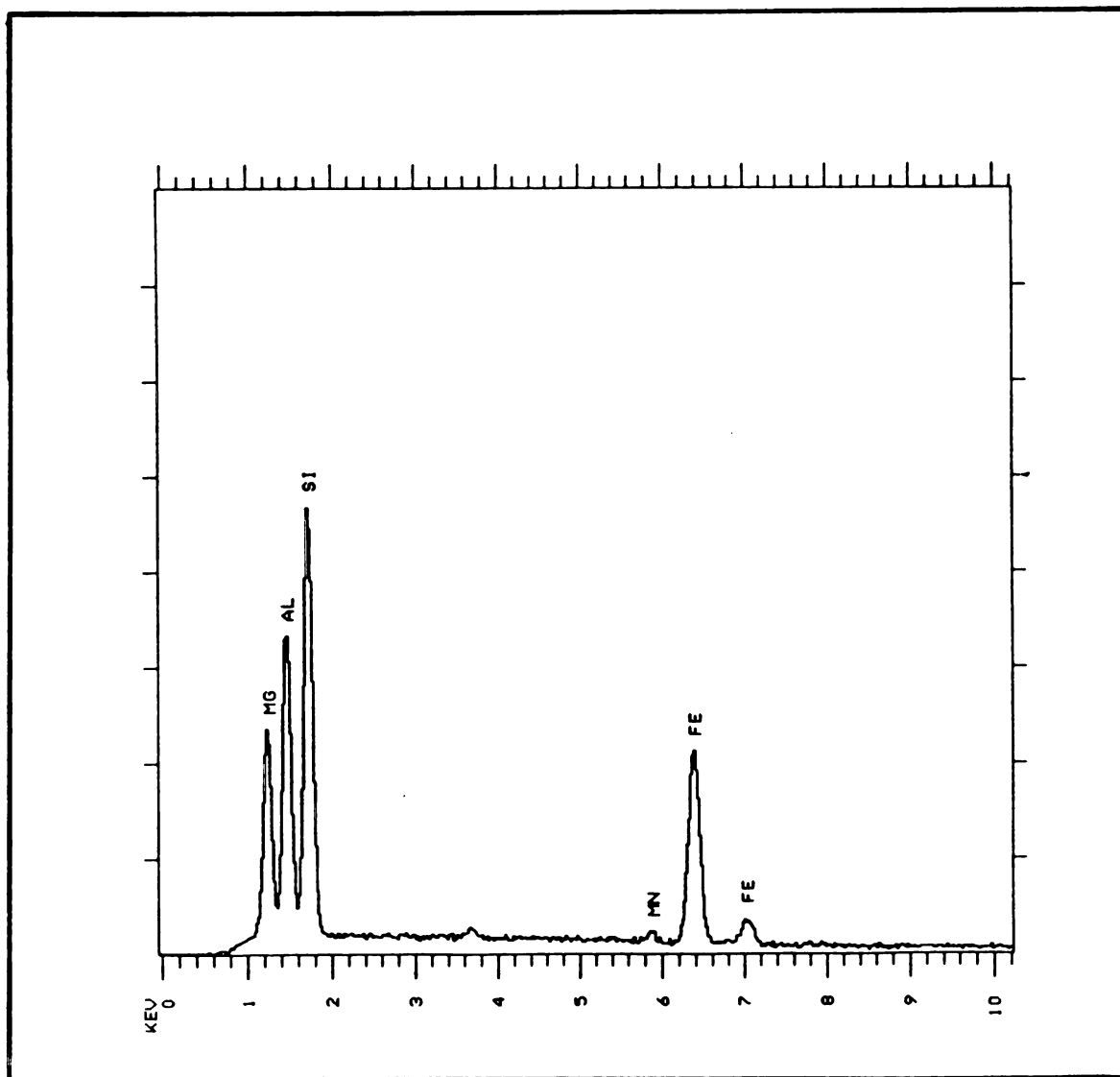
Figure 63 EDS pattern showing relatively Mg-rich chlorite at stop (4). Sample # NH-4-6.
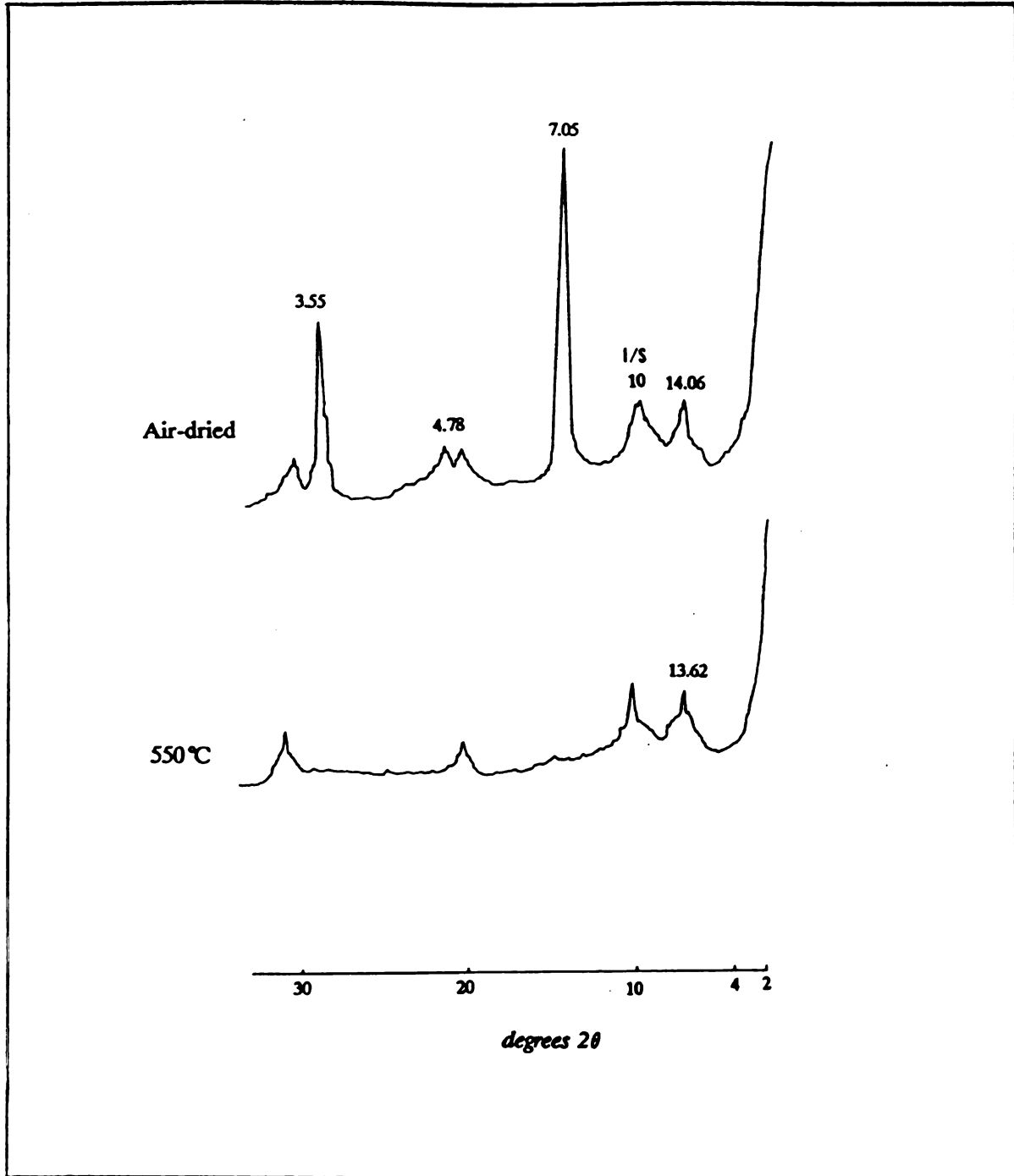
Figure 64 XRD pattern of the authigenic pore-lining clay assemblage showing the marked differences in intensity of the (001) and (002) basal reflections of chlorite and the slight shift in spacing of the (001) reflection after heating. Illite/smectite (I/S) is also recorded. Sample # NH-4-1.

solvation, although a slight reduction in intensity was noted. When heated to 500 degrees celsius, the (002) reflection decreased slightly in intensity.

On the basis of XRD alone, the chlorite has suppressed (001) reflections that, in the absence of chemical data, would be characteristic of a typical chamosite structure (Wilson, 1987). A weak, low intensity 001 reflection and intense (002) reflection would seem to be a characteristic of authigenic chlorites (Wilson, 1987; Humphreys et al., 1989).

ELECTRON MICROPROBE ANALYSIS

Use of an electron microprobe allows the chemistry of the chlorites, in particular the relative amounts of Fe, Mg and Al, to be determined. There are limitations to these analyses. The principal drawback is that the probe can not separate ferrous from ferric iron. Another serious problem results from the fine grain size of the authigenic chlorite and its common occurrence coating detrital grains; it is often difficult to direct the beam onto the clay plates without probing the host detrital grain or other contaminants because the volume analyzed (the surface area, about 2 microns in diameter, and also the depth of penetration into the sample of about 5 microns) is often greater than the dimensions of individual clay particles (Humphreys et al., 1989). With respect to spatial resolution, probe analyses are thus inferior to those obtained from analytical transmission electron microscopy (ATEM). Minor discrepancies in chemical

analyses might occur between the two techniques because of normalization of data with ATEM. Finally, there is the possibility of minerals such as hematite becoming attached to the clay plates and adversely affecting the measured Fe:Mg:Al ratios (Curtis et al., 1984). Given these difficulties, seven authigenic chlorite samples were probed.

Whittle (1986) estimated the compositions of authigenic chlorite from XRD data using the equation after Brindley (1961) and Shirozu (1958). The regression equation of Brindley (1961) allow the estimation of chlorite tetrahedral compositions to within 10%, or 0.1% Al. He estimated the octahedral composition to within 10% Fe using the regression equation after Shirozu (1958), providing the species are trioctahedral. Post and Plummer (1972) investigated IIb chlorites from Flagstaff Hill, California by XRD, DTA and IR spectroscopy and found that Brindley's equation gave a good correlation between tetrahedral Al and basal spacing. However, Whittle (1986) concluded that the compositions of the Ib chlorites derived by calculation from XRD are not the same as compositions of the same material determined by TEM/EDS. He reported major differences in compositions between both methods for both the tetrahedral and octahedral sheets. Therefore, caution should be exercised when estimating the composition of sedimentary chlorites by XRD.

Probe analyses for a total of seven samples from the New Haven Arkose and the East Berlin Formation are summarized in Appendix D. Although authigenic chlorites of similar optical

characteristics have commonly been described in the recent literature (Hayes, 1970; Curtis et al., 1984, 1985), there is considerable variation in their reported chemical compositions (Appendix D). In this study, variation in composition of authigenic chlorite were detected within the same polished thin-section (e.g. sample NH-4-2; Appendix D).

Compared to the average structural formula for the authigenic chlorites recorded in the literature (Boles and Franks, 1979; Curtis et al., 1984, 1985; Whittle, 1986), the Triassic New Haven Arkose chlorites (stop 4) are notably Si-rich and include high amounts of Mg. However, other samples representing East Berlin grain-coating chlorites are equally Mg-rich.

CHLORITE POLYTYPE ANALYSES

Generally, the various polytypes of a given species result from different ways of stacking identical layers. The (001) reflections for any stack of such layers are identical; the differences appear mainly in the hkl reflections. The best way of determining polytypes is by comparing the XRD pattern of an unknown with standard patterns. A ripidolite chlorite (Ib type) sample number CCA-1 from Flagstaff Hill, El Dorado County, California, was used as a clay standard for the polytype study. Mixtures of two polytypes, or presence of additional minerals, can create difficulties in interpreting these polytypes (Eslinger and Pevear, 1988). Polytypism refers to different ways structural unit layers of

the same composition may be superimposed in the crystalline state. During crystal growth, one of a number of possible stacking sequences will form, dependent upon such factors as temperature, pressure, growth rate, and nature and activity of the reactants (Brown and Bailey, 1962; Hayes, 1970).

All chlorites are based on the same structural scheme; one 2:1 layer (talc-like) and one hydroxide sheet (brucite-like) combine to form the structural unit layer (Hayes, 1970). Brown and Bailey (1962) demonstrated that a hydroxide sheet may be placed upon a 2:1 layer in four different ways, to give four different types of chlorite structural unit layers, called Ia, Ib, IIa, and IIb.

The IIb polytype is by far the most stable and abundant in nature, being the high-temperature form in low-grade metamorphic rocks and detrital sediments (Brown and Bailey, 1962). The Ia and Ib polytypes are more typical of diagenetic, authigenic, and pedogenic chlorites (Hayes, 1970). Type IIa has not yet been identified in nature (Eslinger and Pevear, 1988).

Results of chlorite polytype analyses of the East Berlin Formation and the New Haven Arkose show the presence of Ib and IIb polytypes. Chlorite polytypes were identified by h0l reflections (Hayes, 1970). Because relative intensities and d-values depend on composition and are greatly affected by the presence of illite (as its presence makes identification of IIb polytype difficult unless chlorite is the dominant clay mineral; Hayes 1970; Gottfried and Kotra, 1988), samples were

analyzed where illite peaks were weak or nearly absent. Generally, analysis of chlorite polytypes is hindered by the ubiquitous occurrence of illite.

In the East Berlin Formation samples, where chlorite polytypes could be analyzed, the IIb polytype is dominant with minor occurrences of Ib type (Figure 65 and 66). The IIb polytype, characterized by 2.59, 2.55, 2.45, 2.39, and 2.26 Angstrom reflections (Hayes, 1970; Moore and Reynolds, 1989), implies a higher temperature origin (metamorphic or hydrothermal) for the chlorite and would be expected to be found in deeply buried sediments or as a detrital mineral.

The New Haven Arkose samples are dominated by IIb and Ib polytypes. The Ib polytype, as identified by intense 2.51, 2.15, 2.69, and 2.65 Angstrom reflections (Brown and Bailey, 1962; Hayes, 1970; Bailey, 1980; Moore and Reynolds, 1989), represents diagenetic chlorite. Characteristic reflection of the IIb chlorite polytype are similar to those of the East Berlin Formation.

Hayes (1970) investigated the polytypism and chemistry of sedimentary chlorites by XRD and discovered that a restricted range of polytypes occurs within sediments which have not been subjected to metamorphism. Hayes suggested an evolutionary sequence from disordered material Ib_d through Ib ($\beta = 90°$) polytypes. Where sediments had been subjected to temperatures associated with metamorphism, Ib polytypes were converted to IIb polytypes (Whittle, 1986). Most chlorites in the study area were found to be the Ib ($\beta = 90°$) and IIb
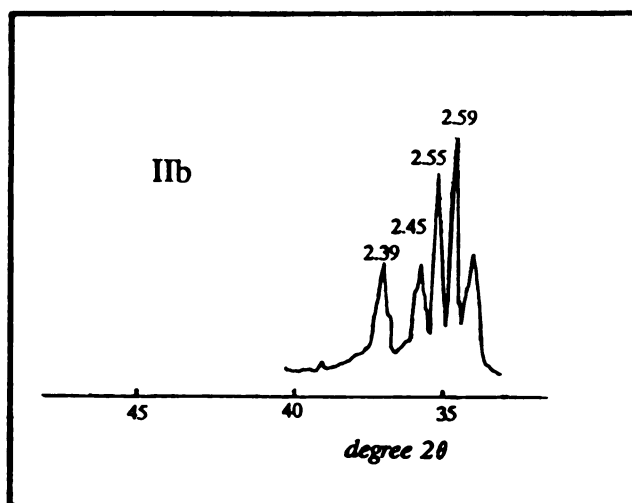
Figure 65 XRD pattern of type IIb chlorite polytype, New Haven Arkose. Notice the intensity of 2.59 and 2.55 Angstrom reflections. Sample # EB-1-17.
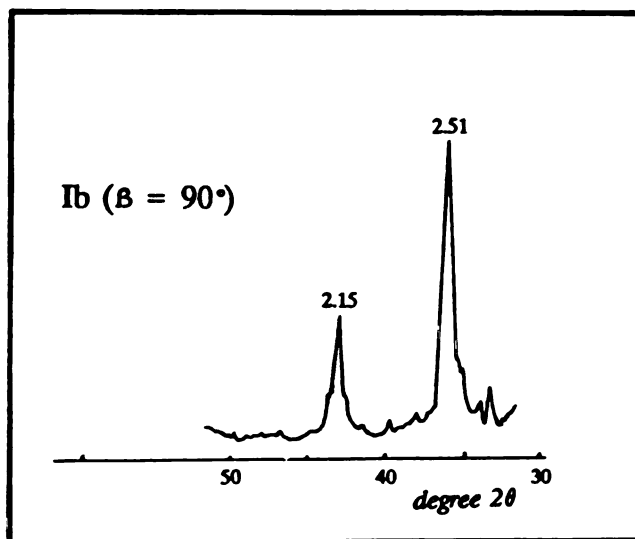
Figure 66 XRD pattern of type Ib chlorite polytype. Notice the characteristic reflections at 2.51 and 2.15 Angstrom. Sample # NH-4-15.

polytypes, with IIb polytype is the most predominant type.

ORIGIN OF THE CHLORITES

Petrographic, SEM, and XRD investigations suggest the presence of both detrital and authigenic chlorites. Chlorite polytype study verifies the presence of both varieties and defines the conditions under which each type was formed. The following is a discussion of the origin of each type.

Detrital chlorite

Detrital chlorite is present in both the New Haven Arkose and East Berlin Formation. Polytype analysis suggests that the detrital chlorite is type IIb. As mentioned earlier the IIb polytype is the most stable high temperature type. Hayes (1970) mentioned that IIb polytype also can form authigenically, probably from type Ib material, at temperatures approaching those of low-grade metamorphism.

There is more than one possible explanation for the origin of this chlorite. It can be transported into the basin as a physical or chemical weathering product of pre-existing, pre-Triassic crystalline rocks in the highlands outside the basin. Once it brought into the basin, it may be in chemical equilibrium with its surroundings, and persist unchanged through burial history and diagenesis. This idea is supported by the presence of IIb chlorite polytype in the sandstones of the study area. Type IIb suggests a sediment source area with a high relief, abundant rainfall, and which contain type IIb chlorite-bearing metamorphic rocks that can be transported,

deposited, and buried as a terrigenous, detrital clay component of sediment (Hayes, 1970).

Authigenic chlorite

A possible source of chlorite can be the basalt. The New Haven Arkose overlies the Milford Chlorite Schist and underlies the Talcott Basalt. Similarly, the East Berlin Formation overlies the Holyoke Basalt and underlies the Hampden Basalt (Figure 2). Therefore, Mg can easily be derived from the overlying basalts, possibly from hydrothermal solutions (April, 1980). These solutions may also have resulted from syndepositional weathering of basalt fragments incorporated in the upper part of the floodplain sediments. EDS qualitative analysis shows intense Fe and Mg peaks of samples about 5-20 cm below the basalt. These high Fe and Mg concentrations may be relicts of the in situ weathering of these basalt fragments by superheated pore waters.

The New Haven Arkose (stop 4) is dominated by authigenic pore-filling and pore-lining chlorite cements, whereas minor amounts of pore-filling chlorite cement were noticed in samples from stops 3 and 2 of the New Haven Arkose. The depth of burial of both formations may account for the difference in authigenic chlorite distribution. Stratigraphically, as we move down section (from the uppermost stop 1 to the lower most stop 4) there is a notable increase in chloritization. Hower et al. (1976) and Moncure et al. (1984) reported a notable increase in chlorite cement at depth greater than 3 km. Therefore, the increase in chlorite near the base of the

section (stop 4) could be depth and temperature related.

Two generations of chlorite cement are present in the sediments of the Hartford basin: 1) early diagenetic grain-coating chloritic clays (Figure 67) and pore-lining; 2) later diagenetic pore-filling chlorite cement. Both generations of cement show similar XRD patterns; the (001) basal reflection of 14.0-14.24 Angstroms is broad and of low intensity, whereas the (002) reflection at 7.01-7.13 Angstroms is sharp and moderately intense.

Different origins for the different authigenic chlorites are suggested by their habits as observed with SEM and X-ray analyses.

Grain-coating Chloritic Clays- These coatings occur only in the East Berlin Formation. An origin related to alteration of a precursor swelling chlorite or corrensite was proposed by several workers (Dunoyer de Segonzac, 1970; Humphreys et al., 1989; and Curtis et al., 1985), based on the morphological and chemical grounds, for the early grain-coating chlorite.

Dunoyer de Segonzac (1970) and Curtis et al. (1985) drew attention to a potential transformation from a precursor smectite through an intermediate swelling chlorite to chlorite. Little is known about the effect of burial diagenesis on this transformation. Helmold and Van de Kamp (1984) documented a decrease in expandability of a grain-coating mixed-layer chlorite/smectite with depth in Paleogene sandstones and suggested that chlorite rim cements in the same
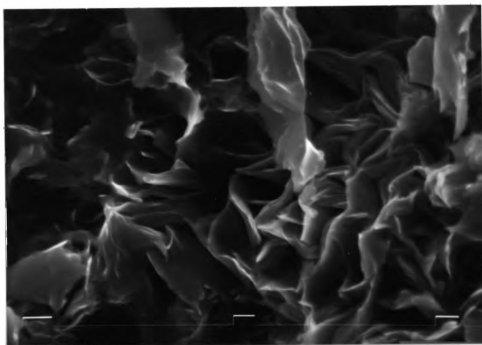
Figure 67 SEM photomicrograph showing similar morphology between grain-coatings and corrensite. Sample # EB-1-25. Tic mark = 10 μm.

sequence were the product of transformation of a precursor swelling phase. Humphreys et al. (1989) reported that the origin of grain-coating chlorite in the Late Triassic sandstones from the Central Graben, North Sea, is due to alteration of a precursor corrensite.

The East Berlin Formation may record the intermediate stage in the grain-coatings transformation process (aggrading model, Chapter 4). The grain-coatings in the East Berlin Formation probably started out as a mixed-layer clays (similar to those of Dunoyer de Segonzac, 1970; Humphreys et al., 1989; and Curtis et al., 1985) but unlike them they were never completely transformed to chlorite.

As mentioned earlier, the grain-coatings are early in the paragenetic sequence, and they are probably related to the eruptive emplacement of the basalt immediately after the deposition of the East Berlin Formation, i.e. because the heat and Mg-source (basalt) was emplaced very shortly after the deposition of the East Berlin Formation. Geologic (relation of grain-coatings to basalt) as well as petrographic (grain-coatings are early in the paragenetic sequence) evidences support this origin.

The occurrence of dolomite cements in the sediments of the East Berlin Formation indicates that sources of Mg and Fe were available. The dolomite formed early in the paragenetic sequence, and the source of Mg was probably the waters of the alkaline Jurassic lakes. The scarcity of authigenic chlorite in these sediments suggests that burial was not deep enough

to form abundant chlorite like that of the New Haven Arkose. Pore-filling and Pore-lining Chlorites- A model involving a precursor swelling chlorite has its attraction for the origin of the early grain-coating chlorites, but cannot explain the distribution of pore-filling and pore-lining chlorites in the fluvial sandstones. The delicate and euhedral morphology of many of the later diagenetic chlorites is suggestive of direct precipitation from solutes in porewaters. Probe data show that grain-coating chlorite has a high silica content similar to the corrensite composition, i.e., reflects minor interstratification of chlorite with smectite or vermiculite.

Direct precipitation from porewaters is favored for the origin of the pore-filling and pore-lining chlorites. The common occurrence of ferroan coatings and cement indicates that sources of Mg and Fe were available in the porewaters at times during burial. Some of the required ions such as Si could also have been supplied by freshwater recharge from the fluvial environment during early burial. Gradual dissolution of feldspar (particularly type 1 K-feldspar albitization; Chapter 5) would have released plentiful supplies of Al and Si into solution. Textural relationships suggest the main phase of feldspar dissolution post-dates formation of the grain-coating chlorites, but was before precipitation of the pore-filling chlorite (Chapter 3). Fe and Mg would also have been supplied to porewaters from the breakdown of detrital chlorite and biotite grains (Hubert and Reed, 1978), some of which show fan-like terminations composed of a low

birefringent clay (Figure 68).

This model of direct precipitation is especially applicable to the pore-filling and pore-lining chlorites because they are not constrained by the depositional environments. During burial diagenesis, porewaters could have migrated through fluvial sediments, allowing direct precipitation of euhedral chlorite in all permeable sandstone beds.

Hoffman and Hower (1979) reported that type-I chlorites are pre-greenschist facies and polytype Ib forms over a temperature range between 100-200°C. The Ib to IIb conversion occurs at a metamorphic grade coincident with the lithologic change from shale to slate at temperature range >200°C. On the other hand, they reported the presence of laumontite at temperature between 100-190°C. They concluded that generally chlorites reflects a higher metamorphic grade than laumontite.
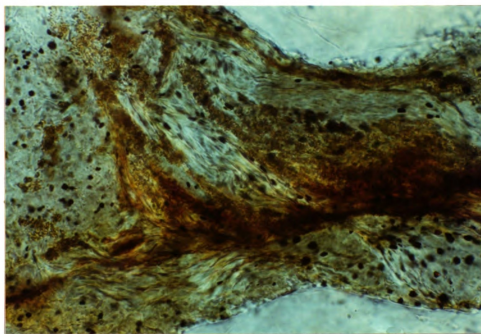
Figure 68 Photomicrograph showing fan-like terminated clay due to the breakdown of mica. Sample # NH-4-6. (Frame dim.: 0.16 mm x 0.24 mm)

CHAPTER 7

ZEOLITES

Zeolites are among the most common authigenic silicate minerals found in unmetamorphosed sedimentary rocks (Hay, 1966 and 1978). Zeolites are hydrous aluminosilicates consisting of a tetrahedral framework of O atoms surrounding either a Si or an Al atom extended in three-dimensional network, which typically provides structural channels (Zelazny and Calhoun, 1982). Ghent (1979) defined the zeolite facies to bridge the gap between diagenesis and metamorphism. He concluded that the zeolitic assemblages can form under conditions ranging from seawater-sediment interface to contact metamorphic aureoles.

Previous studies have proven the occurrence of two main types of zeolites in the sandstones of the Hartford Basin. Heald (1956) reported that many arkoses in Hamden and northern New Haven, Connecticut, contain a considerable amount of the laumontite variety of zeolite. He noticed that in some specimens the zeolite fills pore spaces and partly replaces the feldspar. He concluded that laumontite was formed after at least initial compaction of the sediments as it occupies cracks in fractured detrital grains and surrounds deformed mica.

Van Houten (1962) found analcime in some sandstones in the Triassic Lockatong formation of the Newark Series rift-valley sediments. April (1978) also found analcime in the

168

black shale and gray mudstone of the lacustrine sediments of the East Berlin Formation.

In this study, two varieties of zeolite were found in the studied formations of the Hartford Basin. Analcime is only present in the upper gray mudstone of the East Berlin Formation, whereas laumontite is present in two stops of the New Haven Arkose.

LAUMONTITE

Laumontite has been identified in only seven samples from stop 3 and four samples from stop 2 in the middle and upper parts of the New Haven Arkose. Laumontite was not detected in stop 4 of the New Haven Arkose or in the East Berlin Formation.

Laumontite was identified principally by thin-section petrography, and later confirmed by XRD, SEM, and EDS techniques. Microscopically, its color is mainly light yellowish-gray to optically clear, of low-birefrengence, with well-developed cleavage and undulatory extinction. It occurs as pore-filling cement interstitial to framework grains. It also occurs as partial replacement of detrital plagioclase grains.

Laumontite pore-fillings are partially surrounded by earlier-formed hematite and authigenic clay or silicate (mainly quartz) overgrowth, suggesting that laumontite is late in the paragenesis (Figure 69). Laumontite cement may be optically continuous with laumontite replacing detrital
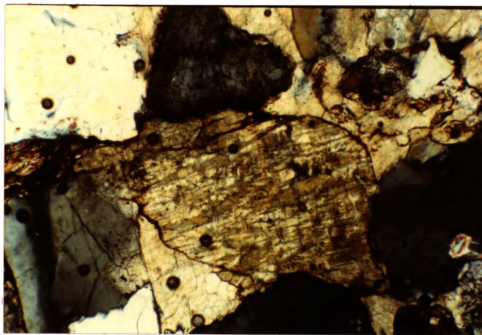
Figure 69 Photomicrograph laumontite pore-filling cement and replacement of feldspar. Sample # NH-3-10. (Frame dim.: 1.0 mm x 1.5 mm)

feldspar, and where replacement is pervasive, distinction between the two modes is especially difficult.

Laumontite replacement of detrital plagioclase varies from incipient alteration to complete replacement, and is the most common mode of occurrence of laumontite. Where replacement is extensive, the laumontite is usually murky brown and contains inclusions of sericite (?) and epidote inherited from the plagioclase precursor.

XRD diffractograms show the diagnostic intense laumontite peak at 4.15 Angstroms and the characteristic peaks at 3.5, 9.40-9.42, 3.26, and 6.84 Angstroms (Gude, 1981), (Figure 70). Under the SEM, laumontite appears as a blocky pore-filling cementing detrital quartz and feldspar grains. Chemical analyses of laumontite in low-grade metamorphic rocks indicate that the zeolite is typically free of sodium and potassium and is near ideal compositions, $Ca(Al_2Si_4O_{12}) \cdot 4H_2O$ (Ghent, 1979; Mumpton, 1981). The laumontite of the New Haven Arkose has the typical composition according to EMP analysis (Appendix E). EDS analysis also indicates that laumontite is composed of the major elements Ca, Si and Al (Figure 71). EDS pattern of laumontite matches perfectly those given by Welton (1984).

Controls on laumontite formation

As evident by optical microscopy, laumontite crystallization postdates the formation of all other authigenic minerals except calcite. Laumontite replacement of detrital grains, and its sharp boundary relationships with silicate overgrowths and authigenic clay rims, all support its
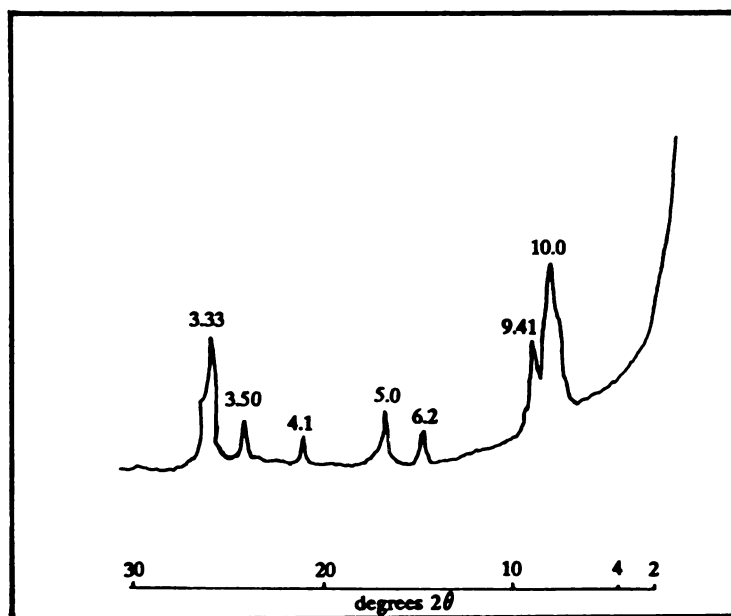
Figure 70 XRD pattern of random powder sample showing the distinctive peaks of laumontite along with illite.
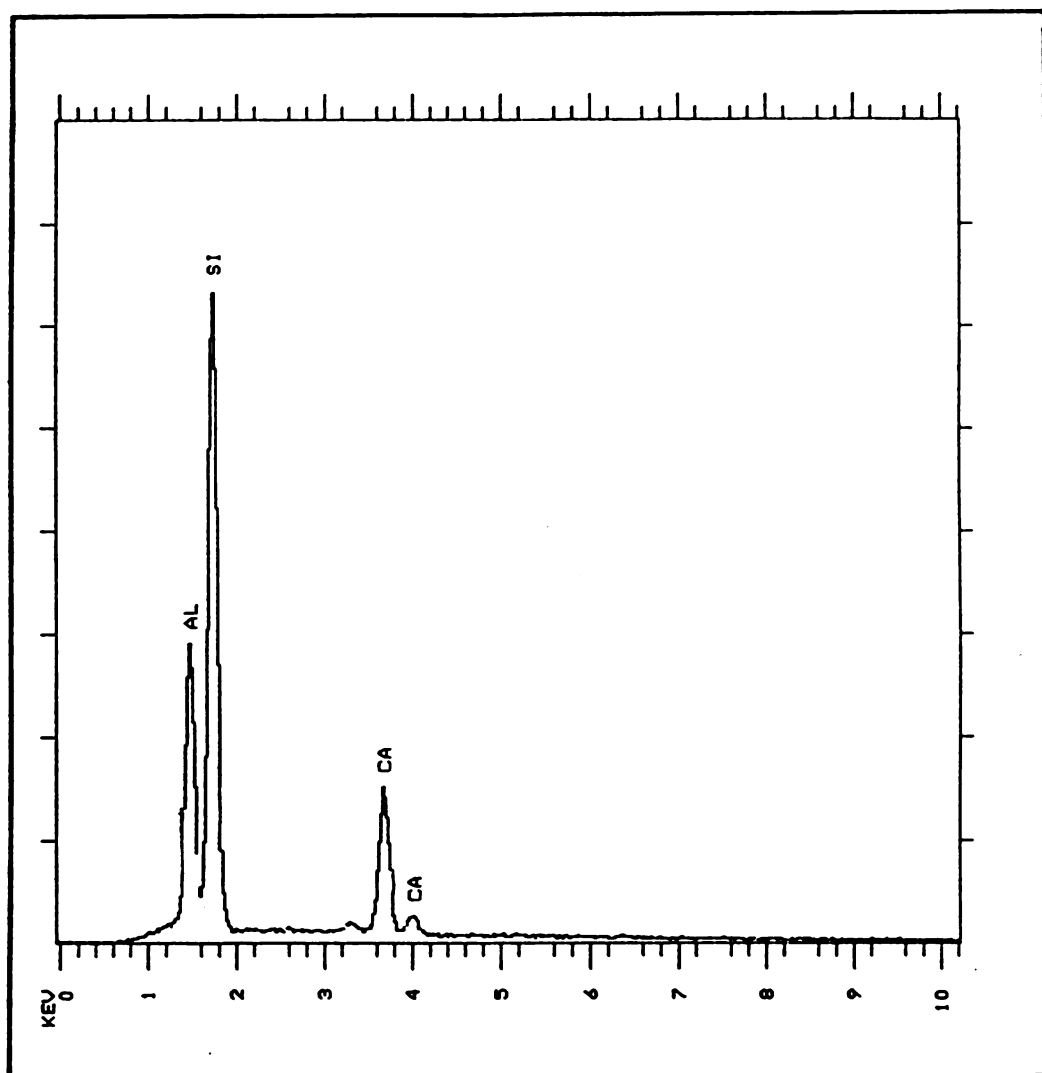
Figure 71 EDS spectrum showing characteristic elemental composition of laumontite (Ca, Al, and Si). Sample # NH-3-10.

late origin.

The presence of laumontite is often taken to indicate low-grade metamorphic conditions (pre-greenschist facies) and thus its thermal stability limits are of interest (Boles, 1981). Boles (1981), after Seki et al. (1969), reported the apparent formation of laumontite at 75 ± 5°C in the Katayama geothermal field, Japan. However, if laumontite is authigenic, it may have formed at temperatures considerably lower than described above (Boles, 1981). The range and upper thermal stability limit are better known. Hoffman and Hower (1979) reported the presence of laumontite in the faulted disturbed belts of Montana, at temperatures between 100-190°C. Ghent (1979) agreed with their temperature ranges and added that laboratory tests show possible formation of laumontite at temperatures up to 185°C.

In the laumontite-producing reaction the anorthite component in detrital plagioclase, with the addition of silica and water, is converted into laumontite; albite is another product of this alteration (Helmold and Van de Kamp, 1984):

$$NaAlSi_3O_8 \cdot CaAl_2Si_2O_8 + 2SiO_2 + 4H_2O = NaAlSi_3O_8 +$$

$$CaAl_2Si_4O_{12} \cdot H_2O \cdot 4H_2O \tag{5}$$
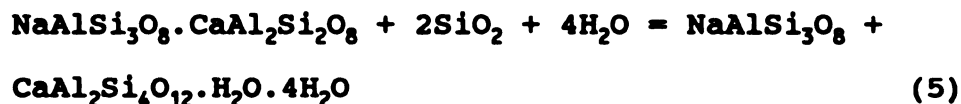
One possible explanation of the formation of laumontite can be due to the variation in the pore-fluid chemistry and fluid pressure. One possible model to explain the variation in fluid pressure between petrologically similar sandstones requires the formation of laumontite in a overpressured zone, a zone where diagenetic reactions proceeded very slowly

because of the rate of pore-fluid throughput (Hayes, 1966). Overpressuring may have occurred in the New Haven Arkose during the time of laumontite formation; this is supported by the fact that laumontite is restricted to the deeply buried New Haven Arkose (stop 3 and 2) and was not detected in the East Berlin Formation. In this situation, pore fluids enriched in Na^+ from the dewatering of smectite-rich shales deliver enough Na^+ to the sandstones to allow albitization of feldspars and possibly of some calcium-bearing plagioclase, which in turn supplied Ca^{+2} necessary for the formation of laumontite. The absence of any calcite cementation or replacement textures in the laumontite rich beds of stop 3 and 2 suggests that all of Ca^{++} was consumed in the formation of laumontite. Boles and Coombs (1977) illustrated the above mentioned process by the following reaction:

$$Plagioclase + 2\ SiO_2 + 4\ H_2O \rightarrow NaAlSi_3O_8 + CaAl_2Si_4O_{12} \cdot 4H_2O\ (6)$$
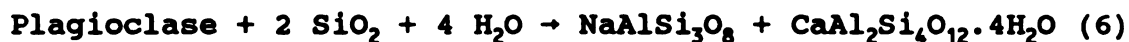
Laumontite distribution appears to be controlled by pore-fluid chemistry and post-compaction permeability variation. Compaction, formation of laumontite, and precipitation of late stage calcite are the three principle processes adversely affecting reservoir properties of the New Haven sandstones.

The fact that laumontite occupies cracks in fractured detrital grains and surrounds deformed mica indicates that it formed at least after initial compaction of the sediments. Although laumontite may result from alteration of original feldspar in sediments, part of the material for the laumontite in the Triassic may have been introduced because much of it

occurs as interstitial filling. The introduced material may be of igneous origin, for laumontite is present in near some disbases in Hampden (stop 3).

A possible explanation for the absence of laumontite in stop 4 of the New Haven Arkose may be related to burial depth. Increasing burial depth (and temperature) as we move downscetion toward stop (4), laumontite become unstable. This implies that the basal New Haven Arkose exceeded the upper thermal stability limit of laumontite (100-200°C, Hoffman and Hower, 1979).

ANALCIME

As mentioned earlier, XRD analysis was the only technique with which analcime was detected. Diffraction patterns show the presence of characteristic peaks at 3.42, 5.59, and 2.92 Angstroms (Figure 72).

Controls on analcime formation

The fact that analcime ($NaAlSi_2O_6.H_2O$) could not be identified in thin-section or with SEM suggests that the mineral exists as a well dispersed cement and may have formed as a direct precipitate from concentrated alkaline solutions (April, 1978; Fuchtbauer, 1983), or as a syngenetic alteration product of a zeolite or clay mineral precursor (Hay, 1966).

Van Houten (1962) found analcime in and associated with some sandstones of the Upper Triassic Lockatong Formation, New Jersey. He concluded that this is due to the deposition of the Lockatong rocks in a lacustrine environment as groups of
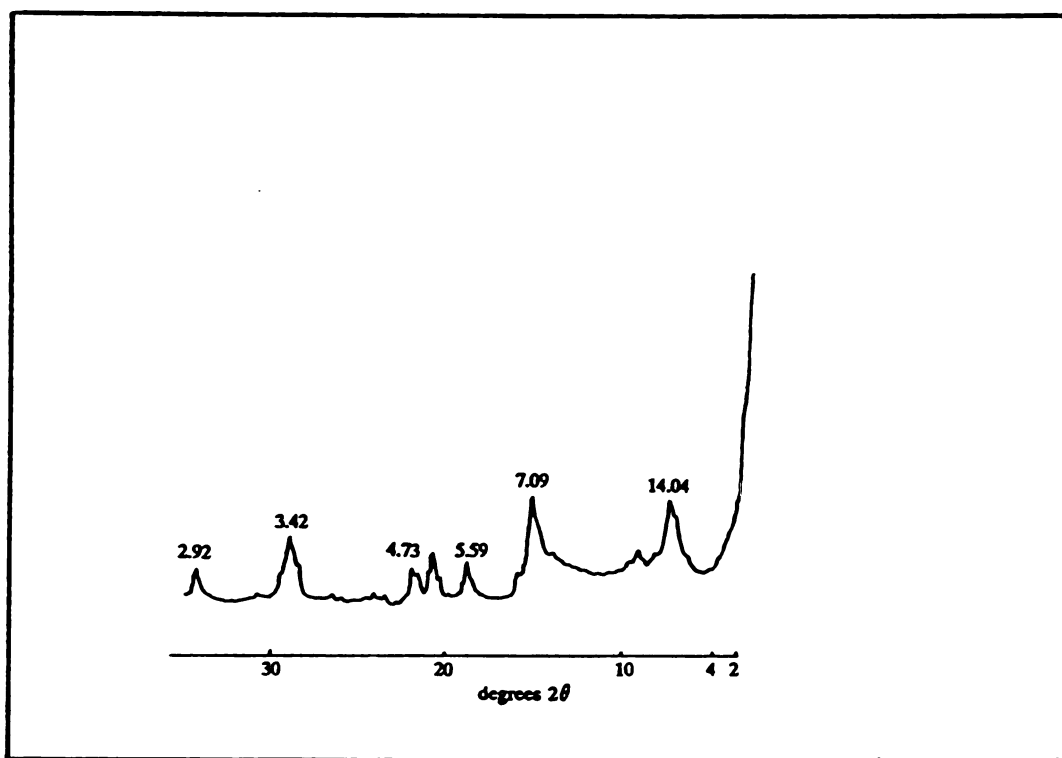
Figure 72 XRD pattern of analcime in the Jurassic East Berlin
Formation. Notice the presence of chlorite peaks
in this sample

detrital and chemical cycles related to climate. Analcime in the Lockatong rocks probably formed at an early stage of diagenesis from a colloidal precursor or aluminosilicate mineral (Van Houten, 1965).

Precipitation of analcime in the East Berlin lake water might have occurred as pH values of 9 or 10 were reached in the lake or pore waters as evaporation proceeded (April, 1981). Hay (1966) reported observing precipitation of analcime directly from strongly alkaline (pH = 9.70), sodium carbonate brines in Lake Natron, Tanzania.

The lack of any microscopic and SEM evidences of analcime textures limit the knowledge about its paragenetic and diagenetic relationships to the different detrital grains and to other diagenetic minerals.

CHAPTER 8

SUMMARY AND CONCLUSIONS

Despite the difference in depositional environment and paleoclimate between the New Haven Arkose and the East Berlin Formation, the paragenetic sequence, in general, shows only minor variations of the diagenetic features between the two. This relates to burial diagenesis rather than depositional facies controls. The only exception to this among the silicates is the presence of analcime, which points to a slightly evaporitic environment of alkaline East Berlin lakes.

The variation in the diagenetic features between stops 2, 3 and 4 of the New Haven Arkoses and stop 1 of the East Berlin Formation are believed to be due to stratigraphic and thermal controls. Stratigraphically, the New Haven outcrops are arranged in the folowing order, from deeper to shallower: stop 4, 2, and 3 (Chapter 1, 2). The East Berlin Formation is hundreds of meters or more higher in the section than the outcrops of the New Haven Arkose examined in this study. The paragenetic sequence of the studied formations shows a variation in the diagenetic minerals with depth. Stop 4 (depply buried) contains no zeolite and minor amounts of albitization but it has abundant pore-filling and -lining chlorites and calcite; stop 2 has zeolite (laumontite), albitized K-feldspar, calcite, and late pore-filling chlorite; and at stop 3 (shallower) minor early pore-filling chlorite, abundant albitized K-feldspar, and zeolite (laumontite) are

present. At stop 1, in the East Berlin Formation, minor amounts of early grain-coating interstratified chlorite, calcite, pressure solution and minor albitized K-feldspar and zeolite (analcime) are the diagenetic features. It is clear that by increasing burial we move from very minor grain-coating interstratified chlorite towards a gradual increase in chlorite plus zeolite and ultimately large amounts of chlorite.

The Portland Arkose is above the oil window (immature), the East Berlin and Shuttle Meadow formations fall within the oil window (mature), and the lower New Haven Arkose below the oil window and in the gas window (overmature), (Pratt et al., 1988). This suggests that the East Berlin falls in the temperature range (90°-110°C) whereas the deeply buried New Haven Arkose was subjected to higher temperature (> 110°C). Throughout the stratigraphic thickness of the New Haven Arkose, facies varies from a zeolite facies (stop 3), to a zeolite/chlorite facies (stop 2), and finally to a chlorite facies (stop 4) with increasing burial depth. Table 5 summerizes the authigenic mineral composition of the four stops of the New Haven Formation and the East Berlin Formation in relation to depth, temperature ranges of metamorphic facies (Hoffman and Hower, 1979; Figure 73), and burial temperatures from the organic maturation indicies of Pratt et al. (1988). This supports the above discussion that by increasing depth the authigenic mineral composition varies the different temperature ranges until it reaches the zeolite (pre-

Table 5. Variation of authigenic aluminosilicate minerals with change in burial depth and temperature.

DEPTH	STOP	FM.	AUTH.AL-SI MINERAL	T°C RANGE MET.FACIES	T°C (BURIAL) O.M.I. (Pratt et al.,1988)
	1	E.B.	Analcime	80-100°C	90-110°C
	3	N.H.	Laumontite	100-200°C	> 110°C
	2	N.H.	Laumontite Chlorite	100-200°C 70-550°C	> 110°C
INCREASE →	4	N.H.	Chlorite	70-550°C	> 110°C
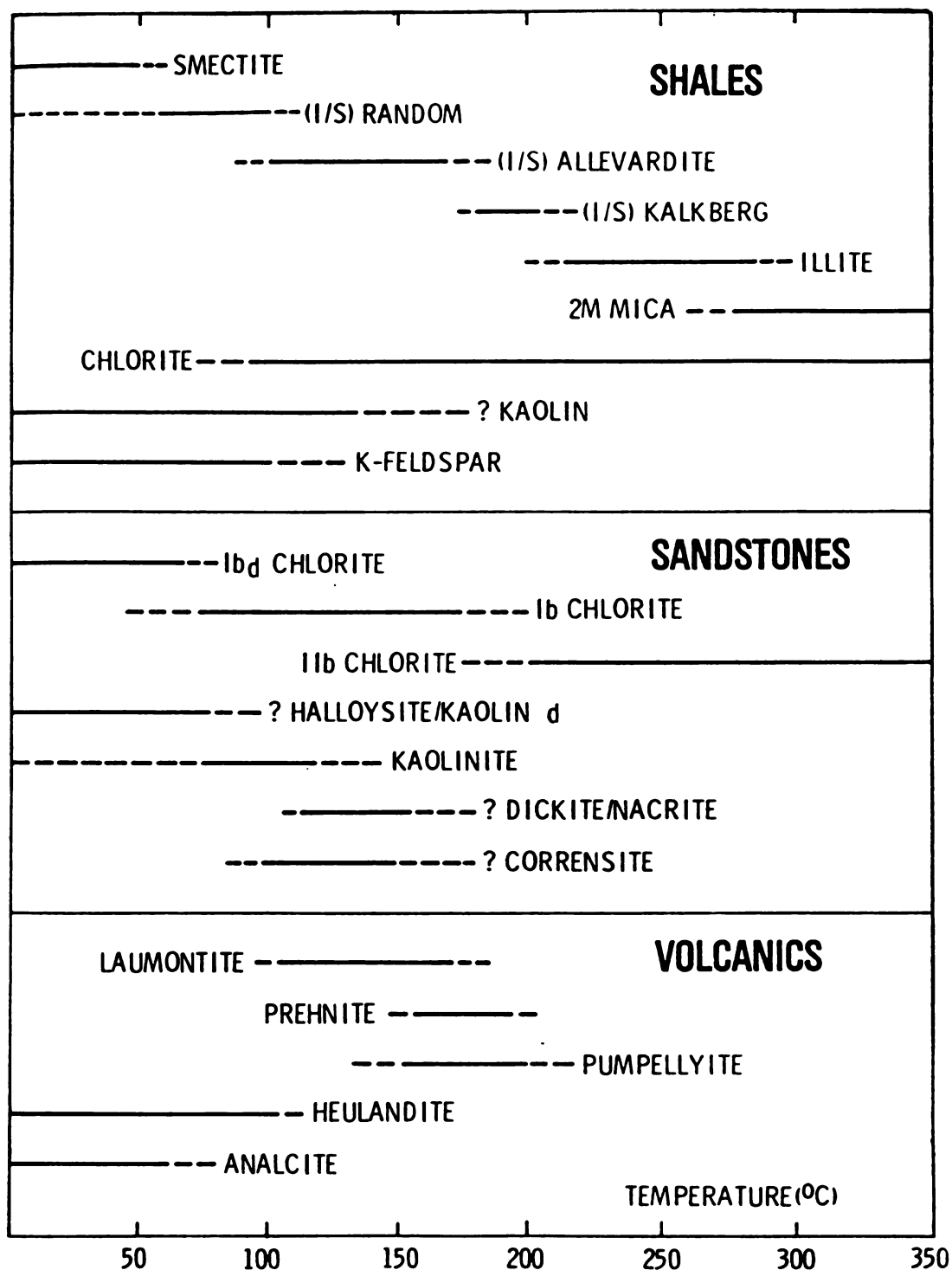
Figure 73 Correlation of the temperature-dependent mineral assemblages in shales, sandstones, and volcanogenic rocks (after Hoffman and Hower, 1979).

greenschist) facies of stop 4. Philpotts' (1990) temperature/pressure diagrams (Figure 74 and 75), confirm these temperature ranges.

Study of paragenetic sequences shows that compaction was the earliest process followed by fracturing of these rocks. The dissolution or albitization of K-feldspars is the main source of K^+ for the smectite-illite transformation and for sericitization (?). Sources of Na^{++} for albitization in the East Berlin Formation could be from the alkaline rich lake water and pore waters rich in sodium or it could be supplied from the smectite-illite transformation; in the New Haven Arkose, Na^{++} either came from external sources, or from smectite illitization. The down section increase of pore-filling chlorite (Table 1 and 2) might suggest a local source of Mg^{++} from the underlying metamorphic rocks. Recall that pore-filling chlorite is late in the paragenetic sequence in the lower New Haven Arkose at stop 4 (Figure 27), and stop 2 (Figure 29). Also, the breakdown of detrital biotite can be a possible source of Mg^{++} in the New Haven arkose. The Mg^{++} source for the chlorite in the East Berlin Formation could be from the redistribution of Mg^{++} rich alkaline lake waters and/or early-formed dolomite. Detrital calcite was present in caliche rich New Haven Arkoses, and it has been redistributed and recrystallized to a complex generations of cements. Calcium needed for the formation of zeolites could be from the redistribution of preexisting Ca^{++} in the caliche; a minor part of it came from albitization of detrital
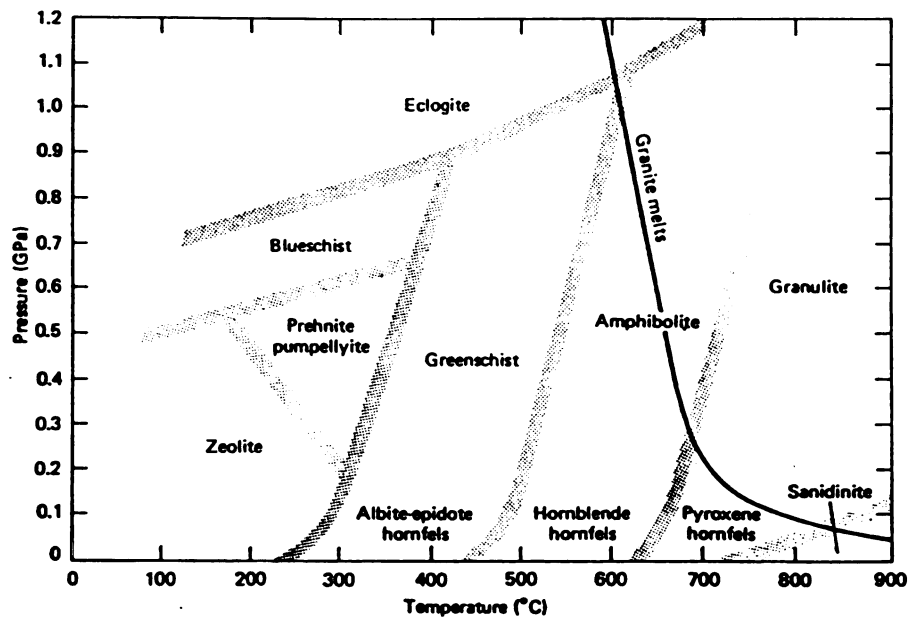
Figure 74 Approximate pressures and temperatures under which various metamorphic mineral facies form (after Philpotts, 1990).
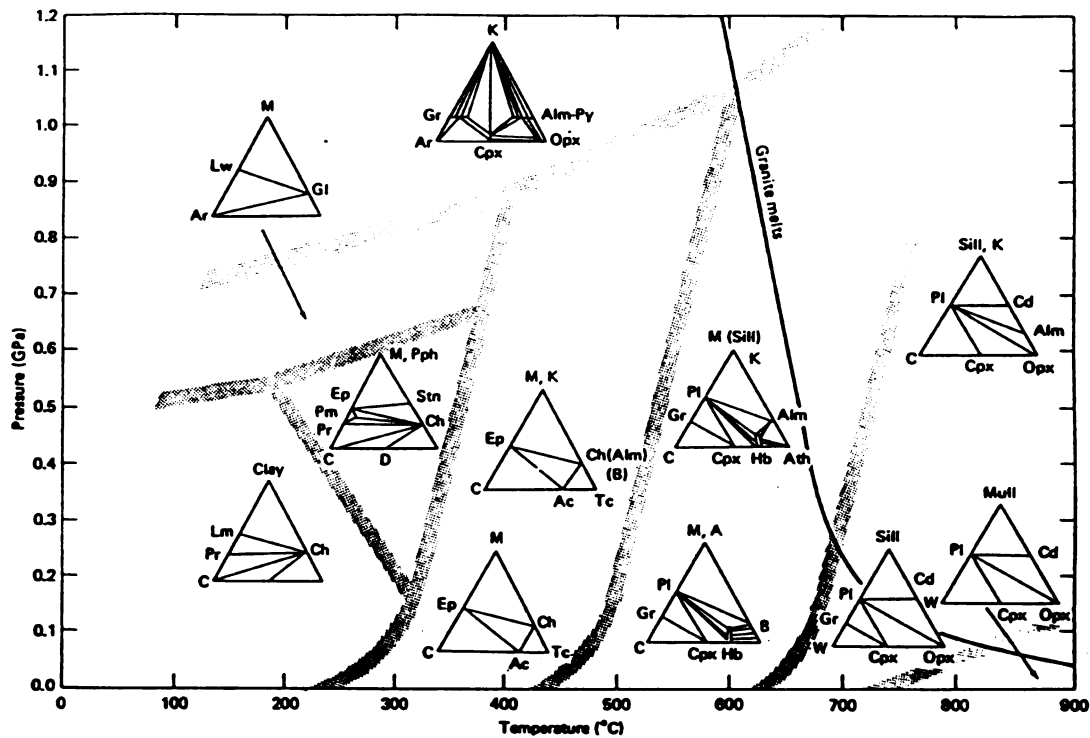
Figure 75 ACF (Al Ca Fe) plots of common quartz-bearing mineral assemblages in the metamorphic facies. Boundaries and conditions are the same as in Figure 74 (after Philpotts, 1990).

plagioclase.

Table 6 is a summary of the possible origin of the important elements of aluminosilicate minerals. Where smectite-illite transformation reaction can produce Na for albitization and K for illitization:

$$3.93K^+ + 1.57KNaCa_2Mg_4Fe_4Al_{14}Si_{38}O_{100}(OH)_{20} \cdot 10H_2O =$$

$$K_{5.5}Mg_2Fe_{1.5}Al_{22}Si_{35}O_{100}(OH)_{20} + 1.57Na^+ + 3.14Ca^{++} + 4.28Mg^{++} +$$

$$4.78Fe^{+3} + 24.66Si^{+4} + 57O^{-2} + 11.4OH^- + 15.7H_2O$$
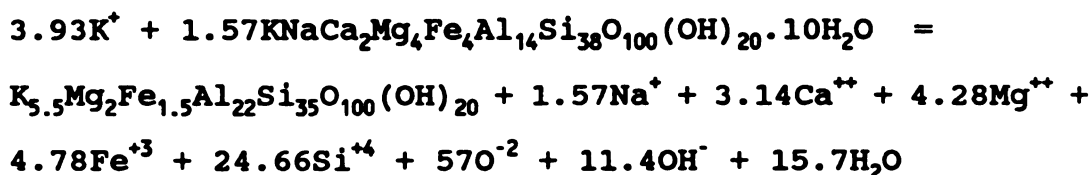
(Boles & Franks, 1979).

Other sources for K for illitization and Ca (for laumontite) are albitization reactions of K-feldspar and Plagioclase respectively:

A- <u>K-fledspar</u>:

$$KAlSi_3O_8 + Na^+ = NaAlSi_3O_8 + K^+ \qquad \text{(Walker, 1984).}$$

B- <u>Plagioclase</u>:

$$Na_{0.74}Ca_{0.27}Al_{1.24}Si_{2.75}O_8 + 0.23H_2O + 0.54H^+ =$$

$$0.74NaAlSi_3O_8 + 0.25Al_2Si_2O_5(OH)_4 + 0.27Ca^{++} + 0.03SiO_2$$

(Land, 1984).
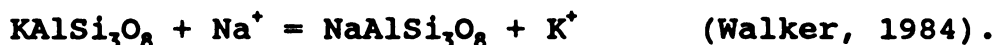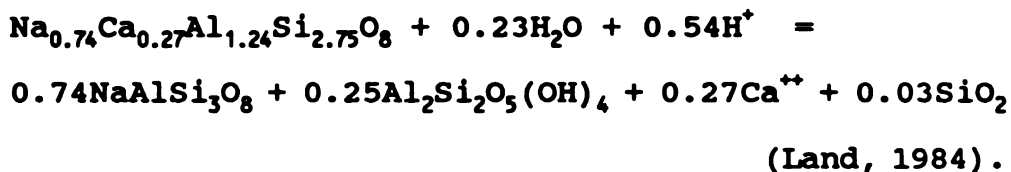
To conclude, I believe that the main diagenetic processes are depth related. The fact that albitization of K-feldspars is minor at shallower depths and lower temperatures in the East Berlin Formation, with a notable increase towards the deeper parts of the basin (New Haven Arkose) supports this inference. Also, within the New Haven Arkose, the change from laumontite facies (stop 2) to laumontite/ Ib chlorite polytype (stop 3) and finally to type Ib/IIb chlorite (stop 4) suggests temperature/depth controls.

Table 6. Summary of possible origin of elements required for the main diagenetic processes.

ELEMENT	PROCESS	POSSIBLE ORIGIN
Na	Albitization	a- Mobile pore-fluids that carried Na from outside the basin. b- Smectite to illite transformation. c- Hydrothermal solutions associated with dike emplacement (stop 3). d- Saline pore fluids derived from evaporative lake or other surface waters.
K	Illitization	a- Albitization of K-feldspars. b- Breakdown of detrital biotite.
Ca	Laumontite replacement & cementation	a- Caliche paleosols (New Haven Fm.). b- Albitization of plagioclase.
Mg	Chloritic cementation	a- Pore water from breakdown of detrital chlorite and biotite (New Haven Fm.). b- Early dolomite (stop 1). c- Hydrothermal solution from the overlying basalt (stop 1) or underlying Milford Chlorite Schist (stop 4).

Future Studies

This study is considered as the opening for later differently directed projects. My main concern in this study was the diagenesis of some aluminosilicate minerals.

Further studies can include the complex calcite distribution, isotope study of different diagenetic chlorite types, albitization near and away from igneous intrusions, and detailed study on the zeolite facies in the New Haven Arkose and East Berlin Formation, and may later explore the similarity or differences in the Shuttle Meadow Formation and the Portland Arkose of the Hartford Basin. Also, detailed studies of illite-smectite interstratification is strongly suggested.

APPENDICES

APPENDIX A

Microprobe analysis of albitized K-feldspar

Appendix A. Microprobe analysis of albitized K-feldspar.

New Haven Arkose (stop 4)

SAMPLE	NH-4-1	NH-4-1	NH-4-2	NH-4-3	NH-4-3
NA$_2$O	12.251	11.495	11.646	11.588	11.452
MGO	0.011	0.019	0.000	0.013	0.000
AL$_2$O$_3$	20.053	20.584	19.674	19.487	20.281
SIO$_2$	68.408	67.320	67.293	67.057	67.281
K$_2$O	0.010	0.120	0.026	0.108	0.151
CAO	0.026	0.616	0.056	0.079	0.628
TIO$_2$	0.028	0.003	0.006	0.009	0.019
MNO	0.023	0.014	0.000	0.000	0.012
FEO(T)	0.181	0.075	0.043	0.051	0.015
BAO	0.062	0.041	0.062	0.000	0.072
TOTAL	101.054	100.287	98.805	98.391	99.910
AB	99.9	96.5	99.6	99.0	96.3
OR	0	0.7	0.1	1.0	1.0
AN	0.1	2.8	0.3	0	3.0

Stop 4 (Cont'd.)

SAMPLE	NH-4-4
NA_2O	11.325
MGO	0.000
AL_2O_3	20.097
SIO_2	67.067
K_2O	0.086
CAO	0.659
TIO_2	0.002
MNO	0.014
FEO(T)	0.073
BAO	0.000
TOTAL	99.323
AB	96.4
OR	0.5
AN	3.1

New Haven Arkose (stop 3)

SAMPLE	NH-3-3	NH-3-7a	NH-3-7b	NH-3-7c	NH-3-7d
NA_2O	10.681	11.851	11.700	11.667	11.404
MGO	0.028	0.001	0.000	0.000	0.008
AL_2O_2	21.457	20.221	19.938	19.904	19.931
SIO_2	66.212	70.073	69.294	69.085	68.512
K_2O	0.112	0.020	0.042	0.067	0.098
CAO	1.858	0.201	0.184	0.250	0.359
TIO_2	0.000	0.004	0.034	0.021	0.000
MNO	0.028	0.000	0.000	0.044	0.032
FEO(T)	0.087	0.000	0.017	0.022	0.030
BAO	0.041	0.000	0.021	0.051	0.082
TOTAL	100.504	102.37	101.229	101.110	100.456
AB	90.1	99.1	99.1	98.4	97.7
OR	1.0	0.0	0.0	0.4	0.6
AN	8.9	0.9	0.9	1.2	1.7

Stop 3 (Cont'd.)

SAMPLE	NH-3-9	NH-3-9	NH-3-9	NH-3-9	NH-3-11
NA_2O	11.243	11.569	11.678	11.666	11.078
MGO	0.005	0.000	0.000	0.01	0.051
AL_2O_3	19.622	20.023	20.186	19.978	20.044
SIO_2	65.285	69.341	69.666	68.852	67.928
K_2O	0.379	0.054	0.023	0.073	0.243
CAO	0.323	0.511	0.414	0.225	0.179
TIO_2	0.000	0.027	0.020	0.000	0.029
MNO	0.014	0.002	0.000	0.016	0.058
FEO(T)	0.000	0.019	0.009	0.000	0.094
BAO	0.000	0.000	0.062	0.133	0.000
TOTAL	96.873	101.547	102.057	100.953	100.334
AB	96.3	97.6	98.1	98.5	97.9
OR	2.1	0.0	0	0.4	1.3
AN	1.6	2.4	1.9	1.1	0.8

Stop 3 (Cont'd.)

SAMPLE	NH-3-11	NH-3-16	NH-3-16	NH-3-16	NH-3-16
NA$_2$O	11.868	11.460	8.414	11.821	11.806
MGO	0.010	0.009	0.000	0.003	0.002
AL$_2$O$_3$	19.925	20.072	20.929	20.229	20.207
SIO$_2$	68.184	68.803	70.277	69.489	69.110
K$_2$O	0.079	0.118	0.045	0.043	0.046
CAO	0.171	0.272	0.405	0.314	0.333
TIO$_2$	0.000	0.006	0.039	0,035	0.045
MNO	0.000	0.014	0.014	0.000	0.000
FEO(T)	0.101	0.034	0.049	0.074	0.028
BAO	0.000	0.062	0.000	0.062	0.134
TOTAL	100.339	100.848	100.172	102.071	101.711
AB	98.8	98.1	97.2	99.0	98.0
OR	0.4	0.6	0	0	0
AN	0.8	1.3	2.8	1.0	2.07

Stop 3 (Cont'd.)

SAMPLE	NH-3-16	NH-3-16	NH-3-16	NH-3-23	NH-3-25
NA$_2$O	11.664	11.084	11.445	11.614	11.847
MGO	0.005	0.000	0.000	0.000	0.010
AL$_2$O$_3$	20.055	20.052	20.536	19.881	20.274
SIO$_2$	68.215	67.932	67.129	67.471	69.085
K$_2$O	0.068	0.824	0.069	0.029	0.023
CAO	0.231	0.172	0.673	0.613	0.173
TIO$_2$	0.000	0.016	0.000	0.020	0.020
MNO	0.039	0.007	0.039	0.018	0.023
FEO(T)	0.000	0.085	0.055	0.052	0.000
BAO	0.072	0.010	0.000	0.010	0.041
TOTAL	100.351	100.182	99.947	99.708	101.496
AB	99.0	94.0	97.0	97.2	99.2
OR	0	5.0	0.0	0	0.0
AN	1.0	1.0	3.0	2.8	0.8

Stop 3 (Cont'd.)

SAMPLE	NH-3-27	NH-3-27	NH-3-27	NH-3-27	NH-3-27
NA_2O	11.342	11.553	11.829	11.811	11.265
MGO	0.004	0.005	0.000	0.000	0.051
AL_2O_3	19.654	19.986	20.049	20.040	20.419
SIO_2	66.702	68.490	68.325	68.813	67.615
K_2O	0.066	0.069	0.060	0.057	0.305
CAO	0.316	0.380	0.205	0.309	0.351
TIO_2	0.000	0.000	0.007	0.000	0.000
MNO	0.038	0.014	0.018	0.009	0.039
FEO(T)	0.051	0.000	0.064	0.011	0.038
BAO	0.040	0.041	0.000	0.083	0.052
TOTAL	98.213	100.538	100.557	101.132	100.135
AB	98.5	97.8	99.0	99.0	95.9
OR	0	0.4	0.0	0.0	2.1
AN	1.5	1.8	1.0	1.0	2.0

Stop 3 (Cont'd.)

SAMPLE	NH-3-28	NH-3-30	NH-3-30	NH-3-30	NH-3-30
NA$_2$O	11.454	11.843	11.839	11.792	11.643
MGO	0.004	0.000	0.000	0.007	0.000
AL$_2$O$_3$	20.551	19.876	19.954	20.276	19.611
SIO$_2$	68.741	67.884	67.602	68.574	69.146
K$_2$O	0.038	0.017	0.190	0.078	0.042
CAO	0.642	0.285	0.294	0.380	0.145
TIO$_2$	0.002	0.030	0.000	0.000	0.000
MNO	0.000	0.000	0.035	0.000	0.016
FEO(T)	0.047	0.006	0.055	0.064	0.013
BAO	0.051	0.021	0.000	0.000	0.082
TOTAL	101.620	99.963	99.969	101.171	100.699
AB	97.0	99.0	98.0	98.0	99.1
OR	0	0.0	1.0	0.0	0.2
AN	3.0	1.0	1.0	2.0	0.7

New Haven Arkose (stop 2)

SAMPLE	NH-2-4	NH-2-4	NH-2-10	NH-2-10	NH-2-12
NA_2O	12.015	11.771	11.728	11.332	10.876
MGO	0.000	0.000	0.000	0.005	0.000
AL_2O_3	19.897	19.887	19.900	20.118	21.147
SIO_2	68.996	67.612	67.784	65.881	65.346
K_2O	0.071	0.104	0.057	0.091	0.293
CAO	0.122	0.233	0.200	0.786	1.332
TIO_2	0.013	0.007	0.000	0.008	0.007
MNO	0.000	0.000	0.000	0.009	0.000
FEO(T)	0.049	0.000	0.021	0.024	0.000
BAO	0.031	0.000	0.021	0.000	0.031
TOTAL	101.194	99.614	99.711	98.252	99.032
AB	99.1	98.3	99.1	95.8	92.1
OR	0.4	0.6	0	0.5	1.6
AN	0.5	1.1	0.9	3.7	6.3

Stop 2 (Cont'd.)

SAMPLE	NH-2-12	NH-2-12	NH-2-13	NH-2-13	NH-2-13
NA_2O	11.446	11.248	11.127	11.620	11.674
MGO	0.000	0.005	0.000	0.006	0.003
AL_2O_3	19.202	20.414	21.210	20.095	19.937
SIO_2	64.009	66.376	65.013	66.815	66.977
K_2O	0.098	0.051	0.124	0.650	0.103
CAO	0.336	0.773	1.419	0.172	0.267
TIO_2	0.000	0.000	0.000	0.000	0.002
MNO	0.046	0.000	0.007	0.000	0.011
FEO(T)	0.000	0.009	0.011	0.009	0.004
BAO	0.000	0.103	0.031	0.010	0.000
TOTAL	95.137	98.979	98.943	99.376	98.980
AB	97.9	96.1	92.8	95.7	98.2
OR	0.5	0.3	0.7	3.5	0.6
AN	1.6	3.6	6.5	0.8	1.2

Stop 2 (Cont'd.)

SAMPLE	NH-2-13	NH-2-14	NH-2-14	NH-2-14	NH-2-17
NA_2O	11.815	11.512	10.734	10.983	11.909
MGO	0.000	0.000	0.014	0.000	0.000
AL_2O_3	20.275	20.505	21.258	21.397	20.195
SIO_2	68.069	67.056	64.953	64.575	67.870
K_2O	0.127	0.126	0.083	0.070	0.011
CAO	0.282	0.693	1.823	1.810	0.263
TIO_2	0.025	0.000	0.013	0.000	0.000
MNO	0.012	0.018	0.037	0.000	0.000
FEO(T)	0.000	0.024	0.017	0.028	0.021
BAO	0.000	0.021	0.082	0.021	0.000
TOTAL	100.605	99.956	99.015	98.884	100.271
AB	98.0	96.1	91.0	91.3	98.8
OR	0.7	0.7	0.5	0.4	0
AN	1.3	3.2	8.5	8.3	1.2

Stop 2 (Cont'd.)

SAMPLE	NH-2-17	NH-2-19	NH-2-19	NH-2-30	NH-2-30
NA$_2$O	11.763	10.543	11.218	11.850	11.972
MGO	0.001	0.009	0.003	0.000	0.006
AL$_2$O$_3$	20.319	19.652	20.651	20.169	20.323
SIO$_2$	67.143	68.090	66.869	68.352	67.903
K$_2$O	0.026	2.181	0.100	0.057	0.061
CAO	0.355	0.051	0.923	0.162	0.298
TIO$_2$	0.004	0.003	0.021	0.016	0.029
MNO	0.000	0.005	0.028	0.005	0.000
FEO(T)	0.030	0.000	0.034	0.021	0.056
BAO	0.000	0.124	0.010	0.031	0.031
TOTAL	99.643	100.656	99.858	100.662	100.679
AB	98.4	87.8	95.1	98.9	98.7
OR	0	12.0	0.6	0.3	0
AN	1.6	0.2	4.3	0.8	1.3

Stop 2 (Cont'd.)

SAMPLE	NH-2-34	NH-2-34	NH-2-35	NH-2-35	NH-2-35
NA$_2$O	12.047	11.702	11.658	11.094	11.778
MGO	0.007	0.000	0.000	0.000	0.004
AL$_2$O$_3$	20.139	20.205	20.444	20.828	20.344
SIO$_2$	67.329	67.431	67.314	66.067	67.801
K$_2$O	0.012	0.014	0.112	0.066	0.052
CAO	0.127	0.198	0.406	1.304	0.273
TIO$_2$	0.000	0.003	0.000	0.021	0.009
MNO	0.039	0.019	0.002	0.002	0.012
FEO(T)	0.009	0.000	0.131	0.082	0.000
BAO	0.000	0.000	0.000	0.021	0.062
TOTAL	99.709	99.572	100.068	99.486	100.333
AB	99.4	99.1	97.5	93.5	98.7
OR	0	0.0	0.6	0.4	0
AN	0.6	0.9	1.9	6.1	0.6

East Berlin Fm. (stop 1)

SAMPLE	EB-1-1	EB-1-1	EB-1-2	EB-1-2	EB-1-3
NA_2O	11.988	11.221	12.102	11.974	11.037
MGO	0.005	0.077	0.000	0.009	0.001
AL_2O_3	19.925	21.352	19.770	19.427	19.329
SIO_2	67.640	66.818	67.450	67.370	66.999
K_2O	0.026	0.758	0.039	0.048	0.040
CAO	0.032	0.144	0.073	0.031	0.040
TIO_2	0.020	0.000	0.000	0.019	0.010
MNO	0.007	0.000	0.000	0.037	0.009
$FEO(T)$	0.049	0.120	0.075	0.015	0.028
BAO	0.052	0.000	0.021	0.000	0.041
TOTAL	99.744	100.489	99.529	98.930	97.534
AB	99.7	95.1	99.5	96.6	99.6
OR	0.1	4.2	0.2	0.3	0.2
AN	0.2	0.7	0.3	0.1	0.2

Stop 1 (Cont'd.)

SAMPLE	EB-1-4	EB-1-4	EB-1-5	EB-1-5	EB-1-6
NA_2O	11.234	9.500	10.114	11.872	12.387
MGO	0.013	0.052	0.124	0.008	0.021
AL_2O_3	20.818	23.309	22.631	19.884	20.105
SIO_2	67.295	64.259	64.704	68.045	67.790
K_2O	0.119	0.949	1.117	0.075	0.016
CAO	0.874	2.303	1.091	0.027	0.024
TIO_2	0.000	0.000	0.001	0.000	0.000
MNO	0.000	0.009	0.000	0.016	0.009
FEO(T)	0.000	0.098	0.125	0.054	0.045
BAO	0.072	0.031	0.000	0.000	0.000
TOTAL	100.425	100.511	99.905	99.982	100.397
AB	95.2	83.5	88.3	99.5	99.9
OR	0.7	5.2	6.4	0.4	0
AN	4.1	11.3	5.3	0.1	0.1

Stop 1 (Cont'd.)

SAMPLE	EB-1-6	EB-1-6	EB-1-6	EB-1-7	EB-1-7
NA_2O	11.937	11.851	11.756	12.105	11.741
MGO	0.000	0.000	0.001	0.065	0.010
AL_2O_3	20.013	20.129	19.803	20.089	20.224
SIO_2	67.944	66.720	67.178	68.638	66.766
K_2O	0.009	0.071	0.018	0.151	0.089
CAO	0.023	0.359	0.088	0.103	0.476
TIO_2	0.022	0.002	0.005	0.004	0.000
MNO	0.000	0.002	0.000	0.000	0.000
FEO(T)	0.077	0.024	0.000	0.172	0.004
BAO	0.010	0.000	0.031	0.041	0.000
TOTAL	100.036	99.158	98.880	101.369	99.309
AB	99.9	98.0	99.5	98.7	97.3
OR	0	0.4	0.1	0.8	0.5
AN	0.1	1.6	0.4	0.5	2.2

Stop 1 (Cont'd.)

SAMPLE	EB-1-10	EB-1-12	EB-1-12	EB-1-12
NA_2O	11.895	11.373	12.386	12.247
MGO	0.027	0.049	0.000	0.000
AL_2O_3	19.769	20.120	20.814	20.837
SIO_2	67.696	68.404	71.125	69.955
K_2O	0.039	0.279	0.047	0.088
CAO	0.060	0.176	0.232	0.451
TIO_2	0.013	0.025	0.012	0.009
MNO	0.000	0.000	0.000	0.000
FEO(T)	0.068	0.282	0.051	0.036
BAO	0.103	0.000	0.052	0.000
TOTAL	99.669	100.708	104.719	103.622
AB	99.5	97.6	98.7	98.0
OR	0.2	1.6	0.3	0
AN	0.3	0.8	1.0	2.0

APPENDIX B

Microprobe analysis of plagioclase feldspar

Appendix B. Microprobe analysis of plagioclase feldspar.

New Haven Arkose (stop 3)

SAMPLE	NH-3-1	NH-3-1	NH-3-1	NH-3-3	NH-3-3
NA_2O	9.827	9.895	8.935	10.027	10.080
MGO	0.000	0.015	0.000	0.004	0.000
AL_2O_3	22.634	22.480	23.059	21.843	21.849
SIO_2	65.076	65.255	62.455	64.696	64.960
K_2O	0.323	0.311	0.306	0.288	0.580
CAO	3.072	3.136	4.420	2.587	2.316
TIO_2	0.000	0.026	0.015	0.000	0.000
MNO	0.028	0.000	0.000	0.030	0.000
FEO(T)	0.009	0.036	0.026	0.000	0.006
BAO	0.010	0.021	0.031	0.021	0.000
TOTAL	100.977	101.176	99.246	99.495	99.792
AB	83.7	83.6	77.2	86.0	85.9
OR	1.8	1.7	1.7	2.0	3.2
AN	14.5	14.7	21.1	12.0	10.9

Stop 3 (Cont'd.)

SAMPLE	NH-3-7	NH-3-9	NH-3-10	NH-3-10	NH-3-16
NA_2O	10.119	9.828	10.847	10.678	9.171
MGO	0.000	0.001	0.002	0.001	0.002
AL_2O_3	21.859	22.305	21.167	21.204	22.437
SIO_2	65.619	65.376	67.140	66.905	62.113
K_2O	0.361	0.328	0.157	0.170	0.297
CAO	2.150	2.866	1.598	1.594	3.406
TIO_2	0.001	0.025	0.018	0.006	0.028
MNO	0.000	0.000	0.011	0.014	0.021
FEO(T)	0.022	0.039	0.034	0.099	0.039
BAO	0.000	0.010	0.000	0.062	0.000
TOTAL	100.132	100.779	100.973	100.732	97.514
AB	87.6	84.5	91.7	91.5	81.5
OR	2.1	1.8	0.9	1.0	1.7
AN	10.3	13.7	7.4	7.5	16.8

Stop 3 (Cont'd.)

SAMPLE	NH-3-23	NH-3-25	NH-3-25	NH-3-27	NH-3-30
NA$_2$O	10.289	9.913	9.751	8.885	8.535
MGO	0.000	0.006	0.000	0.009	0.000
AL$_2$O$_3$	21.536	22.112	22.069	23.123	24.253
SIO$_2$	64.496	64.285	63.781	62.221	61.617
K$_2$O	0.158	0.150	0.116	0.238	0.149
CAO	2.097	2.897	2.958	4.127	5.194
TIO$_2$	0.014	0.003	0.024	0.019	0.026
MNO	0.041	0.000	0.043	0.007	0.002
FEO(T)	0.034	0.032	0.088	0.036	0.058
BAO	0.000	0.040	0.030	0.000	0.113
TOTAL	98.665	99.437	98.861	98.665	99.948
AB	89.1	85.4	85.1	78.5	74.2
OR	0.9	0.8	0.7	1.4	0.8
AN	10.0	13.8	14.2	20.1	25.0

New Haven Arkose (stop 2)

SAMPLE	NH-2-4	NH-2-4	NH-2-4	NH-2-10	NH-2-12
NA$_2$O	10.066	9.206	10.351	9.454	10.617
MGO	0.000	0.007	0.000	0.000	0.013
AL$_2$O$_3$	22.326	22.776	22.067	22.478	21.122
SIO$_2$	64.807	63.147	64.813	62.794	64.598
K$_2$O	0.169	0.533	0.188	0.198	0.399
CAO	3.093	4.010	2.576	3.433	1.658
TIO$_2$	0.009	0.018	0.000	0.020	0.004
MNO	0.000	0.021	0.000	0.000	0.000
FEO(T)	0.013	0.113	0.019	0.000	0.028
BAO	0.000	0.021	0.052	0.062	0.021
TOTAL	100.482	99.851	100.066	98.438	98.459
AB	85.1	78.2	87.0	82.3	90.0
OR	0.9	3.0	1.0	1.1	2.2
AN	14.0	18.8	12.0	16.6	7.8

Stop 2 (Cont'd.)

SAMPLE	NH-2-14	NH-2-19	NH-2-19
NA_2O	10.079	9.871	10.321
MGO	0.000	0.000	0.003
SIO_2	22.660	22.503	21.453
AL_2O_3	62.397	64.136	64.553
K_2O	0.138	0.368	0.327
CAO	3.075	3.185	2.354
TIO_2	0.000	0.034	0.024
MNO	0.000	0.021	0.000
FEO(T)	0.024	0.015	0.030
BAO	0.000	0.000	0.000
TOTAL	98.372	100.133	99.064
AB	84.9	83.2	87.2
OR	0.8	2.0	1.8
AN	14.3	14.8	11.0

East Berlin Fm. (stop 1)

SAMPLE	EB-1-5	EB-1-7	EB-1-12
NA$_2$O	10.550	9.387	9.888
MGO	0.000	0.005	0.010
AL$_2$O$_3$	21.659	23.845	23.402
SIO$_2$	63.595	61.631	65.155
K$_2$O	0.158	0.032	0.184
CAO	2.218	4.535	3.265
TIO$_2$	0.018	0.000	0.008
MNO	0.000	0.018	0.000
FEO(T)	0.000	0.086	0.043
BAO	0.062	0.000	0.000
TOTAL	98.259	99.540	101.955
AB	81.1	78.8	83.7
OR	9.4	0.2	1.0
AN	9.5	21.0	15.3

APPENDIX C

Microprobe analysis of K-feldspar

Appendix C. Microprobe analysis of K-feldspar.

New Haven Arkose (stop 4)

SAMPLE	NH-4-1	NH-4-2	NH-4-3	NH-4-3	NH-4-3
NA$_2$O	0.961	0.290	0.625	0.790	1.097
MGO	0.006	0.000	0.000	0.009	0.011
AL$_2$O$_3$	19.124	18.730	18.719	18.999	18.969
SIO$_2$	63.285	64.036	63.904	64.603	64.940
K$_2$O	14.599	15.570	14.434	14.035	13.994
CAO	0.019	0.000	0.000	0.000	0.002
TIO$_2$	0.000	0.000	0.001	0.000	0.000
MNO	0.035	0.009	0.005	0.000	0.000
FEO(T)	0.000	0.017	0.002	0.017	0.015
BAO	0.270	0.363	0.218	0.000	0.000
TOTAL	98.300	99.015	97.908	98.453	99.028
AB	9.1	2.8	6.2	7.8	10.9
OR	90.9	97.2	93.8	92.2	89.1
AN	0	0	0	0	0

Stop 4 (Cont'd.)

SAMPLE	NH-4-6
NA_2O	0.927
MGO	0.000
AL_2O_3	18.793
SIO_2	63.965
K_2O	14.288
CAO	0.003
TIO_2	0.041
MNO	0.000
$FEO(T)$	0.094
BAO	0.125
TOTAL	98.236
AB	9.0
OR	91.0
AN	0

New Haven Arkose (stop 3)

SAMPLE	NH-3-7	NH-3-7	NH-3-7	NH-3-9	NH-3-9
NA$_2$O	1.226	0.898	1.211	0.401	0.677
MGO	0.000	0.002	0.000	0.011	0.000
AL$_2$O$_3$	18.857	18.520	18.883	18.464	18.802
SIO$_2$	65.163	64.539	64.612	63.357	65.528
K$_2$O	15.537	15.823	15.177	16.360	15.983
CAO	0.012	0.011	0.019	0.000	0.000
TIO$_2$	0.001	0.011	0.000	0.000	0.011
MNO	0.000	0.000	0.000	0.007	0.000
FEO(T)	0.006	0.034	0.021	0.032	0.000
BAO	0.186	0.176	0.124	0.331	0.299
TOTAL	100.988	100.015	100.047	98.963	100.301
AB	10.7	7.9	10.8	3.5	6.1
OR	89.3	92.1	89.2	96.5	93.9
AN	0	0	0.0	0	0

Stop 3 (Cont'd.)

SAMPLE	NH-3-16	NH-3-16	NH-3-16	NH-3-16	NH-3-25
NA_2O	4.106	0.916	1.082	1.272	0.936
MGO	0.000	0.002	0.004	0.009	0.003
AL_2O_3	11.564	18.703	18.927	18.791	18.556
SIO_2	42.762	64.061	63.961	64.916	65.213
K_2O	0.035	15.511	15.333	14.769	15.749
CAO	19.779	0.028	0.006	0.064	0.000
TIO_2	18.564	0.027	0.000	0.013	0.000
MNO	0.002	0.028	0.000	0.009	0.000
FEO(T)	0.430	0.047	0.030	0.002	0.000
BAO	0.000	0.104	0.042	0.010	0.000
TOTAL	97.243	99.425	99.384	99.856	100.456
AB	27.4	92.0	9.9	11.2	8.3
OR	0	8.0	90.1	88.8	91.7
AN	72.6	0	0.0	0.0	0

Stop 3 (Cont'd.)

SAMPLE	NH-3-27	NH-3-27	NH-3-27	NH-3-27	NH-3-28
NA_2O	1.213	1.423	0.983	0.938	2.505
MGO	0.029	0.000	0.012	0.000	0.002
AL_2O_3	18.782	19.221	18.202	18.716	19.042
SIO_2	64.570	65.142	63.525	64.385	63.563
K_2O	14.666	14.391	15.366	15.923	12.857
CAO	0.043	0.010	0.003	0.044	0.077
TIO_2	0.000	0.002	0.018	0.010	0.000
MNO	0.000	0.032	0.000	0.000	0.135
FEO(T)	0.070	0.002	0.015	0.028	0.062
BAO	0.591	0.208	0.233	0.041	0.896
TOTAL	99.964	100.431	98.346	100.085	99.140
AB	11.3	13.4	8.9	8.2	22.8
OR	88.7	86.6	91.1	91.8	76.9
AN	0	0.0	0	0	0.3

Stop 3 (Cont'd.)

SAMPLE	NH-3-30	NH-3-30	NH-3-30	NH-3-30	NH-3-30
NA_2O	1.027	1.056	1.164	1.227	1.377
MGO	0.024	0.006	0.011	0.000	0.020
AL_2O_3	18.793	18.939	19.079	19.155	18.872
SIO_2	64.826	64.179	64.757	64.236	64.614
K_2O	15.764	14.668	14.273	13.721	13.582
CAO	0.006	0.050	0.035	0.023	0.043
TIO_2	0.000	0.015	0.011	0.000	0.000
MNO	0.030	0.000	0.000	0.000	0.000
FEO(T)	0.103	0.040	0.013	0.047	0.023
BAO	0.000	0.176	0.313	0.302	0.166
TOTAL	100.572	99.129	99.656	98.710	98.698
AB	9.0	10.3	10.6	12.0	13.0
OR	91.0	89.7	89.4	88.0	87.0
AN	0	0	0.0	0.0	0.0

New Haven Arkose (stop 2)

SAMPLE	NH-2-10	NH-2-12	NH-2-13	NH-2-14	NH-2-17
NA_2O	1.059	0.250	1.253	0.299	1.206
MGO	0.009	0.000	0.014	0.007	0.000
AL_2O_3	18.940	18.610	19.033	18.914	18.990
SIO_2	63.821	63.373	63.964	64.088	62.798
K_2O	14.802	16.012	14.588	16.127	14.377
CAO	0.049	0.000	0.102	0.080	0.065
TIO_2	0.000	0.032	0.017	0.000	0.002
MNO	0.018	0.000	0.000	0.011	0.000
FEO(T)	0.051	0.000	0.000	0.023	0.034
BAO	0.279	0.000	0.227	0.000	0.621
TOTAL	99.030	98.277	99.197	99.550	98.093
AB	9.8	2.3	11.5	2.7	11.3
OR	90.2	97.7	88.0	96.9	88.7
AN	0	0	0.5	0.4	0

Stop 2 (Cont'd.)

SAMPLE	NH-2-19	NH-2-35	NH-2-35
NA$_2$O	0.699	1.056	0.430
MGO	0.000	0.000	0.011
AL$_2$O$_3$	18.851	18.749	18.618
SIO$_2$	64.962	63.585	63.734
K$_2$O	15.305	14.584	15.326
CAO	0.000	0.040	0.000
TIO$_2$	0.000	0.022	0.000
MNO	0.000	0.000	0.000
FEO(T)	0.019	0.011	0.056
BAO	0.000	0.290	0.218
TOTAL	99.837	98.338	98.392
AB	6.5	9.9	4.1
OR	93.5	90.1	95.9
AN	0	0	0

East Berlin Fm. (stop 1)

SAMPLE	EB-1-4	EB-1-4	EB-1-4	EB-1-4	EB-1-7
NA_2O	0.492	0.307	0.338	0.688	0.376
MGO	0.007	0.009	0.007	0.000	0.024
AL_2O_3	19.231	18.610	19.217	18.711	18.688
SIO_2	64.066	63.482	65.678	64.174	64.510
K_2O	14.975	14.878	14.776	15.836	15.350
CAO	0.007	0.009	0.009	0.010	0.001
TIO_2	0.032	0.047	0.000	0.009	0.000
MNO	0.000	0.000	0.000	0.041	0.000
FEO(T)	0.008	0.376	0.036	0.004	0.000
BAO	0.923	0.540	0.550	0.340	0.010
TOTAL	99.742	98.259	100.611	99.814	98.961
AB	4.4	3.3	3.4	6.2	3.6
OR	95.6	96.7	96.6	93.8	96.4
AN	0.0	0.0	0	0	0.0

Stop 1 (Cont'd.)

SAMPLE	EB-1-10	EB-1-12	EB-1-12
NA$_2$O	0.651	1.030	0.760
MGO	0.019	0.000	0.002
AL$_2$O$_3$	18.936	18.909	18.754
SIO$_2$	63.001	63.478	62.548
K$_2$O	14.766	13.709	15.549
CAO	0.002	0.117	0.000
TIO$_2$	0.000	0.007	0.008
MNO	0.041	0.002	0.000
FEO(T)	0.002	0.000	0.017
BAO	0.682	0.125	0.774
TOTAL	98.100	97.377	98.411
AB	6.3	9.9	6.9
OR	93.7	90.1	93.1
AN	0	0	0.0

APPENDIX D

Microprobe analysis of chlorite

Appendix D. Microprobe analysis of chlorite.

New Haven Arkose (stop 4)

SAMPLE	NH-4-1	NH-4-2	NH-4-2	NH-4-3	NH-4-3
NA_2O	0.051	0.116	0.065	0.070	0.069
MGO	18.829	15.414	16.212	16.299	17.104
AL_2O_3	18.945	25.263	23.405	24.959	26.164
SIO_2	29.547	30.673	28.578	33.109	34.063
K_2O	0.193	0.532	0.230	0.602	0.647
CAO	0.717	0.188	0.074	0.195	0.163
TIO_2	0.011	0.050	0.036	0.037	0.000
MNO	0.443	1.309	1.044	0.528	0.518
FEO(T)	14.664	14.028	18.574	12.488	11.981
BAO	0.000	0.000	0.019	0.000	0.000
TOTAL	83.399	87.573	88.328	88.287	90.709

East Berlin Fm. (stop 1)

SAMPLE	EB-1-2	EB-1-2
NA_2O	0.064	0.060
MGO	20.964	16.533
AL_2O_3	20.369	22.130
SIO_2	30.252	33.932
K_2O	0.068	0.927
CAO	0.109	0.313
TIO_2	0.000	0.046
MNO	0.681	0.608
FEO(T)	15.031	13.294
BAO	0.050	0.010
TOTAL	87.588	87.854

APPENDIX E

Microprobe analysis of zeolite

Appendix E. Microprobe analysis of zeolite.

New Haven Arkose (stop 3)

SAMPLE	NH-3-10	NH-3-10	NH-3-10	NH-3-10	NH-3-11
NA_2O	0.033	0.086	0.037	0.295	0.081
MGO	0.010	0.000	0.000	0.013	0.000
AL_2O_3	21.345	22.213	22.131	22.090	23.038
SIO_2	50.853	51.734	51.901	52.934	54.335
K_2O	0.788	0.547	0.536	1.326	0.822
CAO	10.730	11.399	11.355	10.533	11.280
TIO_2	0.017	0.011	0.000	0.001	0.009
MNO	0.000	0.000	0.000	0.032	0.000
FEO(T)	0.056	0.058	0.056	0.045	0.006
BAO	0.000	0.021	0.000	0.010	0.031
TOTAL	83.833	86.070	86.010	87.280	89.601

Stop 3 (Cont'd.)

SAMPLE	NH-3-11	NH-3-11	NH-3-11
NA$_2$O	0.296	0.090	0.161
MGO	0.017	0.000	0.000
AL$_2$O$_3$	22.866	22.231	21.805
SIO$_2$	54.805	51.386	50.666
K$_2$O	1.681	0.655	0.955
CAO	10.607	11.310	10.933
TIO$_2$	0.008	0.017	0.010
MNO	0.000	0.000	0.016
FEO(T)	0.023	0.000	0.028
BAO	0.031	0.031	0.031
TOTAL	90.334	85.721	84.605

APPENDIX F

SEM and BSEM analyses

Appendix F.   SEM and BSEM analyses

Stop	Sample	SEM	BSEM
	NH-4-6	x	x
	NH-4-5	–	–
	NH-4-4	x	x
4	NH-4-3	x	x
	NH-4-2	x	x
	NH-4-1	x	x
	NH-3-36	–	x
	NH-3-35	–	x
	NH-3-34	–	–
	NH-3-33	x	–
	NH-3-32	–	–
	NH-3-31	–	–
	NH-3-30	x	x
	NH-3-29	–	–
3	NH-3-28	x	x
	NH-3-27	x	x
	NH-3-26	–	–
	NH-3-25	x	x
	NH-3-24	–	x
	NH-3-23	x	x
	NH-3-22	–	–

Appendix F (Cont'd.)

Stop	Sample	SEM	BSEM
	NH-3-21	-	-
	NH-3-20	-	-
	NH-3-19	x	x
	NH-3-18	-	x
	NH-3-17	-	-
	NH-3-16	x	x
	NH-3-15	-	-
	NH-3-14	x	-
	NH-3-13	-	-
	NH-3-12	-	-
	NH-3-11	x	x
3	NH-3-10	x	x
	NH-3-9	x	x
	NH-3-8	-	-
	NH-3-7	x	x
	NH-3-6	-	-
	NH-3-5	-	-
	NH-3-4	-	-
	NH-3-3	x	x
	NH-3-2	x	-
	NH-3-1	x	x

Appendix F (Cont'd.)

Stop	Sample	SEM	BSEM
	NH-2-35	x	x
	NH-2-34	x	x
	NH-2-33	x	-
	NH-2-32	-	-
	NH-2-31	-	-
	NH-2-30	x	x
	NH-2-29	-	x
	NH-2-28	-	-
	NH-2-27	-	-
	NH-2-26	x	-
	NH-2-25	-	x
2	NH-2-24	x	-
	NH-2-23	-	-
	NH-2-22	x	x
	NH-2-21	-	-
	NH-2-20	-	-
	NH-2-19	x	x
	NH-2-18	-	-
	NH-2-17	x	x
	NH-2-16	-	-
	NH-2-15	-	-
	NH-2-14	x	x
	NH-2-13	x	x

Appendix F (Cont'd.)

STOP	Sample	SEM	BSEM
	NH-2-12	x	x
	NH-2-11	−	−
	NH-2-10	x	x
	NH-2-9	x	x
	NH-2-8	−	−
	NH-2-7	x	x
2	NH-2-6	−	−
	NH-2-5	−	−
	NH-2-4	x	x
	NH-2-3	−	−
	NH-2-2	x	x
	NH-2-1	−	−
	EB-1-28	−	x
	EB-1-27	−	−
	EB-1-26	−	−
	EB-1-25	x	x
	EB-1-24	−	−
1	EB-1-23	−	x
	EB-1-22	−	−
	EB-1-21	x	x
	EB-1-20	−	−
	EB-1-19	−	−

Appendix F (Cont'd.)

STOP	Sample	SEM	BSEM
	EB-1-18	-	x
	EB-1-17	-	-
	EB-1-16	x	-
	EB-1-15	-	-
	EB-1-14	x	-
	EB-1-13	-	-
	EB-1-12	x	x
	EB-1-11	-	-
	EB-1-10	x	x
1	EB-1-9	-	-
	EB-1-8	-	-
	EB-1-7	x	x
	EB-1-6	x	x
	EB-1-5	x	x
	EB-1-4	x	x
	EB-1-3	x	x
	EB-1-2	x	x
	EB-1-1	x	x

x = analysis performed

- = not analysed

LIST OF REFERENCES

LIST OF REFERENCES

Aagaard, P., Egeberg, P. K., Saigal, G. C., Morad, S., and Bjorlykke, K., 1990, Diagenetic albitization of detrital K-feldspars in Jurassic, Lower Cretaceous and Tertiary clastic reservoir rocks from offshore Norway. II. Formation water chemistry and kinetic considerations: Jour. Sed. Petrology, v. 60, 575-581.

Adams, W. L., 1964, Diagenetic aspects of Lower Morrowan, Pennsylvanian sandstones, Northwestern Oklahoma: Am. Assoc. of Petrol. Geol. Bull., v. 48, p. 1568-1580.

Almon, W. R., Fullerton, L. B., and Davies, D. K., 1976, Pore space reduction in Cretaceous sandstones through chemical precipitation of clay minerals: Jour. Sed. Petrology, v. 46, p. 89-96.

Anderson, G. H., 1937, Granitization, albitization, and related phenomena in the northern Inyo Range of California-Nevada: Geol. Soc. Amer. Bull., v. 48, p. 1-74.

April, R. H., 1978, Clay mineralogy and geochemistry of the Triassic - Jurassic sedimentary rocks of the Connecticut Valley: Ph. D. diss., Dept. of Geology / Geography, Univ. Mass., Amherst, Mass., 206 p.

April, R. H., 1980, Regularly interstratified chlorite / vermiculite in contact metamorphosed red beds, Newark Group, Connecticut Valley: Clays and Clay Minerals, v. 28, p. 1-11.

April, R. H., 1981, Trioctahedral smectite and interstratified chlorite / smectite in Jurassic strata of the Connecticut Valley: Clays and Clay minerals, v. 29, p. 31-39.

Austin, J. A., Jr., Uchupi, E., Shaughnessy, D. R., and Ballard, R. D., 1980, Geology of New England passive margin: Am. Assoc. of Petrol. Geol. Bull., v. 64, p. 501-526.

Bailey, E. H., and Stevens, R. E., 1960, Selective staining of K-feldspar and plagioclase of rocks slabs and thin sections: Amer. Min., v. 45, p. 1020-1025.

Bailey, S. W., 1980, Structures of layer silicates:in Crystal Structures of Clay Minerals and their X-ray Identification, G. W. Brindley and G. Brown (eds.), Mineralogical Society, Monograph 5, London, p. 1-123.

Berner, R. A., 1981, A new geochemical classification of sedimentary environments: Jour. Sed. Petrology, v.51, No. 2, p. 359-365.

Blatter, C. L., Roberson, H. E., and Thompson, G. R., 1973, Regularly interstratified chlorite-dioctahedral smectite in dike-intruded shales, Montana: Clays and Clay Minerals, v. 21, p. 207-212.

Boles, J. R., 1981, Zeolites in low-grade metamorphic rocks: in Mineralogy and Geology of Natural Zeolites, F. A. Mumpton (ed.), 2nd printing, Reviews in Mineralogy, v. 4, p. 103-135.

Boles, J. R., 1982, Active albitization of plagioclase, Gulf Coast Tertiary: Am. Jour. Sci., v. 282, p. 165-180.

Boles, J. R., 1984, Secondary porosity reactions in the Stevens Sandstone, San Joaquim Valley, California: in Clastic Diagenesis, D. A. McDonald and R. C. Surdam (eds.), Am. Assoc. of Petrol. Geol. Mem. 37, p. 217-224.

Boles, J. R., and Franks,S. G., 1979, Clay diagenesis in the Wilcox sandstones of southeast Texas: Implications of smectite diagenesis on sandstone cementation: Jour. Sed. Petrology, v. 49, p. 55-70.

Bradley, W. F., and Weaver, C. E., 1956, A regularly interstratified chlorite vermiculite clay mineral: Amer. Min., v. 41, p. 497-504.

Brindley, G. W., 1961, Chlorite minerals: in The X-ray Identification and Crystal Structures of Clay Minerals, G. Brown (ed.), The Mineralogical Society, London, p. 242-296.

Brown, G., and Brindley, G. W., 1980, X-ray diffraction procedures for clay mineral identification: in Crystal Structures of Clay Minerals and their X-ray Identification: Mineralogical Society, Monograph No. 5, London, p. 305-360.

Brown, G., 1961, The X-ray Identification and Crystal Structures of Clay Minerals: Mineralogical Society, London, 544 p.

Brown, B. E., and Bailey, S. W., 1962, Chlorite polytypism: I. Regular and semi-random one-layer structures: Amer. Min., v. 47, p. 819-850.

Carstea, D. D., Harward, M. E., and Knox, E. G., 1970, Formation and stability of hydroxy-Mg interlayers in phyllosilicates: Clays and Clay Minerals, v. 18, p. 213-222.

Cornet, B., and Traverse, A., 1975, Palynological contributions to the chronology and stratigraphy of the Hartford Basin in Connecticut and Massachusetts: Geosci. and Man, v. 11, p. 1-33.

Curtis, C. D., Ireland, B. J., Whiteman, J. A., Mulvaney, R., and Whittle, C. K., 1984, Authigenic chlorites: problems with chemical analysis and structural formula calculation: Clay Minerals, v. 19, p. 471-481.

Curtis, C. D., Hughes, C. R., Whiteman, J. A., and Whittle, C. K., 1985, Compositional variation within some sedimentary chlorites and some comments on their origin: Mineral. Mag., v. 49, p. 375-386.

Dana, J. D., 1883, Origin of Jura-Trias of eastern North America: Am. Jour. Sci., v. 25, p. 383-386.

Demicco, R. V., and Gierlowski-Kordesch, E. G., 1986, Facies sequences of a semi-arid closed basin: the lower Jurassic East Berlin Formation of the Hartford Basin, New England, USA: Sedimentology, v. 33, p. 107-118.

Dickinson, W. R., and Suczek, C. A., 1979, Plate tectonics and sandstone compositions: Am. Assoc. of Petrol. Geol. Bull., v. 63, p. 2164-2182.

Drever, J. I., 1973, The preparation of oriented clay mineral specimens for x-ray diffraction analysis by a filter membrane peel technique: Amer. Min., v. 58, p. 553-554.

Dunoyer De Segonzac, G., 1970, The transformation of clay minerals during diagenesis and low-grade metamorphism: A review: Sedimentology, v. 15, p. 281-346.

Dypvik, H., 1983, Clay mineral transformation in Tertiary and Mesozoic sediments from North Sea: Am. Assoc. of Petrol. Geol. Bull., v. 67, p. 160-165.

Early, J. W., Brindley, G. W., McVeagh, W. J., and Vanden Heuvel, R. C., 1956, A regularly interstratified montmorillonite-chlorite: Amer. Min., v. 41, p. 258-267.

Eslinger, E., and Pevear, D., 1988, Clay minerals for petroleum geologists and engineers: SEPM Short Course Notes No. 22, 356 p.

Fisher, M. J., and Jeans, C. V., 1982, Clay mineral stratigraphy in the Permo-Triassic red beds sequences of BNOC 72/10-1A, Western Approaches, and the south Devon coast: Clay Minerals, v. 17, p. 79-89.

Fuchtbauer, H., 1983, Facies controls on sandstone diagenesis: in Sediment Diagenesis, A. Parker and B. W. Sellwood (eds.), Nato ASI Series C, 115, D. Reidel, Dodrecht, p. 269-288.

Ghent, E. D., 1979, Problems in zeolite facies geothermometry, geobarometry and fluid compositions: SEPM Special Pub. No. 26, p. 81-87.

Gold, P. B., 1987, Textures and geochemistry of authigenic albite from Miocene sandstones, Louisiana Gulf Coast: Jour. Sed. Petrology, v. 57, p. 353-362

Gottfried, R. M., and Kotra, R. K., 1988, Comparative mineralogy of clay-rich strata in selected Early Mesozoic basins of the eastern United States: in Studies of the Early Mesozoic Basins of the Eastern United States, A. J. Froelich and G. R. Robinson, Jr. (eds.), U. S. Geol. Surv. Bull. 1776, p. 99-103.

Gude, A. J., 3rd, 1981, X-ray powder diffraction patterns of common zeolites found in sedimentary rocks: in Mineralogy and Geology of Natural Zeolites, F. A. Mumpton (ed.), 2nd printing, Reviews in Mineralogy, v. 4, p. 219-225.

Grim, R., E., 1968, Clay Mineralogy: McGraw Hill, N. Y., 596p.

Hall, M. G., and Lloyd, G. E., 1981, The SEM examination of geological samples with a semiconductor back-scattered electron detector: Amer. Min., v. 66, p. 362-368.

Hallam, A., 1971, Mesozoic geology and the opening of the North Atlantic: Jour. of Geol., v. 79, p. 129-157.

Hay, R. L., 1966, Zeolites and zeolitic reactions in sedimentary rocks: Geol. Soc. Amer. Spec. Paper 85, 130p.

Hay, R. L., 1978, Geologic occurrence of zeolites: in Natural Zeolites, L. B. Sand and F. A. Mumpton (eds.), Pergamon Press Ltd., p. 135-143.

Heald, M. T., Cementation on Triassic arkoses in Connecticut and Massachusetts: Geol. Soc. Amer. Bull., v. 67, p. 1133-1154.

Helmold, K. P., and Van de Kamp, P. C., 1984, Diagenetic mineralogy and controls on albitization and laumontite formation in Paleogene arkoses, Santa Ynez Mountains, California: in Clastic Diagenesis, D. A. McDonald and D. C. Surdam (eds.), Am. Assoc. of Petrol. Geol. Mem. 37, p. 239-276.

Hoffman, J., and Hower, J., 1979, Clay mineral assemblages as low grade metamorphic geothermometers: application to the thrust faulted disturbed belt of Montana, U. S. A.: SEPM Special Pub. No. 26, p. 55-79.

Hower, J., Eslinger, E. V., Hower, M. E., and Perry, E. A., 1976, Mechanism of burial metamorphism of argillaceous sediments: 1. Mineralogical and chemical evidence: Geol. Soc. Am. Bull., v. 87, p. 725-737.

Hubert, J. F., 1977, Paleosol caliche in the New Haven Arkose, Connecticut--record of semiaridity in Late Triassic - Early Jurassic time: Geology, v. 5, p. 302-304.

Hubert, J. F., Reed, A. A., and Carey, P. J., 1976, Paleogeography of the East Berlin Formation, Newark Group, Connecticut Valley: Am. Jour. Sci., v. 276, p. 1183-1207.

Hubert, J. F., and Reed, A. A., 1978, Red bed diagenesis in the East Berlin Formation, Newark Group, Connecticut Valley: Jour. Sed. Petrology, v. 48, p. 175-184.

Hubert, J. F., Reed, A. A., Dowdall, W. L., and Gilchrist, J. M., 1978, Guide to Mesozoic red beds of central Connecticut: 1978 Field trip, eastern section of S.E.P.M., contribution 32, Dept. of Geology and Geography, Univ. of Mass., Amherst, Guidebook 3, 129p.

Hubert, J. F., Gilchrist, J. M., and Reed, A. A., 1982, Jurassic redbeds of the Connecticut Valley: (1) brownstone of the Portland Formation; and (2) playa-playa lake-oligomictic lake model for parts of the East Berlin, Shuttle Meadow, and Portland Formations: in Guidebook for field trips in Connecticut and south-central Massachusetts, R. Joesten and S. S. Quarrier (eds.), State Geol. and Nat. Hist. Survey of Connecticut, Guidebook 5, p. 103-141.

Hubert, J. F., and Meriney, P. E., 1988, Diagenesis of sandstones in the Triassic-Jurassic Hartford Rift Basin, Connecticut and Massachusetts: 1988 SEPM Annual Midyear Meeting Abstr., v. V, p. 26.

Humphreys, B., Smith, S. A., and Strong, G. E., 1989, Authigenic chlorite in Late Triassic sandstones from the Central Graben, North Sea: Clay Minerals, v. 24, p. 427-444.

Iijima, A., and Utada, M., 1966, Zeolites in sedimentary rocks, with reference to the depositional environments and zonal distribution: Sedimentology, v. 7, p. 327-357.

Ingersoll, R. V., Bullard, T. F., Ford, R. L., Grimm, J. P., Pickle, J. D., and Sares, S. W., 1984, The effect of grain size on detrital modes: a test of the Gazzi-Dickinson point-counting method: Jour. Sed. Petrology, v. 54, p. 103-116.

Johnson, L. J., 1964, Occurrence of regularly interstratified chlorite-vermiculite as a weathering product of chlorite in a soil: Amer. Min., v. 49, p. 556-572.

Kaiser, W. R., 1984, Predicting reservoir quality and diagenetic history of the Frio Formation (Oligocene) of Texas: in Clastic Diagenesis, D. McDonald and R. Surdam (eds.), Am. Assoc. of Petrol. Geol. Mem. 37, p. 195-215.

Kastner, M., 1971, Authigenic feldspars in carbonate rocks: Amer. Min., v. 56, p. 1403-1442.

Kastner, M., and Siever, R., 1979, Low temperature feldspars in sedimentary rocks: Am. Jour. Sci., v. 279, p. 435-479.

Keller, W. D., 1970, Environment aspects of clay minerals: Jour. Sed. Petrology, v. 40, p. 788-813.

Keller, W. D., Reynolds, R. C., and Inoue, A., 1986, Morphology of clay minerals in the smectite-to-illite conversion series by Scanning Electron Microscopy: Clays and Clay Minerals, v. 34, No. 2, p. 187-197.

Klein, G. de V., 1969, Deposition of Triassic sedimentary rocks in separate basins, eastern North America: Geol. Soc. Amer. Bull., v. 80, p. 1825-1832.

Krinsley, D. M., Pye, K., and Kearsley, A. T., 1983, Applications of backscattered electron microscopy: Geological Magazine, v. 120, p. 109-114.

Krynine. P. D., 1950, Petrology, stratigraphy and origin of the Triassic sedimentary rocks of Connecticut: Conn. Geol. and Nat. Hist. Survey Bull., v. 73, 247p.

Lajoie, J., 1973, Albite of secondary origin in Charny sandstones, Quebec: Discussion: Jour. Sed. Petrology, v. 43, p. 575-576.

Land, L. S., and Milliken, K. L., 1981, Feldspar diagenesis in the Frio Formation, Brazoria County, Texas Gulf Coast: Geology, v. 9, p. 314-318.

Lorenz, J. C., 1988, Triassic-Jurassic Rift-Basin Sedimentology: Van Nostrand Reinhold, N. Y., 315p.

Lippmann, F., 1956, Clay minerals from the Rot Member of the Triassic near Gottingen, Germany: Jour. Sed. Petrology, v. 26, p. 125-139.

Mack, G. H., and Suttner, L. J., 1977, Paleoclimate interpretation from a petrographic comparison of Holocene sands and the Fountain Formation (Pennsylvanian) in the Colorado Front Range: Jour. Sed. Petrology, v. 47, p. 89-100.

Martin Vivaldi, J. L., and MacEwan, D. M. C., 1960, Corrensite and swelling chlorite: Clays and Clay Minerals, v. 4, p. 173-181.

Middleton, G. V., 1972, Albite of secondary origin in Charny sandstones, Quebec: Jour. Sed. Petrology, v. 42, p. 341-349.

Milliken, K. L., 1989, Petrography and composition of authigenic feldspars, Oligocene Frio Formation, south Texas: Jour. Sed. Petrology, v. 59, p. 361-374.

Milliken, K. L., Gold, P. B., and Land, L. S., 1985, Feldspar diagenesis in Neogene sediments, northern Gulf of Mexico: Am. Assoc. of Petrol. Geol., Annual Meeting Abstr.

Millot, G., 1970, Geology of Clays: Springer-Verlag, N. Y., 429p.

Moncure, G. K., Lahann, R. W., and Siebert, R. M., 1984, Origin of secondary porosity and cement distribution in a sandstone/shale sequence from the Frio Formation (Oligocene): in Clastic Diagenesis, D. A. McDonald and R. C. Surdam, Am. Assoc. Petrol. Geol. Mem. 37, p. 151-161.

Moore, D. M., and Reynolds, R. C., 1989, X-ray Diffraction and the Identification and Analysis of Clay Minerals: Oxford Univ. Press, New York, 332p.

Morad, S., Bergan, M., Knarud, R., and Nystuen, J. P., 1990, Albitization of detrital plagioclase in Triassic reservoir sandstones from the Snoree Field, Norwegian North Sea: Jour. Sed. Petrology, v. 60, p. 411-425.

Mumpton, F. A., 1981, Natural zeolites: in Mineralogy and Geology of Natural Zeolites, F. A. Mumpton (ed.), Reviews in Mineralogy, v. 4, p. 1-17.

Olsen, P. E., 1978, On the use of the term Newark for Triassic and Early Jurassic rocks of eastern North America: Newsletters on Stratigraphy, v. 7, p. 90-95.

Olsen, P. E., 1986, A 40-million-year lake record of early

Mesozoic orbital climatic forcing: Science, v. 234, p. 842-848.

Ogunyomi, O., Martin, R. F., and Hesse, R., 1981, Albite of secondary origin in Charny sandstones, Quebec: a reevaluation: Jour. Sed. Petrology, v. 51, p. 597-606.

Oshchudlak, M. A., and Hubert, J. F., 1988, Petrology of Mesozoic sandstones in the Newark basin, central New Jersey and adjacent New York: in Triassic-Jurassic Rifting, W. Manspeizer (ed.), Elsevier, Developments in Geotectonics 22, Part A, p. 333-352.

Peterson, M. N. A., 1961, Expandable chloritic clay minerals from the Upper Mississippian carbonate rocks of Cumberland Plateau in Tennessee: Amer. Min., v. 46, p. 1245-1269.

Pettijohn, F. J., Potter, P. E., and Siever, R., 1987, Sand and Sandstone: Springer-Verlag, N. Y., 2nd Ed., 553p.

Philipps, J. D., and Forsyth, D., 1972, Plate tectonics, paleomagnetism, and the opening of the Atlantic: Geol. Soc. Amer. Bull., v. 83, p. 1579-1600.

Philpotts, A. R., 1990, Principles of Igneous and Metamorphic Petrology: Prentice Hall, Englewood Cliffs, N.J., 498p.

Pittman, E. D., 1988, Diagenesis of the Terry Sandstone (Upper Cretaceous), Spindle Field, Colorado: Jour. Sed. Petrology, v. 58, p. 785-800.

Post, J. L., and Janke, N. C., 1974, Properties of "swelling" chlorite in some Mesozoic formations of California: Clays and Clay Minerals, v. 22, p. 67-77.

Post, J. L., and Plummer, C. C., 1972, The chlorite series of Flagstaff Hill area, California: a preliminary investigation: Clays and Clay Minerals, v. 20, p. 271-283.

Pratt, L. M., Shaw, C. A., and Burruss, R. C., 1988, Thermal histories of the Hartford and Newark basins inferred from maturation indicies of organic matter: in Studies of the Early Mesozoic Basins of the Eastern United States, A. J. Froelich and G. R. Robinson, Jr. (eds.), U. S. Geol. Surv. Bull. 1776, p. 58-62.

Pye, K., and Krinsley, D. M., 1983, Mudrocks examined by backscattered electron microscopy: Nature, v. 301, p. 412-413.

Pye, K., and Krinsley, D. M., 1984, Petrographic examination of sedimentary rocks in the SEM using backscattered electron detectors: Jour. Sed. Petrology, v. 54, p. 877-888.

Ramseyer, K., and Boles, J. R., 1986, Mixed-layer illite/smectite minerals in Tertiary sandstones and shales, San Joaquin Basin, California: Clays and clay minerals, v. 34, No. 2, p. 115-124.

Reynolds, R. C., 1980, Interstratified clay minerals: in Crystal Structures of Clay Minerals and their X-ray Identification, G. W. Brindley and G. Brown (eds.), Mineralogical Society, Monograph No. 5, London, p. 249-303.

Rodgers, J., 1968, Introduction to the Triassic rocks of Connecticut: in New England Intercollegiate Geological Conference Guidebook for fieldtrips in Connecticut: Yale Univ., New Haven, Section C-0, p. 1-2.

Ross, G. J., and Kodama, H., 1976, Experimental alteration of a chlorite into a regularly interstratified chlorite-vermiculite by chemical oxidation: Clays and Clay Minerals, v. 24, p. 183-190.

Saigal, G. C., Morad, S., Bjorlykke, K., Egeberg, P. K., and Aagaard, P., 1988. Diagenetic albitization of detrital K-feldspar in Jurassic, Lower Cretaceous, and Tertiary clastic reservoir rocks from offshore Norway, I. Textures and origin: Jour. Sed. Petrology, V. 58, p. 1003-1013.

Sanders, J. E., 1970, Stratigraphy and structure of the Triassic strata of the Gaillard Graben, south-central Connecticut: Conn. Geol. and Nat. Hist. Survey, Guidebook 3, 15p.

Shirozu, H., 1958, X-ray powder patterns and cell dimensions of some chlorites in Japan, with a note on their interference colours: Mineral. Jour., v. 2, p. 209-223.

Smith, J. V., 1974, Feldspar Minerals, v. 2, Chemical and Textural Properties: New York, Springer-Verlag, 690p.

Smith, N. D., 1971, Transverse bars and braiding in the lower Platte River, Nebraska: Geol. Soc. Amer. Bull., v. 82, p. 3407-3420.

Smith, N. D., 1972, Some sedimentological aspects of planner cross-stratification in a sandy braided river: Jour. Sed. Petrology, v. 42, p. 624-634.

Starkey, J., 1959, Chessboard albite from New Brunswick, Canada: Geol. Mag., v. 96, p. 141-145.

Suchecki, R. K., Perry, E. A., and Hubert, J. F., 1977, Clay petrology of the Cambro-Ordovician continental margin, Cow Head Klippe, western Newfoundland: Clays and Clay Minerals, v. 25, p. 163-170.

Suchecki, R. K., Hubert, J. F., and Birney De Wet, C. C., 1988, Isotope imprint of climate and hydrogeochemistry on terrestrial strata of the Triassic-Jurassic Hartford and Fundy rift basins: Jour. Sed. Petrology, v. 58, p. 801-811.

Schwartz, F. W., and Longstaffe, F. J., 1988, Ground water and clastic diagenesis: in Hydrogeology, B. W. Rosenshein and P. R. Seaber (eds.), Boulder, Colorado, Geological Society of America, v. 0-2, p. 413-434.

Tompkins, R. E., 1981, Scanning electron microscopy of a regular chlorite/smectite (corrensite) from a hydrocarbon reservoir sandstone: Clays and Clay Minerlas, v. 29, p. 233-235.

Van Houten, F. B., 1962, Cyclic sedimentation and the origin of analcime-rich Upper Triassic Lockatong Formation, west-central New Jersey and adjacent Pennsylvanian: Am. Jour. Sci., v. 260, p. 561-576.

Van Houten, F. B., 1965, Composition of the Triassic Lockatong and associated formations of Newark Group, central New Jersey and adjacent Pennsylvania: Am. Jour. Sci., v. 263, p. 825-863.

Van Houten, F. B., 1977, Triassic-Liassic deposits of Morocco and Eastern North America: Comparison: Am. Assoc. of Petrol. Geol. Bull., v. 61, p. 79-99.

Velbel, M. A., Saad, M. K., 1991, Palaeoweathering or diagenesis as the principal modifier of sandstone framework composition? A case study from some Triassic rift-valley redbeds of eastern North America: in Developments in Sedimentary Provenance Studies, A. C. Morton et al. (eds.), Geological Society of London, Special Publ. No. 57, p. 91-99.

Velde, B., 1977, Clays and Clay Minerals in Natural and Synthetic Systems: Developments in Sedimentology, v. 21, Elsevier Scientific Pub. Co., Amsterdam, 218p.

Vetter, M., and Brakenridge, G. R., 1986, Hartford and Deerfield basin framework mineralogies: independent evidence for provinance, current directions, and tectonic history: Am. Assoc. of Petrol. Geol. Abstr., v. 70, p. 659.

Walker, T. R., 1978, Discussion: Paleoclimate interpretation from a petrographic comparison of the Holocene sands and the Fountain Formation (Pennsylvanian) in the Colorado Front Range: Jour. Sed. Petrology, v. 48, p. 1011-1013.

Walker, T. R., 1984, Diagenetic albitization of potassium feldspar in arkosic sandstones: Jour. Sed. Petrology, v. 54, p. 3-16.

Weaver, C. E., and Pollard, L. D., 1975, The Chemistry of Clay Minerals: Developments in Sedimentology, v. 15, Elsevier Scientific Pub. Co., Amsterdam, 234p.

Welton, J. E., 1984, SEM Petrology Atlas: Methods in exploration series No. 4, Am. Assoc. of Petrol. Geol. Pub., 237p.

Whittle, C. K., 1986, Comparison of sedimentary chlorite composition by X-ray diffraction and analytical TEM: Clay Minerals, v. 21, p. 937-947.

Wilson, M. J., 1987, A Handbook of Determinative Methods in Clay Mineralogy, Blackie and Son Ltd., Glasgow, 308p.

Wilson, M. D., and Pittman, E.D., 1977, Authigenic clays in sandstones: recognition and influence on reservoir properties and paleoenvironmental analysis: Jour. Sed. Petrology, v. 47, p. 3-31.

Zelazny, L. W., and Calhoun, F. G., 1982, Palygorskite, (attapulgite), sepiolite, talc, pyrophyllite, and zeolite: in Mineral in Soil Environments, J. B. Dixon and S. B. Weed (eds.), 3rd printing, Pub. by Soil Science Society of America, p. 435-470.